Master of Engineering (Electronics)

Feasibility study on developing embedded system for PFAS detection in drinking water

Topic Number and Name:

ENGR9700 ENGINEERING THESIS PROJECT REPORT

Semester and Year:

Semester 1&2 – 2019

Name of Student and ID:

Hao Fu – 2196360

Name of Supervisor:

Prof. Youhong Tang

Date of Report Submitted:

04/ December / 2019

Grade:

Submitted to the College of Science and Engineering in partial fulfillment of the requirements for the degree of Master of Engineering (Electronics) at Flinders University - Adelaide Australia

DECLARATION

I hereby acknowledge that in accordance with the University's policy on plagiarism, and unless otherwise referenced, all material presented in this report is my own.

<FUHAO>

<03/04/2018>

ACKNOWLEDGEMENT

I would like to acknowledge the following for their assistance in producing this report:

I would like to thank my thesis supervisor Youhong Tang from Flinders University. He introduced me to the first step of PFOA design and showed me how to apply embedded system to the medical field. Also thanks my group leader Jinjian Wu. He explained and provided practical experience related to chemicals and combined chemistry knowledge with design to produce the final optimization results. Whenever I have trouble or have questions about the research or writing, they always be happy to help me solve problems and lead me to the right direction.

I would also like to thank Xinyi Zhang for supporting me in the project experiment, and her valuable comments on this thesis. With their enthusiastic participation and contribution, this research project can finally success.

Abstract

In this article, I explain the difficulty of PFAS detection using HPLC-MS, including a long detection time and expensive inspection. Alternatively, image processing is used to collect images of and a coloration reaction of PFOA, which is much simple and easier than HPLC-MS. However, the accuracy of the mobile image recognition system has limitations. That is because that different mobile phone cameras will generate different RGB values. Furthermore, after the collection of RGB, there needs to design an appropriate image interpolation algorithm towards the image recognition system.

In my project, the embedded system is used to drive the camera module. The OV2640 is a 1/4" CMOS UXGA (1632*1232) image sensor from OmniVision. The sensor is small and low in operating voltage. Users have complete control over image quality, data format and transmission. For example, RGB565 format, YUV422 format or Bayer format. All image processing functions including Brightness and contrast can be programmed via the SCCB interface. The output pixels data transformation is passing through the DCMI (Digital camera Interface).

Firstly, analyse image acquisition results for different brightness according to image output formats RGB565 and YUV422. Through the results, it can be found that the best image quality can be obtained when the brightness of the camera module is adjusted to the maximum using the internal registers of the camera module.

Secondly, the accuracy of the whole recognition system is compared by linear algorithm, exponential algorithm and polynomial algorithm. Firstly, the influence of different colours on the whole solution is analysed by calculating the coefficient of determination, and then selected the function expression that best matches the data. The results of the image recognition system show that polynomial algorithm has the highest recognition. Linear algorithm has the lowest recognition.

By using PFAS detection colour recognition with embedded systems, the accuracy of PFAS solution detection can be effectively improved, from 30 ppb of mobile phone recognition system to 5 ppb of embedded system, which can effectively reduce development time and development cost.

Contents

List of Figures

List of Tables

List of Equation

1 Background and Literature Review

1.1 How to detect PFOA detection on previous method

Per- and polyfluoroalkyl substances (PFAS) are a group of man-made chemicals that includes PFOA, PFOS. PFAS have been manufactured and used in a variety of industries around the globe, including in the United States since the 1940s. During 2011 and 2012, the Australia Government department of Health monitored PFOA in raw and finished drinking water in some communities. PFOA was detected in finished water with levels as high as 5600 ng/L. [18]. Perfluoroalkyl materials and polyfluoroalkyl materials (PFAS) comprise a family of compounds synthesized by humans (Buck, R.C., Franklin, J. [1]).They have a wide range of applications such as clothing, upholstery, carpets, food containers, cookware, water-based firefighting foam (Buck, R.C., Franklin, J. [1]).As their widely used artificial materials, they are currently being detected on a global scale, including almost all life forms and environments from the Arctic to the South Pole (Fang, C., Zhang, X. [2]);Studies have shown that PFOA / PFOS is toxic and is often listed as a new contaminant by various tissues (George, A., White L. [3]). Therefore, PFOA / PFOS monitoring is urgently needed.

There are many ways to detect PFAS substances. The first method is HPLC-MS instrumental analysis (Fang, C [4]), it is common method, but it is high cost and long detection time. Secondly, the MBAS and astkCARE TM test paper analysis methods do not have much practical reference value because it has large error depend on Visual recognition. Image inspection is a powerful analytical tool in solution detection. Among them, the portable image sensor has excellent sensitivity and low price, which is the good choice in PFAS detection. The current method is to collect the image of astkCARE ^{TM} through the mobile phone camera and analyse the concentration of the PFAS substance by the value of RGB (Lopez-Ruiz, N., Curto, V.F. [5]), and the difference of the high concentration solution can be successfully distinguished. My main research direction is to address the shortcomings of mobile phone image acquisition module and image processing module, improve the resolution of the image to increase the accuracy of the entire image recognition system.

1.1.1 HPLC-MS method

HPLC-MS is the main technique used to detect PFOA. However, but HPLC-MS testing requires high costs (usually > $100/sample) and longer detection times (usually more than 2 weeks) and must be text in specialized laboratories with complex instruments. As can be seen in Figure 1, HPLC-MS requires many experimental steps to complete test. Special instruments and training are required for PFAS testing.

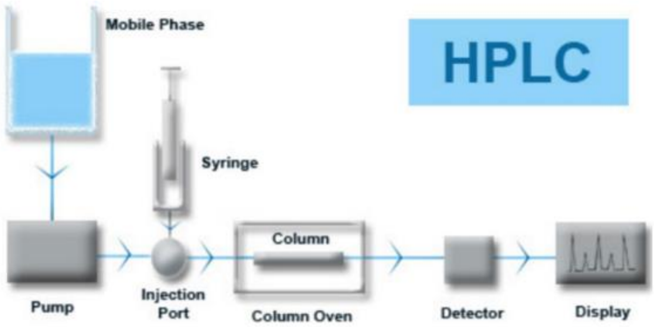

Figure 1 HPLC-MS method to detect PFOA

1.1.2 AstkCARE ™ with the human eye detection

Like pH strips, perhaps colouring is the easiest way to test with the naked eye, such as MBAS and astkCARE™. This visual inspection is highly dependent on colour assessment. Furthermore, interference from background illumination affects subjective results. The background illumination on a sunny, cloudy or rainy day has different results. Although use of PH ribbons significantly reduces the cost of detection. Figure 2 depicts a photographic image of different concentrations of PFOA.

It can be found that in the human eye recognition unable to distinguish the difference in the apparent concentration range whatever the format is RGB565 or YUV422.Therefore, in order to obtain accurate colour readings, it is recommended to use an image scanning device or design image processing unit for naked eye detection.

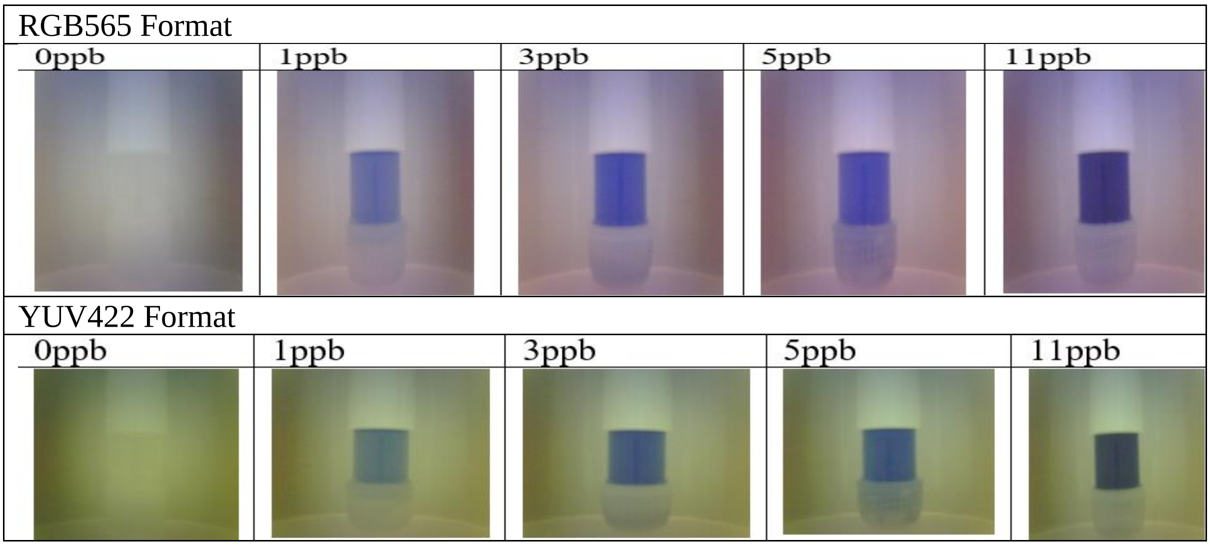

Figure 2 PH ribbons to detect PFOA with human eye

1.1.3 AstkCARE ™ with the smartphone camera detection

The smartphone camera was used to read the coloration of astkCARE™ to instead of the naked eye detection system, as shown in Figure 3, which is the physical map of the entire design. the solution to be tested on clean test tube, and then the test tube is placed on environment of a stable light source, the camera will collect the colour data on PFAS solution. Use a mobile app to read the colour (RGB) and convert it to FPAS concentration.

Figure 3 Smartphone camera detection image system

(Ref: [2] Fang, C and R. Naidu. "Fluoro-spe for Selective Detection of Fluorosurfactants at Ppb Level.")

Through this experiment, it can be found that when the concentration of PFAS substance changes, the RGB value collected by the mobile phone camera has been main changed of the calibration curve. (The whole RGB value ranges from 0 to 255, 0 represents the light and 255 represents the dark.) It can be shown in Figure 4 It can be demonstrated that smartphone cameras can distinguish different FPAS concentration changed, which allows image recognition system to be more sensitive than the naked eye recognition.

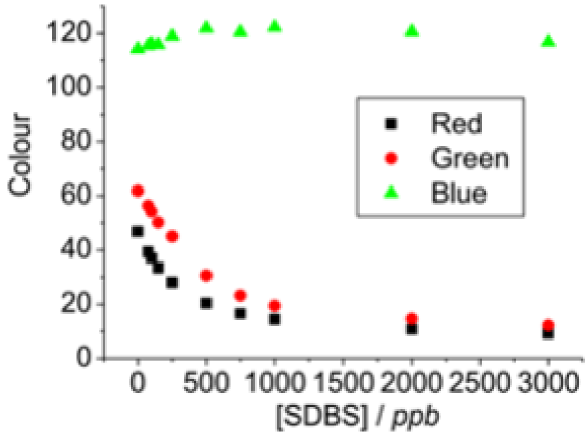

Figure 4 smartphone cameras can distinguish different FPAS concentration with RGB format

1.2 Smartphone camera detection current problems

1.2.1 Different mobile phone cameras have different sensitivity

Although in the mobile phone camera result, it is necessary to reduce the influence of different cameras on different mobile phone, it is unavoidable to increase the error in this experiment. As shown in Figure 5, it can be found that different mobile phones are different in sensitivity to light. However, when the light sensitivity is different, the different RGB values are obtained. Although the RGB trend can be determined, the appropriate threshold cannot be set. it needs to choose the professional camera that is most suitable for astkCARE ™ image acquisition.

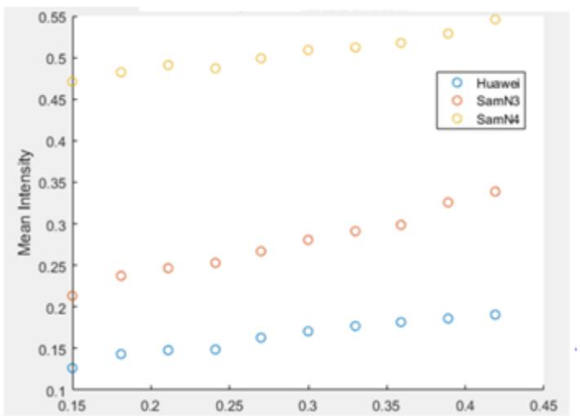

Figure 5 different mobile phones are different in sensitivity to light

1.2.2 Recognition ability on low concentration solution

Although mobile phone camera image processing filter could get high quality picture, Undoubtedly, it removes some important on image. In particular, the fit can be extended to a low concentration range (30%) so it needs to set 10 ppb as the detection limit .as show on Figure 6.the image filter in the phone has been pre-set, it is necessary to redesign an image filter that is most suitable for image acquisition with astkCARE^{TM} to reduce the impact of the image filter on the image system.

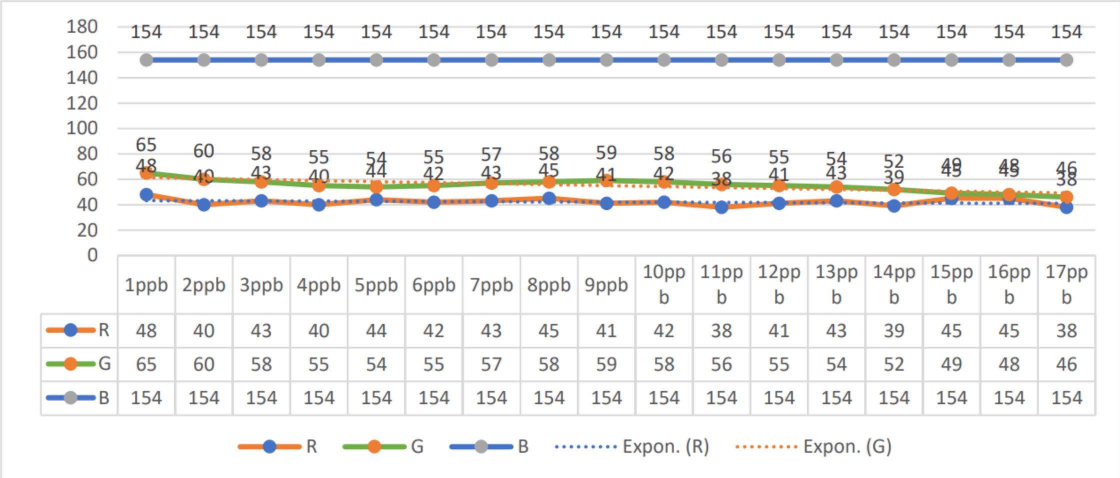

	1ppb	2ppb	3ppb	4ppb	5ppb	6ppb	7ppb	8ppb	9ppb	10ppb	11ppb	12ppb	13ppb	14ppb	15ppb	16ppb	17ppb
R	48	40	43	40	44	42	43	45	41	42	38	41	43	39	45	45	38
G	65	60	58	55	54	55	57	58	59	58	56	55	54	52	49	48	46
B	154	154	154	154	154	154	154	154	154	154	154	154	154	154	154	154	154

Figure 6 Smartphone camera system recognition ability on low concentration

1.3 How to improve Smartphone camera detection

I divided the image recognition system into two parts, which is the image acquisition and processing module, to enhance the recognition of low concentration ranges. It is expected that the original 50 ppb detection limit can be raised to a 10-ppb detection limit. As show in this Figure 7. In the image acquisition module, I used a professional OV2640 camera module instead of a mobile phone camera. In the image processing system, I use the STMF407 chip to replace the mobile phone processing system, because the STMF407 has a Digital Camera Interface to effectively increase the speed of image transmission to reduce image display distortion. In the image processing module, I use single colour capture or the green colour interpolation algorithm to get more effective information on each camera pixel.

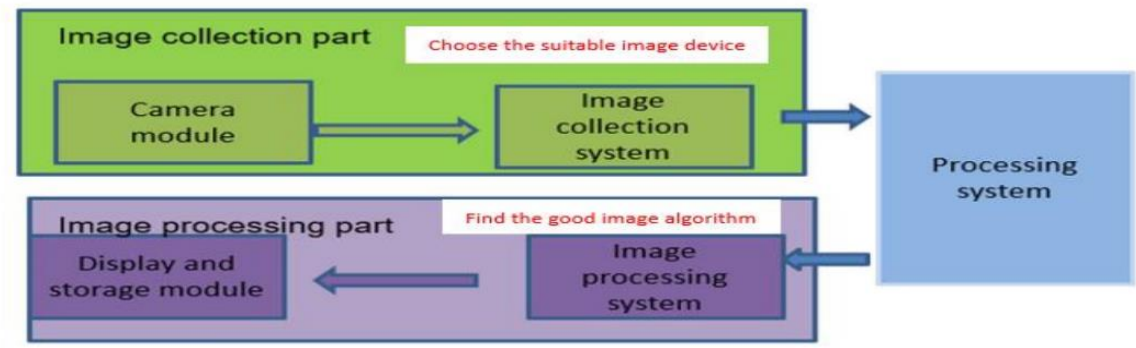

Figure 7 Re-design image recognition system

1.3.1 Image acquisition module

1.3.1.1Bayer format

For colour images, it need to collect a variety of basic colours, such as RGB colours, the easiest way is to use the filter method, the red filter through the red wavelength, the green filter through the green wavelength, The blue filter passes through the blue wavelength. As shown in Figure 8. Bayer format pictures are set in different colours on an algorithm. the RGB values of each pixel must be achieved by interpolation.

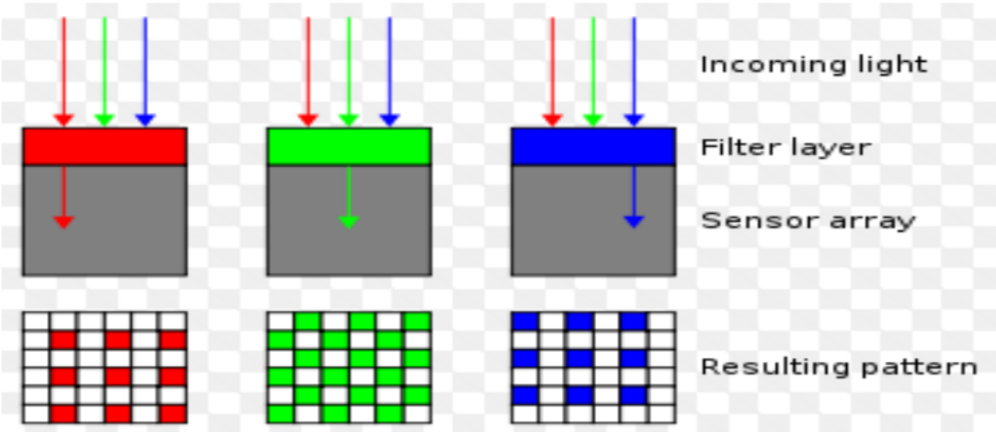

Figure 8 Bayer format on image system

1.3.1.2RGB565 format

The single colour algorithm method can improve triple the effective information in the original image. At present, the RGB acquisition method adopted by the mobile phone camera is in the form of RGB565. The 16-bit valid data is used to save the RGB values of the image. As shown on Figure 12, RED colour has 5 data valid bits, green colour has 6 data valid bits, and blue colour has 5 data valid bits, as show in Figure 9.

It can be found the change on the concentration of the PFAS solution in the image recognition system leads to the most obvious change is the green colour. Image processing system can use all 16 bits of valid data to collect the value of green (light intensity of the green colour).

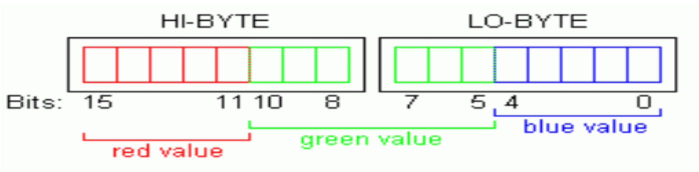

Figure 9 RGB565 format on image system

1.3.1.3YUV 4:2:2 format

In human vision, there are three channels for colour detection, and for many colour systems, three "channels" are enough to represent most colours, such as red, green and blue. In many video systems, the three channels are: luminance and two chrominance channels. In the YUV format, the luminance and chrominance components form a weighted sum of R'G'B' components rather than linear RGB components, as show on Figure 10.

The collection method of YUV 4:2:2 is shown in the Figure 10. The two chrominance components are sampled at half of the luminance sampling rate: the resolution of horizontal chrominance is halved, which reduces the bandwidth of the uncompressed video signal by a third.

Y0	U0	Y1	V0	Y2	U2	Y3	V2	Y4	U4	Y5	V4

Figure 10 YUV 422 format on image system

1.3.2.4 Compared YUV format and RGB format

The RGB format is usually simple: red, green, and blue with a given pixel size. RGB565 is the most common, allowing 16-bit data transmission with a value of 0-255 for each color component. Through image acquisition in RGB format, the RGB value of the solution can be easily obtained and analysed. The problem with RGB, however, is that it does not represent the best mapping of visual perception. The YUV colour space is a more efficient encoding scheme that can reduce more bandwidth than RGB capture. Therefore, most video cards render directly using YUV or brightness/chroma images. The most important component that YUV captures is always the brightness or Y component. Therefore, Y should have the highest sampling rate.

1.3.2 Image processing module

1.3.2.1 Linear algorithm

A linear function is one that is changing at a rate as X changes.

$$Y = AX + B$$

Equation 1 Linear algorithm

1.3.2.2 Exponential algorithm

An exponential function is one that changes at a rate that's always proportional to the value of the function.

$$Y = Be^{AX}$$

Equation 2 Exponential algorithm

1.3.2.3 Polynomial algorithm

A second order polynomial function is one that is changing at a rate as X and X^2changes.

$$Y = AX^2 + BX + C$$

Equation 3 Polynomial algorithm

1.3.2.4 Coefficient of determination

R^2 is a statistic of how close the data is to the fitted regression line. Also is the determination coefficient. The definition of R^2 is simple. Linear model explains the percentage change in response variables: R^2 = current data difference / total difference

Equation 4 Coefficient of determination

R^2 is always between 0 - 100%

When R^2 = 0%, the algorithm does not fit the algorithm to the data. When R^2 = 100%, the algorithm explains all changes in the vicinity of the data. In general, the higher the R^2 will better fit the algorithm to the data.

1.4 Image Parameter configuration

If need to obtain a high-quality image, it needs to adjust not only the image output format of the camera, but also the brightness and contrast of the camera to reduce the impact of external environment such as light noise on the entire image acquisition.

1.4.1 Image brightness

The brightness adjustment is probably the simplest algorithm in the image processing, the image can be brightened or darkened when the brightness of all the pixels is multiplied plus an enhancement factor. As shown in the Table 1, the image performance of the entire FPOA solution collection system under different brightness conditions. As shown in the table 1, the image performance of the entire FPOA solution collection system under different brightness conditions.

Format	**Image brightness: -2**	**Image brightness: 0**	**Image brightness: 2**
RGB565			
YUV422			

Table 1 image brightness effect on image quality

1.4.2 Image contrast

The contrast ratio is the ratio of the picture black and white.the gradient layer from the black to the white. As shown on Table 2. The large is ratio is, the more the gradient layers are and the richer the color performance. The contrast ratio has key impact on the visual effect. Generally, the higher the contrast ratio is, the clearer the image is and the brighter the color is. However, the small contrast ratio will make the whole image grey. High contrast ratio can greatly improve the image definition, detail performance and grey level performance. As shown in the Table 2, the image performance of the entire FPOA solution collection system under different brightness conditions.

Format	**Image brightness : -2**	**Image brightness : 0**	**Image brightness : 2**
RGB565			
YUV422			

Table 2 image contrast effect on image quality

1.4.3 Compared Image brightness and Image contrast configuration

Through the image, it can be found that by adjusting the brightness and contrast of the camera could improve quality of image. That is, more obvious trend changes can be obtained in different colour changes, but when configuring the camera parameters, the brightness should be set first, and then consider the image contrast configuration. Because this can ensure that the colour change is in a normal range (RGB value between 0 to 255), there will be without any distortion.

1.5 Image distortion problem (Digital Camera Interface)

Increasing the display quality or information of an image design green interpolation increases the complexity of the algorithm, as it undoubtedly limits the processing speed of the image processing system. When the processing speed of the image processing system does not reach the scanning speed of the display system, the picture could have some distortion occurs (for example, the scanning speed of the VGA display system is 25 ns) as shown in the Figure 11.

Figure 11 Image distortion problem

In order to solve the problem of image distortion caused by the algorithm. The RGB values of the image acquisition system are generally transmitted through an I2C (Inter-Integrated Circuit). In order to increase the transmission rate of the image acquisition system, an additional digital camera interface is needed to transmit the values of RGB in the image acquisition system to the processing system.

DCMI stands for Digital Camera Interface. (POR P D R.[20])The DCMI interface is used to parallel data port to collect camera image data. The camera generates a parallel data stream and a pixel clock signal (DCMI_PIXCLK) that allows the interface to capture incoming image data. the connection between the micro processing (STMF407) and the camera module (OV2640) required for this design is shown 12. It can be found that when the camera acquires image data, the image data is sent to the digital camera interface, and then transferred to the processing unit by DMA (Direct Memory Access) control. The data transfer by DMA (Direct Memory Access) can obviously improve the processing speed of the image acquisition system.

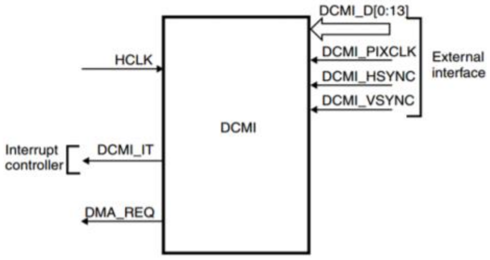

Figure 12 DCMI block diagram

2 Introduction

2.1 Overall system block diagram

2.1.1 System construction environment

The image acquisition system in this paper has three parts, namely ARM image acquisition and recognition system, standard to be tested PFOA solution and airtight acquisition box. As show on Figure 13. Among them, I am mainly responsible for the design of ARM image acquisition and recognition system. J is mainly responsible for the preparation of standard solution to be tested. The primary preparation principle is to mix PFOA with patented reagent so that PFOA can show visible blue. A is mainly responsible for the design of airtight collection boxes. I am focus on the device is mainly able to ensure that the camera module and the solution to be tested are kept at a fixed distance each time the camera acquires images and minimize the influence of external light source on the whole experiment.

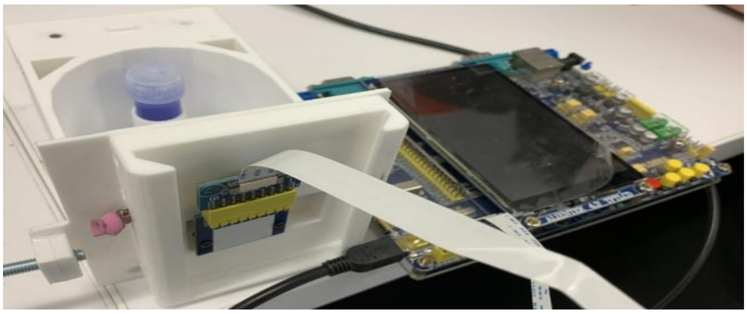

Figure 13 whole system environment

2.1.2 Image acquisition and recognition system

The system hardware part of this paper is mainly composed of four parts, which are acquisition unit, image processing unit, display unit and storage unit. As the most front end of the system, the acquisition unit is mainly utilized the image sensor to complete the acquisition of the original image; Image processing unit is the above all part of the whole image acquisition system, which is mainly used to process the original video image data collected by the front-end image sensor to complete the image acquisition and transmission; As show on Figure 14.The storage unit is the temporary storage of the image data transmitted from the image processing module; Display unit is to display the image information and the image result storage unit is to store whole picture information. The overall system block diagram is shown in the Figure 14.

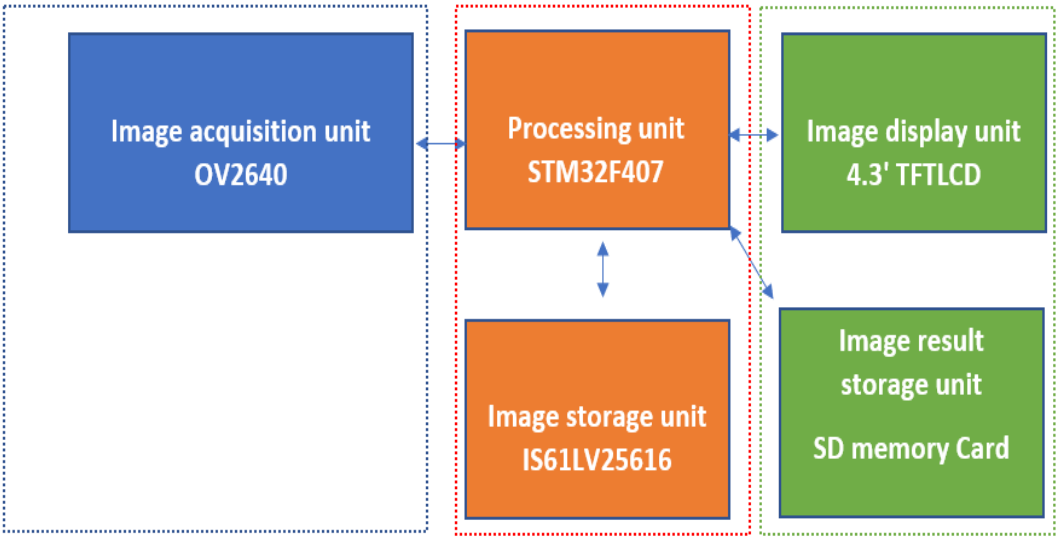

Figure 14 image acquisition and recognition system block diagram

2.2 Image system equipment selection

2.2.1 Processing unit – STM32F407

As the design of image acquisition and transmission system, the selection of processor chip plays a decisive role in the performance of the whole system. At present, there are a variety of ARM chips in the market, which vary greatly in the performance, power consumption, price and processing speed for different application scenarios. Given that the image processing module is the centre of the whole system, and is the core of the whole system in the control module and responsible for the control of the front-end image sensor and the processing of the image data, it is necessary to fully consider the system performance, low power consumption and the scalability of the system when selecting the device of this part. Based on the above considerations, STM32F407ZGT6 chip designed by STMicroelectronics （ST） is selected as the microprocessor of the system.

ST launched STM32F4 series high-performance microcontroller based on ARM; Cortex™ -M4 as a kernel, as shown in the Figure 15, which adopts 90 nm NVM process and ART (Adaptive real-time Memory Accelerator). ART technology makes the program zero-wait execution, improving the efficiency of program execution, and giving full play to the performance of Cortext-M4, so that the STM32 F4 series can reach 168MHz.

Adaptive real-time Memory Accelerator can fully release the performance of cortex-m4 kernel; When the CPU operates at all allowable frequencies (≤168MHz), programs running in flash memory can achieve performance equivalent to zero wait cycles. The STM32F4 series microcontroller integrates single-cycle DSP instruction and FPU (floating point unit), which improves the computing power and can perform some complex calculation and control, including Camera interface, up to 54M bytes /s.

Figure 15 STM32F407 Processing unit layout

2.2.2 Image acquisition unit – OV2640

Image sensor, as the front end of the whole system, is the source of images in the system. Its advantages and disadvantages directly affect the two kinds of image sensors.
the camera image sensor material composition can be divided into CCD and CMOS. The names of CCD and CMOS are related to the materials used for their imaging. CCD is the abbreviation of "Charge Coupled Device", and CMOS is the abbreviation of "Complementary Metal Oxide Semiconductor". By querying the configuration of the phone, it can find that all the mobile phone cameras in this experiment are CMOS cameras. (Litwiller D [13]) The CCD uses a special manufacturing process to create a charge on the chip without distortion.

The CCD camera has a high quality in terms of fidelity and light sensitivity. CMOS chips use a method to process of manufacturing most microprocessors to make cameras. There are some significant differences between CCD and CMOS sensors.As show on Table 3

Category	CMOS	CCD
Cost	Low	High
Production line	General purpose	Dedicated
Radiation resistance	High	Low
Signal to noise ratio	Good	Perfect
Integration status	Monolithic high integration	Low, requires an external chip
Image	Simultaneous read	Sequential scan
Power supply	Single power supply	Multiple power supply
Module size	Small	Large
Circuit structure	Simple	Complicate
Sensitivity	Good	Perfect
Dynamic range	>70dB	>70dB
Blue light sensitivity	High sensitivity	Low sensitivity

Table 3 CCD and CMOS camera different performance

As can be seen from the table, CMOS is better than CCD in terms of cost, integration status, circuit structure and module volume. For a small embedded image acquisition and transmission system, the power consumption, cost and volume of the system should be considered, so CMOS is more suitable than CCD as the image sensor in this design.

The camera module is designed to operate temperature from 0 to 50 degrees The image was captured at a laboratory temperature of 25 degrees. The temperature has on effect on image acquisition during image capture processing.

The sensor is small size and low working voltage, providing all functions of camera and image processor. As shown in the Figure 16, 8-bit image data of various resolutions can be output through SCCB bus control, such as whole frame, sub-sampling, scaling and window fetching. The UXGA image of this product can reach up to 15 frames/second, and the user can fully control the image quality, data format and transmission mode. All image processing functions including gamma curve, white balance, contrast degree and chroma can be programmed through SCCB interface.

Figure 16 OV2640 camera module layout

OmmiVision image sensor applies unique sensor technology to improve image quality and obtain clear and stable colour images by reducing or eliminating optical or electronic defects such as fixed pattern noise, trailing, floating. The features of OV2640 are as follows:

- High sensitivity, low voltage suitable for embedded application standard SCCB interface, compatible with IIC interface;
- Supporting RawRGB, RGB (RGB565), YUV (422) output format;
- Supporting for UXGA, SXGA, SVGA and scaling down to any size from SXGA to 40*30;
- Supporting automatic exposure control, automatic gain control, automatic white balance, automatic elimination of light stripes, automatic black level calibration.
- supporting colour saturation, hue, gamma, sharpness and other settings.
- Supporting image zooming, translation and window setting;
- Supporting image compression, namely output JPEG image data;

2.2.3 Image storage unit - IS61LV25616

This design collects a large amount of image data in the work, which requires a large storage capacity to cache the data. The microcontroller selects STM32F407, and its internal SRAM storage capacity is only 192KB, which cannot meet the requirements of the system, so an external SRAM chip IS62WV51216 is extended.

IS62WV51216 is a high-performance CMOS technology SRAM chip made by ISSI company, with a storage capacity of 8M and consists of four blocks with a size of 2M each as show on Figure 17, taking a short time to complete one storage, up to 8ns at least., which can be connected to the microcontroller via the FSMC (variable static storage controller) bus. FMSC has the following performance advantages:

(1) The FSMC interface of STM32F4 supports many types of static storage including NOR FLASH, NAND FLASH, SRAM.

(2) Multiple types of storage can be expanded simultaneously. Since different Banks are independent of each other, different types of storage can be expanded

(3) FSMC will prevent FSMC bus access conflict by setting the delay time parameter of the bus; flexible data storage operation methods, which not only support asynchronous data read and write operation, but also support SRAM /NAND memory synchronous burst access operation mode.

Figure 17 Storage module layout

2.2.4 Image display unit - 4.3' TFTLCD

TFT-LCD, Thin Film Transistor-Liquid Crystal Display. TFT-LCD is different from the simple matrix of passive TN-LCD and STN-LCD. It has a thin film transistor (TFT) on each pixel of the LCD screen, which can effectively overcome the crosstalk of non-gate, and make the static characteristics of the LCD screen independent of the number of scan lines, thus greatly improving the image quality. As shown on Figure 18

Figure 18 LCD display system layout

2.2.5 SD card memory

Many single chip computer systems need high-capacity storage device for the storage of the data. SD card are the most commonly used. They have their own advantages. Generally, the SD card is the most suitable for single chip system, which can support not only large capacity (32GB above) but also SPI/SDIO drive. In addition, there are different sizes for option (standard SD card size, TF card size), which can meet the requirements of different applications.

The design uses 8G memory card for the storage of image data collected, saves the image in BMP format and JEPG format, reads the image from SD card and displays in LCD. As shown on Figure 19 .SD card is connected to STM32F4 through SDIO interface(secure digital input and output), which can realize the transfer rate of 24M byte per second maximum. At the same time, the built-in FATFS document system in the system software is used for the management of data in SD card. It mainly provides multiple API functions such as f_open, f_read, f_write, f_close in the application layer for users to use and realizes the file read/ write protocol in FATFS module.

Figure 19 SD Card storage module layout

3 Theoretical framework

3.1 Hardware principle

3.1.1 Basic working principle of STM32 GPIO

STM32F407ZGT6 has 7 groups of IO ports, each group of IO ports has 16 IO, a total of 16X7 = 1212 IO. GPIO operation mode can be divided into

- 3 input modes: input pull-up / input pull-down / analog input
- 3 output modes: open drain output / Multiplexing function / push-pull output
- 4 output speeds: 2MHZ/25MHz/50MHz/100MHz

Pull-up and pull-down resistor of M4 is designed by external circuit, so both input and output ports can be pulled up and pulled down by setting. As shown in the Figure 20 is GPIO internal schematic of STM32 divided into two parts which are input module and output module, wherein the input module is passed to the input register through INPUT interface and TTL trigger, and the output module outputs the value of the data register to OUPUT interface through output control module.

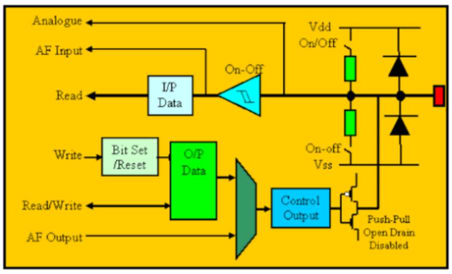

Figure 20 GPIO internal block diagram

3.1.2 Input and output pin settings

Set GPIO before using each pin.as show on Figure 21

1.select the port number that want to set

2. Determine whether the port is an input port or an output port.

3. select the control mode, whether need pull-up or pull-down resistor

4. select the working frequency of the port

5. select the group name of the port to complete port initialization

```
GPIO_InitStructure.GPIO_Pin = GPIO_Pin_9|GPIO_Pin_15;//PG9,15
GPIO_InitStructure.GPIO_Mode = GPIO_Mode_OUT; //output port
GPIO_InitStructure.GPIO_OType = GPIO_OType_PP;//Push-pull
GPIO_InitStructure.GPIO_Speed = GPIO_Speed_50MHz;//100MHz
GPIO_InitStructure.GPIO_PuPd = GPIO_PuPd_UP;//push - up
GPIO_Init(GPIOG, &GPIO_InitStructure);//initialization
```

Figure 21 Input and output pin settings on GPIO

3.2 Software principle

As shown in the Figure 22 is the software design flow chart of PFOA solution identification system. Begins with a new project via KEIL 5 software. KEIL will perform basic I/O configuration according to the chip model selected by the user. Then introduce STM32 support library in KEIL 5, the main aim of introducing library files is to simplify GPIO initialization. When the program design is completed without any error, FLYMcu software generates HEX file that STM407 processor can recognize and download HEX file to STM407 processor.

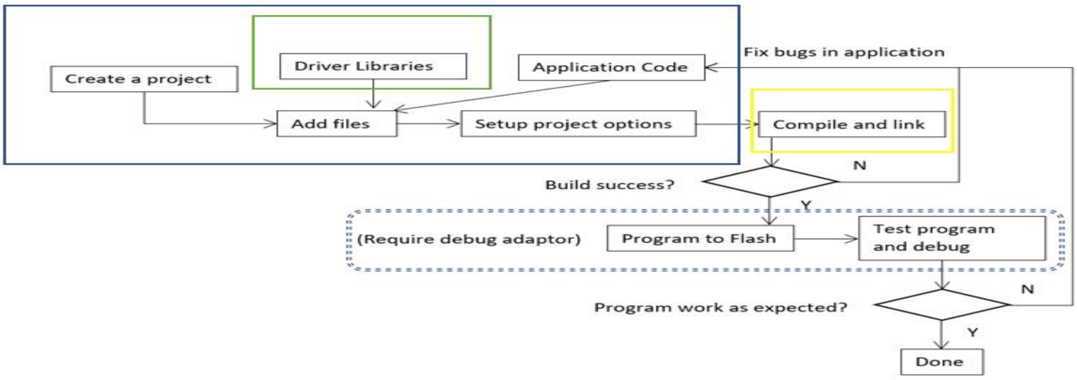

Figure 22 software design and build flow

3.2.1 KEIL5 development kit

This design software development is based on MDK development platform development, it is an embedded development tool for ARM launched by KEIL of Germany. For cortex-m core processor, it is the best development tool and is used by most embedded development engineers all over the world. The latest release from KEIL is MDK5.10, which uses the uVision5 IDE integrated development environment as show on Figure 23.

Vision5 IDE interface integrates powerful project manager, editor and MAKE tools, integrated tools including debugger, C/C + + compilers, macro assemblers, software simulator and link locator. Vision5 IDE working main interface, composed of the toolbar, menu bar, multiple window, status bar, and dialog box and so on, of which, the menu bar and toolbar mainly realize fast operation commands, the project workspace is used to manage files, the output window is used as the interactive window of debugging commands and the display compilation information search keyword results, and the workspace is mainly used for code editing.

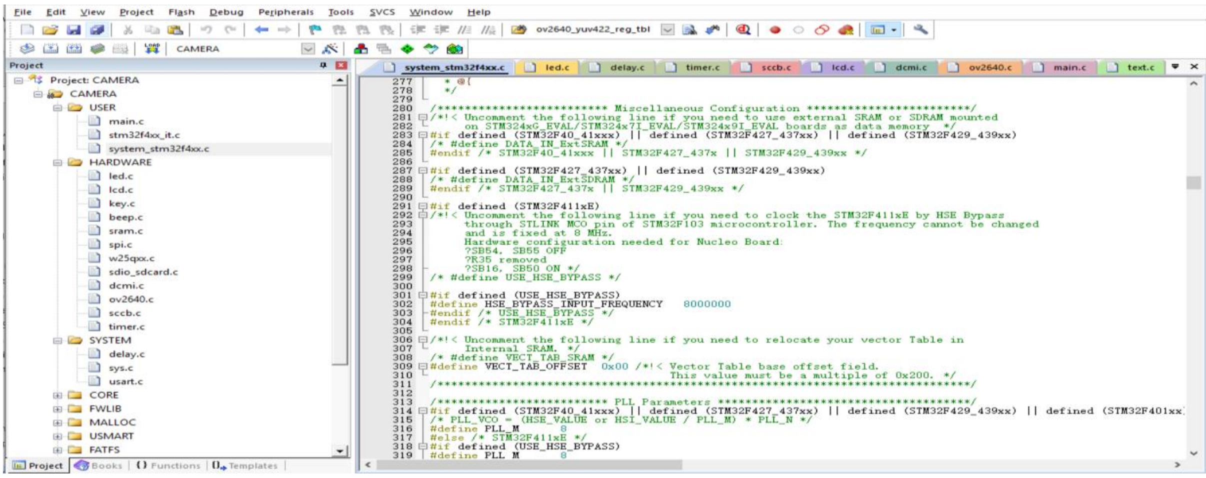

Figure 23 KEIL 5 development software kit

3.2.2 Software design library function support

In the development of SCM, Software design library function support directly operates registers. For example, to control the status of some IO ports, which can be controlled by directly operating registers.

the disadvantage of direct operation of registers is that STM32 can only be used correctly if know how to use each register, and it is not easy to memorize hundreds of registers for a MCU of the STM32 level. ST(stmicroelectronics) then launched its official firmware library, which encapsulates the underlying operations of these registers and provides a complete set of interfaces (apis) for developers to call. Firmware library is a collection of functions, whose function is responsible for dealing directly with registers down and providing the interface (API) for user function calls up.

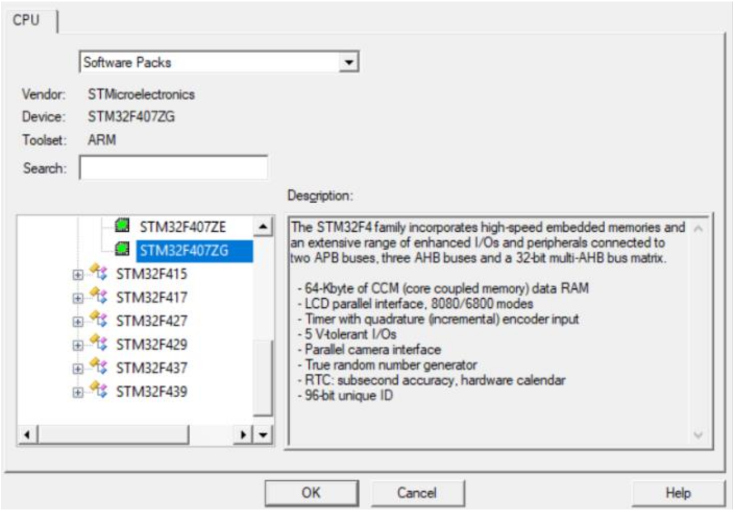

Figure 24 Software design library support

The math.h header defines various mathematical functions. All the functions available in this library take double and return double as the result. In this design, the math library function is used to calculate and analyse the exponential function (EXP) based on the STM407 processing system.

3.2.3 Download software – FlyMcu

Flymcu is the practical and the latest stm32 serial program software, which can help users connect the serial used in the communication, facilitate the program and support programming, verification and read device information. The continuous program mode can be used. The eagleIAP application program can be programmed through IAP and IAP guide program and application program can be programmed through ISP. It is very suitable for professional single chip computer developer. The software can be widely applied in In Circuit Programming (ICP) and In-Application Programming (IAP) field.

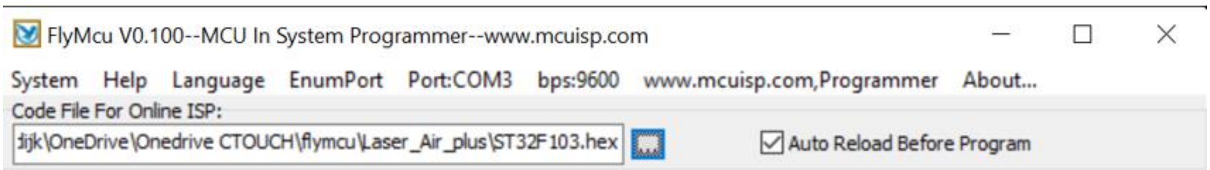

Figure 25 FlyMcu – Download software

4. Hardware Connection

4.1 LCD hardware connection

TFTLCD module adopts 16 bit parallel mode to connect with the external part as shown in the Figure 26.

CS： TFTLCD chip selects the signal

WR： write date in TFTLCD

RD： read data from TFTLCD

D[15：0]： 16 bits two-way data wire

RST： Reset TFTLCD

RS： Command / data label(（0 read/write command, 1 data read and write）

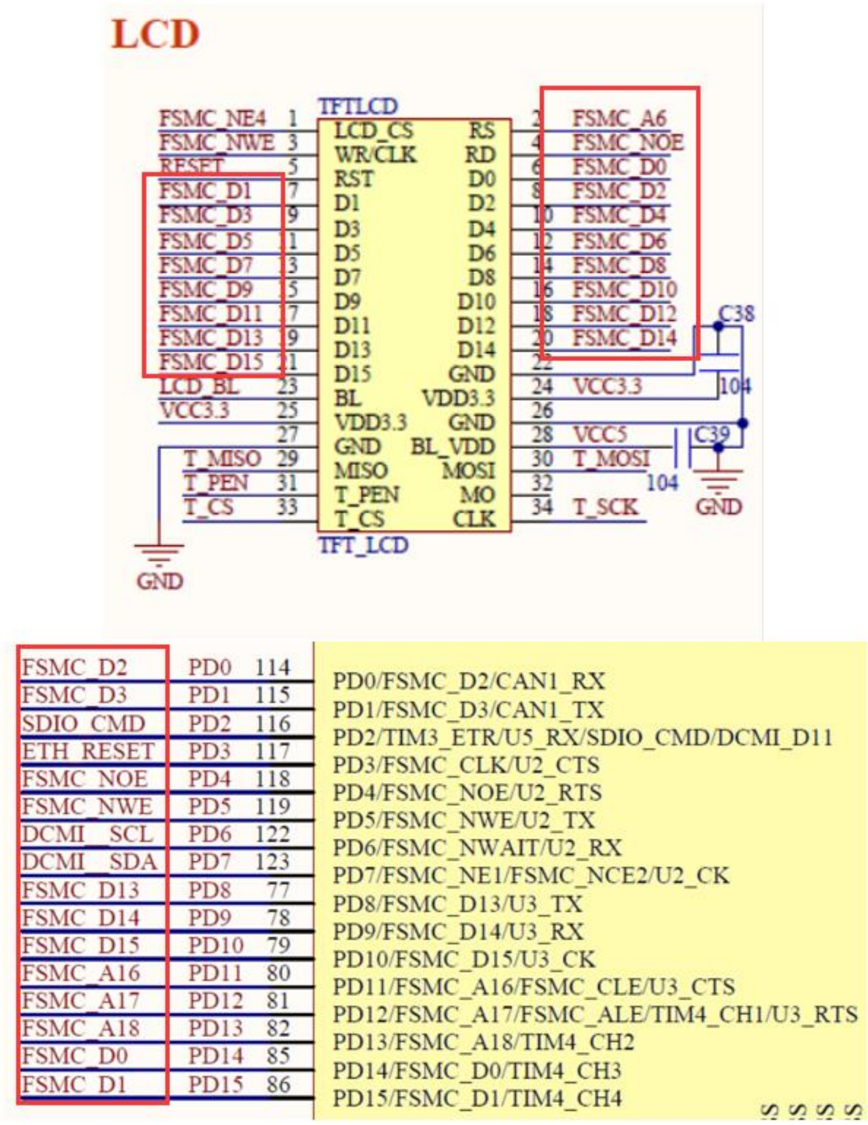

Figure 26 LCD display module Schematic diagram

4.2 SD Card module hardware connection

The STM32F407 development board is connected to the SD card through the SD card interface. The hardware connection schematic as show on Figure 27

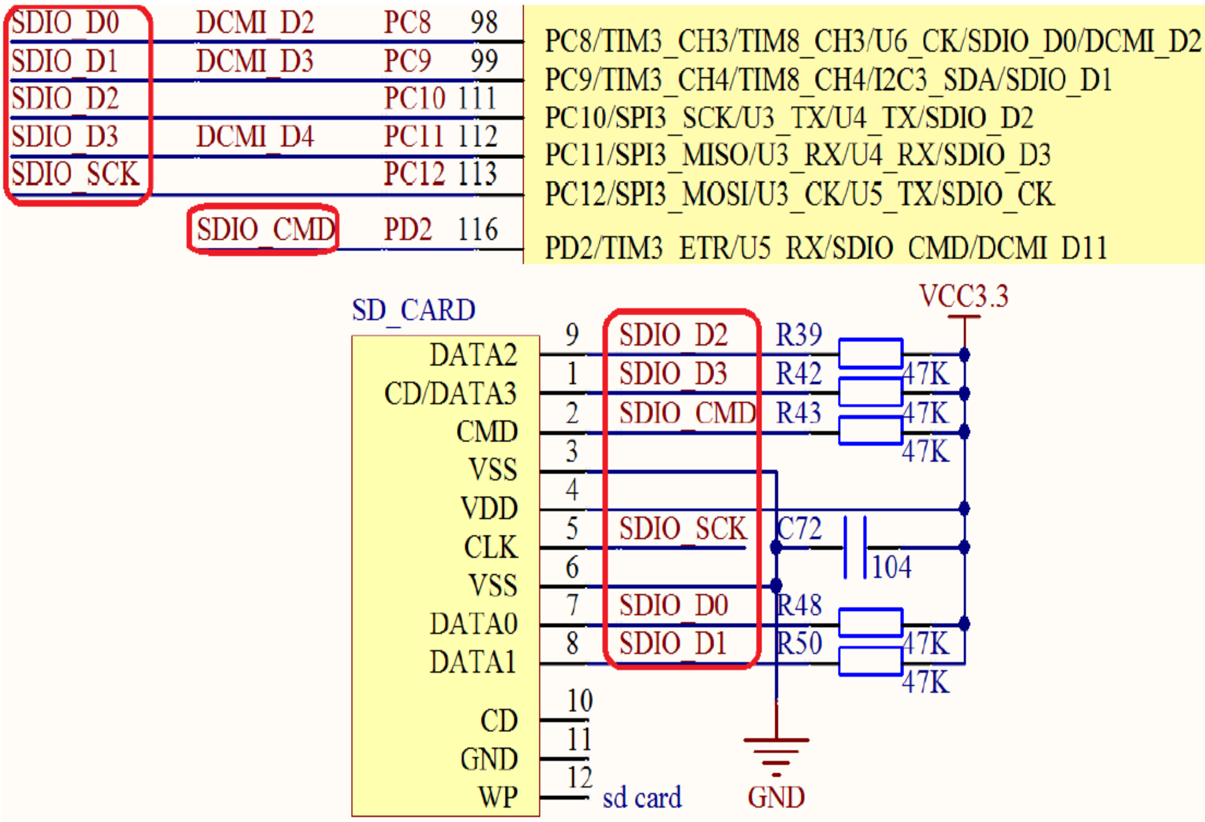

Figure 27 SD Card module Schematic diagram

4.3 KEY button hardware connection

KEY0 on the development board STM32F4 is connected to PE4, KEY1 is connected to PE3, KEY2 is connected to PE2, KEY_UP is connected to PA0 as shown in the Figure 28.

KEY0, KEY1 and KEY2 are valid low level while KEY_UP is valid high level. There is no pullup and pulldown resistance. Therefore, we need to set pullup and pulldown resistance in the internal STM32F4.

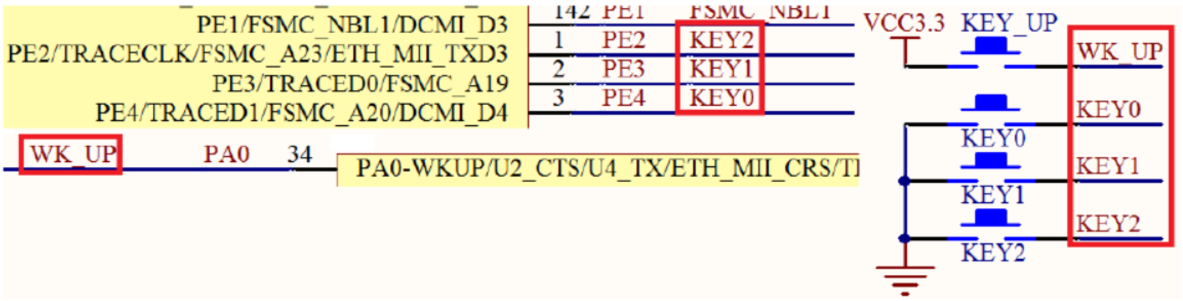

Figure 28 key button Schematic diagram

4.4 SDRAM storage module hardware connection

The stm32f407 development board uses the IS62WV51216 chip packed by TSOP44. This chip is directly connected to STM32F4 FSMC. The IS62WV51216 schematic diagram is shown in the Figure 29.

The connection relation of IS62WV51216 and STM32F4 can be seen from the schematic diagram.

A[0:18] is connected to FMSC_A[0:18]

D [0:15] is connected to FSMC_D[0:15]

UB is connected to FSMC_NBL1

LB is connected to FSMC_NBL0

OE is connected to FSMC_OE

WE is connected to FSMC_WE

CS is connected to FSMC_NE3

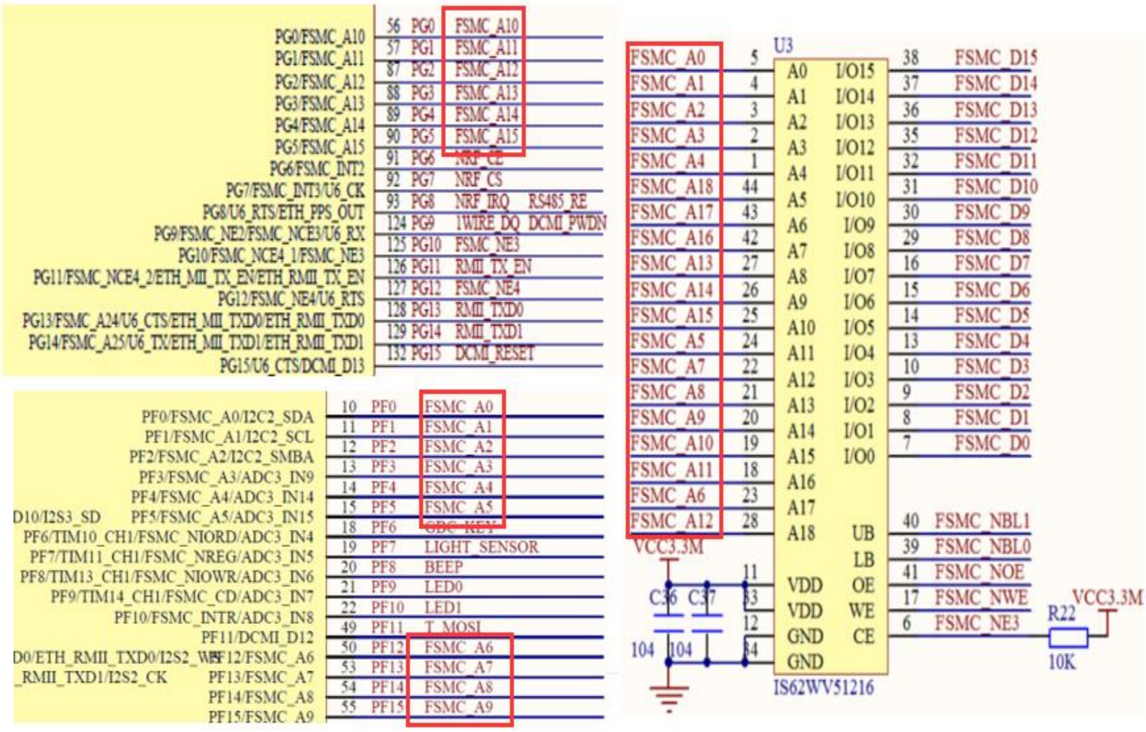

Figure 29 SDRAM storage module Schematic diagram

4.5 OV2640 camera module hardware connection

Camera module schematic diagram is shown in the Figure 30.

Module is connected to the external communication through a 2*9 dual row pin header（P1）and is connected to the external communication signal as shown in the Figure.

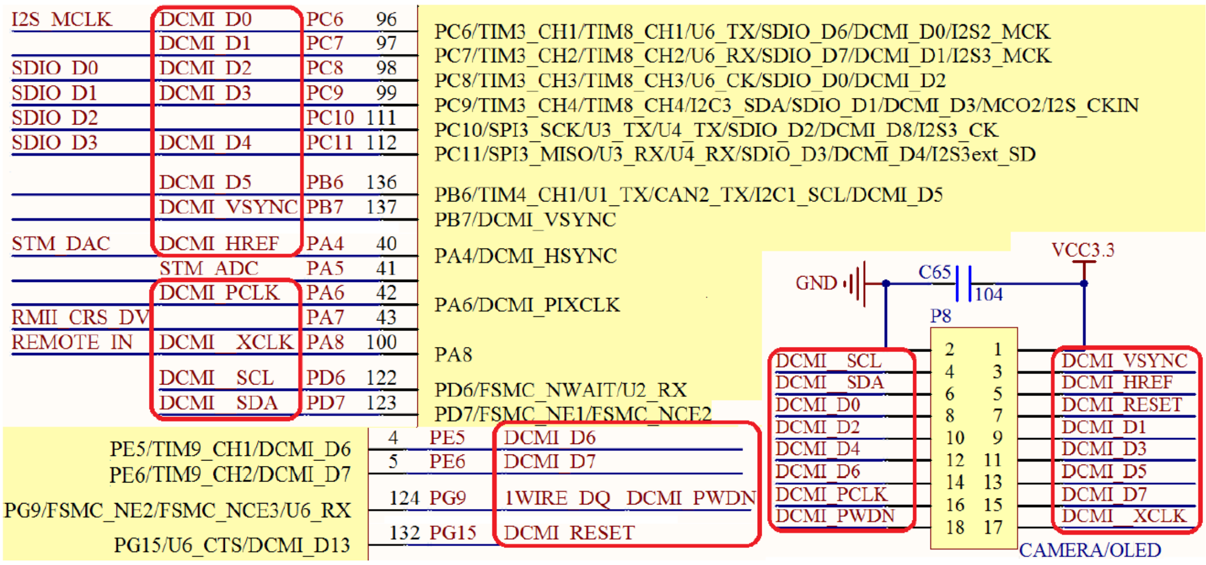

Figure 30 OV2640 Camera module Schematic diagram

5. System equipment working principle

5.1 LCD display module

Module LCD display port read/write process is as show on Figure 31 and 32

1. Set RS high(data)/low(command) according to the data type to write and read.
2. the chip select is pulled down and LCD module is selected.
3. Set RD/WR low according to the data read or data write.
    - Data read: read the data of the data line（D[15:0]）along the rising edge of RD.
    - Data write: Write the data into LCD module along the rising edge of WR.

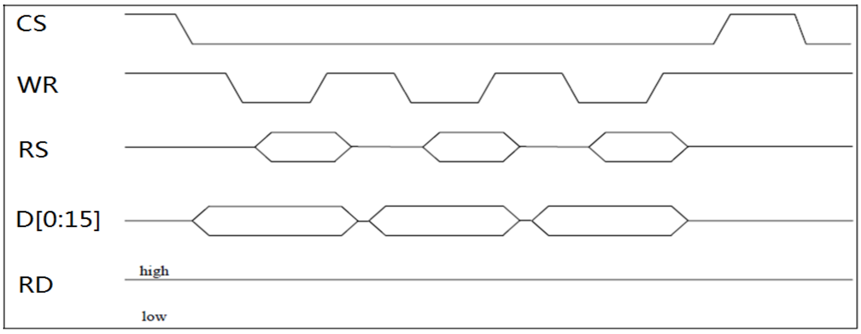

Figure 31Timing sequence write of the parallel port

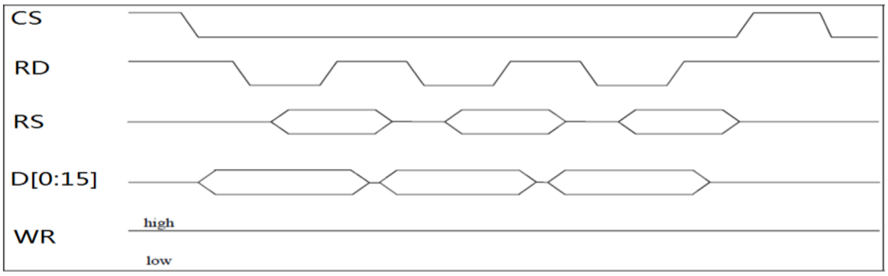

Figure 32 Timing sequence read of the parallel port

5.1.1 LCD read and write command

5.1.1.1 Read ID command

0XD3 is used to read ID of LCD controller. This command is shown in the Table 4. It can be seen from the table that the last two parameters is read to be 0X41. The LCD drive used in this experiment is type 41.

Order	Control			Description									HEX
	RS	RD	WR	D15~D18	D7	D6	D5	D4	D3	D2	D1	D0	
Command	0	1	↑	××	1	1	0	1	0	0	1	1	D3H
parameter 1	1	↑	1	××	0	1	0	0	0	0	0	1	41H

Table 4 LCD Read ID command

5.1.1.2 Control read/write direction command

0X36 to control the read/write direction of ILI9341 memory.

0X36 command is followed by a parameter.it can control the all scanning direction of the whole ILI9341 through the setting of MY, MX and MV, as show on Table 5

If LCD scanning direction is set from the left to the right and from up to down, it only needs to set the coordinate once and then fill the colour data into LCD. In this way, it can greatly improve the display speed.

Control			LCD scan direction (GRAM Self-increasing mode)
MY	MX	MV	
0	0	0	From left to right, from up to down.
1	0	0	From left to right, from down to up.
0	1	0	From right to left, from up to down.
1	1	0	From right to left, from down to up.

Table 5 LCD control write/read direction command

5.1.1.3 Column address setting command

0X2A, column address setting command, with scanning mode from left to right and from up to down. This command is used to set the horizontal ordinate (the x coordinate), as show on Table 6. This command is used for x coordinate setting in default scanning mode. This command has four parameters, 2 coordinate values, SC and EC, the starting value and ending value of column address.

Order	Control			Description									HEX
	RS	RD	WR	D15~D18	D7	D6	D5	D4	D3	D2	D1	D0	
Command	0	1	↑	××	0	0	1	0	1	0	1	0	2AH
Parameter 1	1	1	↑	××	SC15	SC14	SC13	SC12	SC11	SC10	SC9	SC8	SC
Parameter 2	1	1	↑	××	SC7	SC6	SC5	SC4	SC3	SC2	SC1	SC0	
Parameter 3	1	1	↑	××	EC15	EC14	EC13	EC12	EC11	EC10	EC9	EC8	EC
Parameter 4	1	1	↑	××	EC7	EC6	EC5	EC4	EC3	EC2	EC1	EC0	

Table 6 LCD column address setting command

5.1.1.4 Page address setting command

Command: 0X2B, page address setting command, with the scanning mode from left to right and from up to down.

This command is used for y coordinate setting in the default scanning mode. This command has four parameters actually 2 coordinate values, SP, EP.the starting value and ending value of the page address.

Order	Control			Description									HEX
	RS	RD	WR	D15~D18	D7	D6	D5	D4	D3	D2	D1	D0	
Command	0	1	↑	××	0	0	1	0	1	0	1	0	2BH
Parameter 1	1	1	↑	××	SP15	SP14	SP13	SP12	SP11	SP10	SP9	SP8	SP
Parameter 2	1	1	↑	××	SP7	SP6	SP5	SP4	SP3	SP2	SP1	SP0	
Parameter 3	1	1	↑	××	EP15	EP14	EP13	EP12	EP11	EP10	EP9	EP8	EP
Parameter 4	1	1	↑	××	EP7	EP6	EP5	EP4	EP3	EP2	EP1	EP0	

Table 7 LCD Page address setting command

5.1.1.5 Write colour command

0X2C, this command is to write GRAM command. We can write colour data into GRAM LCD after sending this command. This command supports continuous write.

It can be seen from the table that the data valid bit wide becomes 16 bits after receiving command 0X2C. We can continuously write LCD GRAM value. However, GRAM address will be increased according to the scanning direction of MY/MX/MV setting. There is no need to reset the coordinate, thus greatly improving the write speed.

Order	Control			Description									HEX
	RS	RD	WR	D15~D18	D7	D6	D5	D4	D3	D2	D1	D0	
Command	0	1	↑	××	0	0	1	0	1	1	0	0	2CH
Parameter 1	1	1	↑	D1 [15:0]									××
... ...	1	1	↑	D2 [15:0]									××
Parameter n	1	1	↑	Dn [15:0]									××

Table 8 LCD Write colour command

5.2 OV2640 Image module

5.2.1 OV2640 Introduction

Micro controller STM32F407 drives the image sensor OV2640 for the collection of image data through DCMI (Digital Camera Interface). This interface is the fast camera interface for STM32F407 series chip by ST company. It can receive the 8 bit fast data flow sent from external CMOS image sensor and is a synchronous parallel interface supporting the different data formats of YCbCr4:2:2/RGB565 line-by-line video.

STM407 chip relates to OV2640 data signal through DCMI interface as shown in the Figure 33. DCMI DMA request is reflected in DMA2 Channel 1 data flow 1.

There are four different signals in the DCMI interface.

1. 14 bit data input. This design uses 14 bit data format and is mainly used to receive output value of the image sensor.
2. Receive PDCCLK of the image sensor PCLK signal.
3. Receive HSYNC of image sensor HSYNC/HREF signal
4. Receive the VSYNC of image sensor VSYNC.

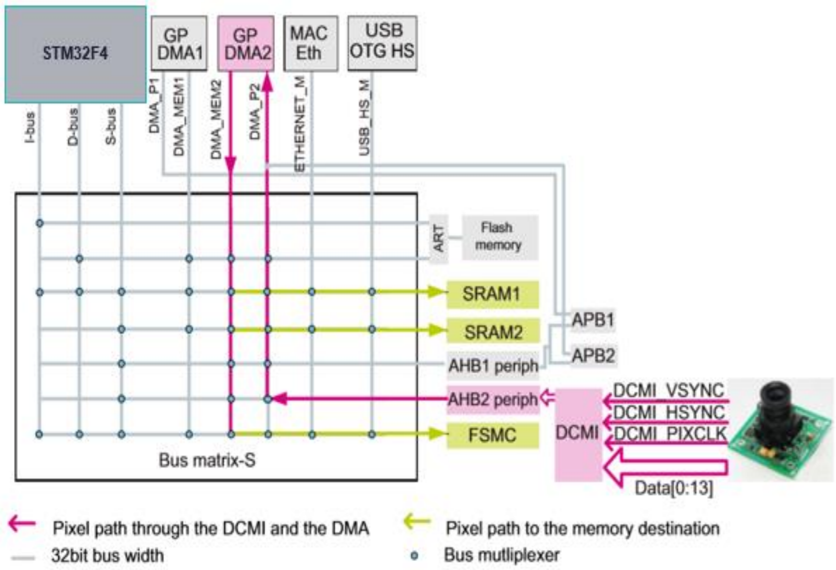

Figure 33 DCMI connection between OV2640 and DMA

DCMI can receive 54MB/S data flow maximum and stores the image data through a 32-bits DCMI_DR in DMA transmission data. The image buffer is managed by DMA not DCMI interface. The received data can be organized according to line/frame. Data flow synchronization can be achieved through the built-in sync code or HSYNC signal or VSYNC signal hardware.

5.2.2 Initialization image sensor

SCCB bus timing sequence analysis

Image sensor OV2640 visits and sets the storage through SCCB bus timing sequence and finally achieves the control for output image. Therefore, SCCB bus programming should be realized first. Two-wire mode SCCB bus and I2C bus share the similar bus protocol.

Data input/output and clock input of the two-wire SCCB bus are respectively data line SIO_D and clock line SIO_C. They complete the SCCB bus function through the coordination of SIO_D and SIO_C. Data line write the parameter needs to be set into the corresponding storage or read the needed date from the corresponding storage according to SCCB bus protocol. Timing sequence of SCCB bus is shown in the Figure 34.

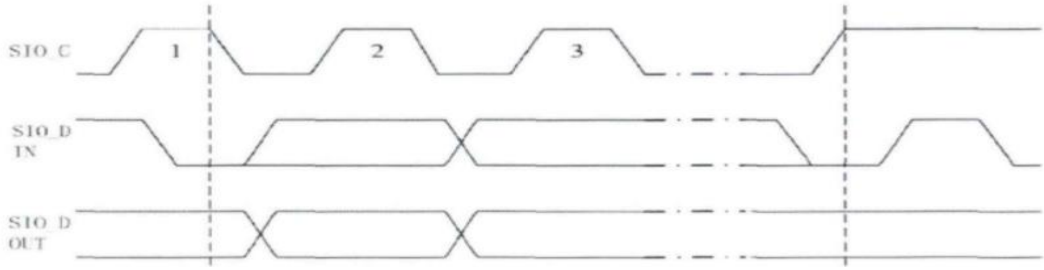

Figure 34 SCCB Clock timing diagram

SCCB is divided into two phrases or three phrases according to different read/write statuses. It is divided into three phrases when we need to write data from STMF407 controller to OV2640. It needs two signals when OV2640 returns data to STMF407. Each phrase has 9 data bits, including 8 sequence data transmission and the 9th bit invalid bit. The maximum valid bit （MSB） is always in the first place of each phrase as shown in the Figure 35.

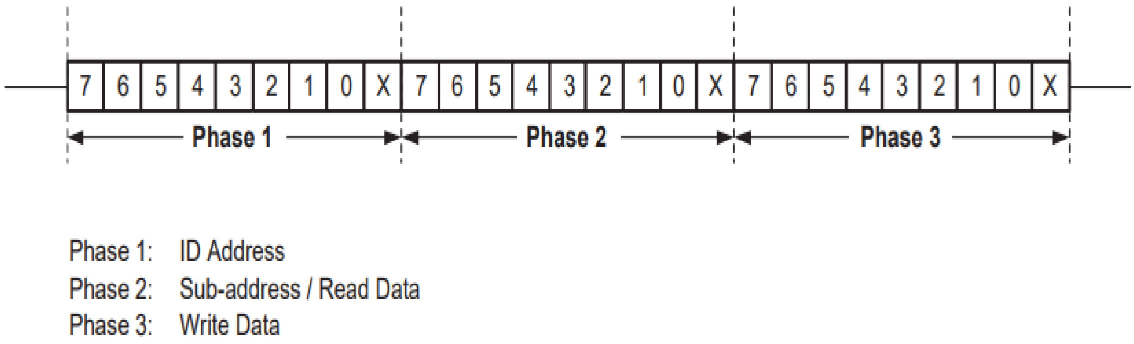

Figure 35 SCCB Command read/write statuses

5.2.3 Image output quality control

The resolution ratio of the image sensor OV2640 in this design is 200W. The image output format setting mainly includes the setting of four parts, respectively sensor window setting, image size setting, image window setting and image output size setting. These four parts can be realized by transferring related functions. These settings are eventually displayed on LCD after the completion of setting. As shown on Figure 36

The sensor window is set through the configuration of OV2640 storage through OV2640_Window_Set function. The storage for configuration is OXO3/OX19/0X1A/OXO7/OX17/OX18.

Image size should not be greater than the sensor window size. It needs the configuration of 0XC0/0XC1/0X8C. The function setting image size, also the output resolution of the selected format, such as UXGA:1600*1200.

Image window setting, i.e., setting image window size. The window size shall not exceed the image size in the previous setting. It needs the configuration of related storage of 0X51/0X52/0X53/0X54/0X55/0X57 .

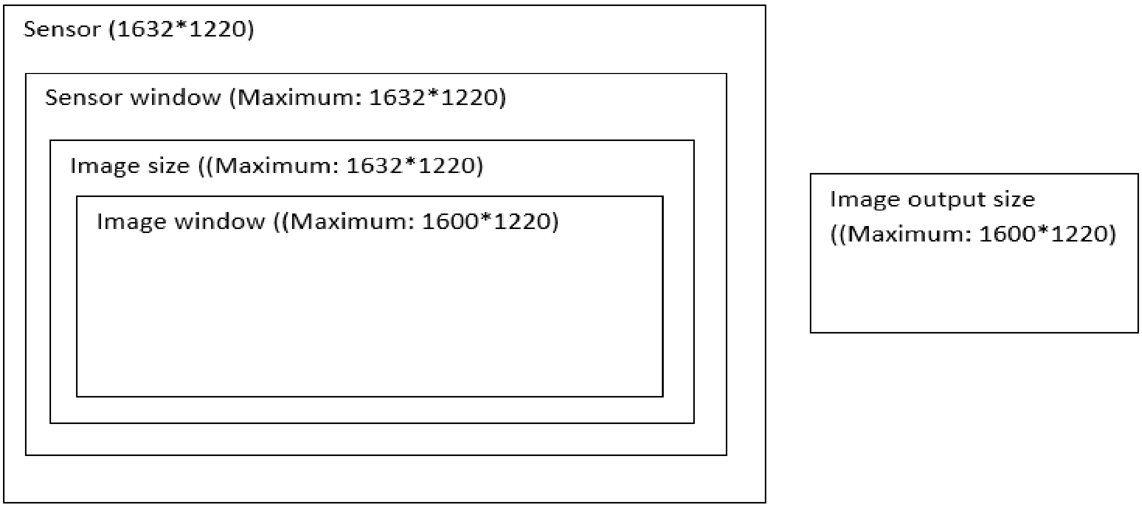

Figure 36 image window setting and output quality control

5.2.4 Image output timing sequence

OV2640 image data format design includes RGB565 and JPEG output mode. Image data output is carried out under the control PCLK(pixel clock, one or half pixel in one cycle), VSYNC and HREF/ HSYNC. The line output timing sequence of OV2640 is shown in the Figure 37.

There will be image data when HREF is high. At this time, there will be 8 bit data of each PCLK . Each PCLK outputs one bit data because the DCMI interface of this design uses 8 bit data mode.

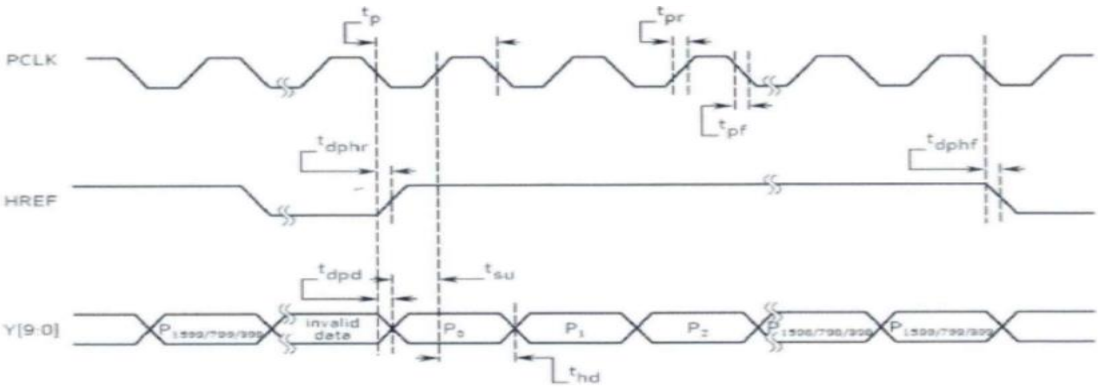

Figure 37 Image module output clock timing diagram

6.Software design

This chapter mainly introduces the software design of the system, which is also one of the most important components of the whole image acquisition system design. The software design is divided into three parts: image acquisition module, image processing module and image transmission module. It is expounded from the aspects of system development software environment, image sensor initialization, collection module and transmission module program design. The design process of system software is shown on Figure 38.

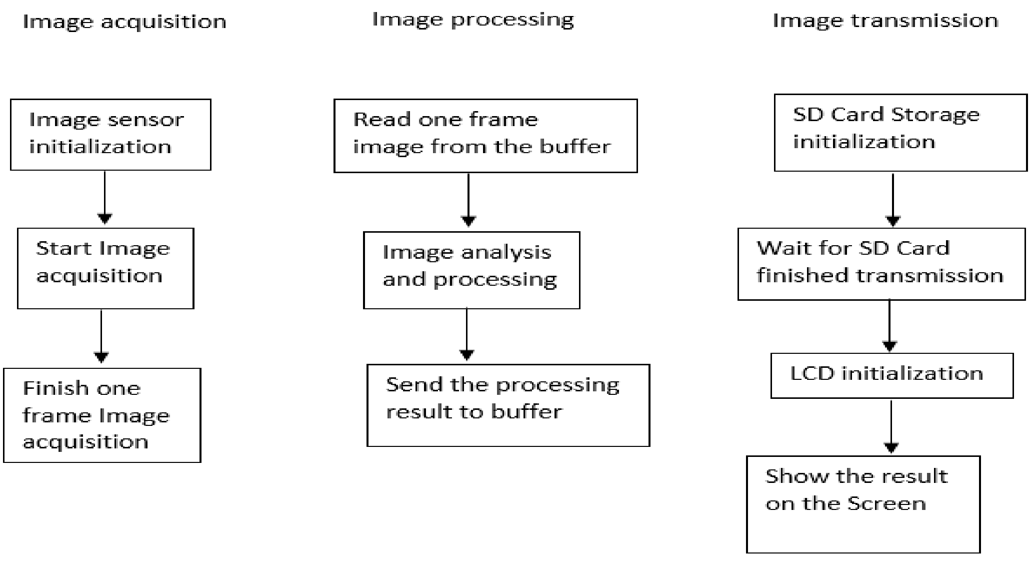

Figure 38 whole system design flow chart

As shown in the Figure 39 is the block diagram of PFOA solution image recognition system, including a camera module, a memory management module, LCD display module, and SD Card storage module. I2C communication command is designed in the camera module to conFigure the register parameters of the camera module. Pixel output reads the output pixel of the camera module according to a certain timing, and finally outputs it to the memory management module through DCMI interface. After receiving the acquisition signal of the camera module, memory management module sends the collected signal to LCD display system and SD card storage system according to the interrupt management principle.

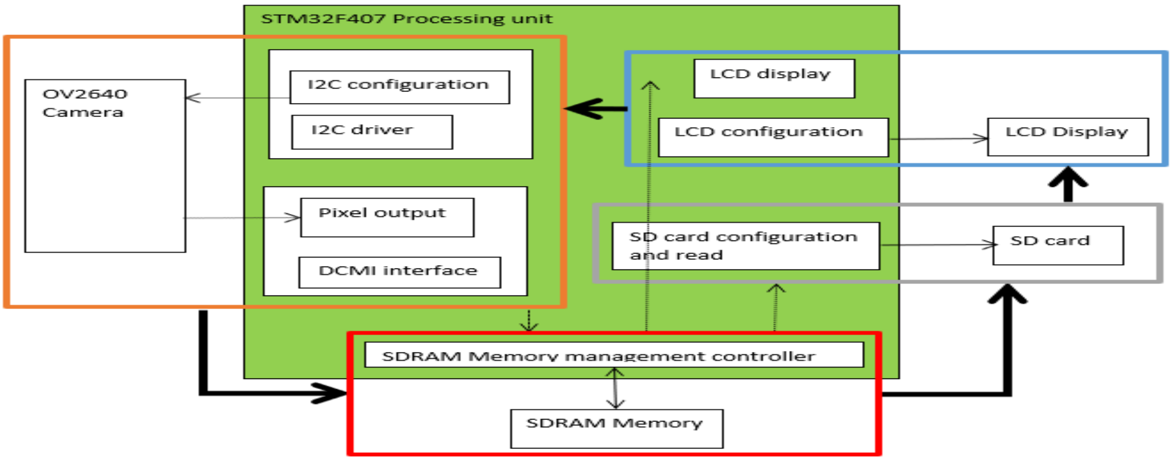

Figure 39 whole system block diagram

6.1 Display system design

6.1.1 LCD design flow chart

The flow chart of this LCD display program is shown below. LCD must be reset and initialized before use. The initialization sequence is provided by LCD manufacturer. As shown on Figure 40

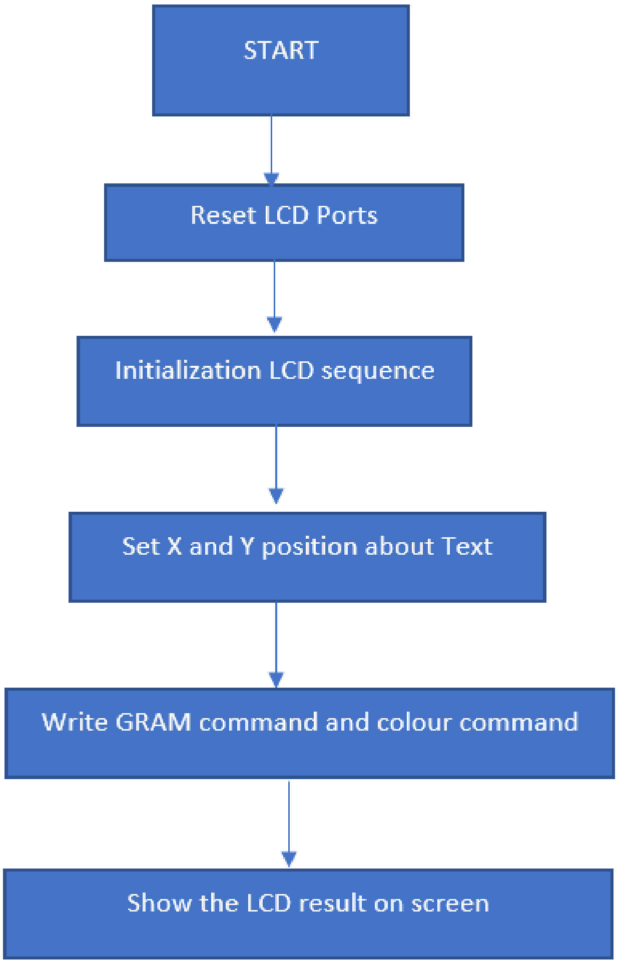

Figure 40 LCD display module design flow chart

6.1.2 LCD internal address structure

LCD instructions are divided into two types which are write register function and a write data function according to the LCD instruction list.

When write register function is required, RS =0.

when write data function is required, RS=1.

According to the hardware circuit, RS port of the LCD is connected to A10 interface of the STMF407 board. (Ref: 4.1 LCD Hardware connection)

LCD_BASE is determined according to the connection of external circuits, such as Bank1.sector4 is start from address 0X6C000000, and 0X000007FE is the offset of A10.. Write 3E with binary: 11 1110, and for 16-bit data, the address is shifted to the right by one bit, corresponding to the address pin, which is: A10: A0=000 0011 1111

At this time, A6 is 0, but if the 16-bit address is incremented by 1 which is 3E+0X01

A10: A0=000 0010 0000, A6 is 1,

which achieves the control of 0 and 1 of RS.

Change this address to LCD_TypeDef structure address,

the address of LCD->LCD_REG is 0X6C00, 003E, the corresponding state to A6 is 0 (RS=0).

the address of LCD->LCD_RAM is 0X6C00, 003F, corresponding state to A10 is 1

(RS = 1).

6.1.3 LCD Initialization flow chart

As shown in the Figure, it is a flowchart of LCD initialization. One of them consists of six parts. The LCD initialization code can be conFigured according to the official configuration, it need not to make any change.

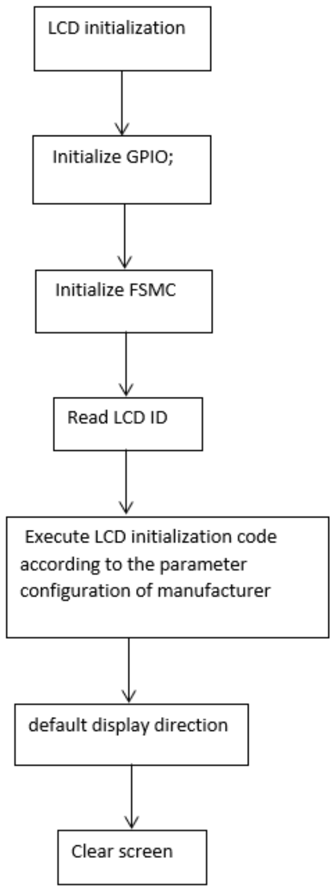

Figure 41 LCD initialization flow chart

6.1.4 LCD library support

As shown in the Figure 42 is the font for LCD display characters in this design. These include the commonly used numbers 0 – 9 and commonly used letters A – Z to meet the basic display requirements and provide portability for the transplant of the entire display interface.

```
const unsigned char asc2_1206[95][12]={
{0x00,0x00,0x00,0x00,0x00,0x00,0x00,0x00,0x00,0x00,0x00,0x00},/*" ",0*/
{0x00,0x00,0x00,0x00,0x3F,0x40,0x00,0x00,0x00,0x00,0x00,0x00},/*"!",1*/
{0x00,0x00,0x30,0x00,0x40,0x00,0x30,0x00,0x40,0x00,0x00,0x00},/*""",2*/
{0x09,0x00,0x0B,0xC0,0x3D,0x00,0x0B,0xC0,0x3D,0x00,0x09,0x00},/*"#",3*/
{0x18,0xC0,0x24,0x40,0x7F,0xE0,0x22,0x40,0x31,0x80,0x00,0x00},/*"$",4*/
{0x18,0x00,0x24,0xC0,0x1B,0x00,0x0D,0x80,0x32,0x40,0x01,0x80},/*"%",5*/
{0x03,0x80,0x1C,0x40,0x27,0x40,0x1C,0x80,0x07,0x40,0x00,0x40},/*"&",6*/
{0x10,0x00,0x60,0x00,0x00,0x00,0x00,0x00,0x00,0x00,0x00,0x00},/*"'",7*/
{0x00,0x00,0x00,0x00,0x00,0x00,0x1F,0x80,0x20,0x40,0x40,0x20},/*"(",8*/
{0x00,0x00,0x40,0x20,0x20,0x40,0x1F,0x80,0x00,0x00,0x00,0x00},/*")",9*/
{0x09,0x00,0x06,0x00,0x1F,0x80,0x06,0x00,0x09,0x00,0x00,0x00},/*"*",10*/
{0x04,0x00,0x04,0x00,0x3F,0x80,0x04,0x00,0x04,0x00,0x00,0x00},/*"+",11*/
{0x00,0x10,0x00,0x60,0x00,0x00,0x00,0x00,0x00,0x00,0x00,0x00},/*",",12*/
{0x04,0x00,0x04,0x00,0x04,0x00,0x04,0x00,0x04,0x00,0x00,0x00},/*"-",13*/
{0x00,0x00,0x00,0x40,0x00,0x00,0x00,0x00,0x00,0x00,0x00,0x00},/*".",14*/
{0x00,0x20,0x01,0xC0,0x06,0x00,0x38,0x00,0x40,0x00,0x00,0x00},/*"/",15*/
{0x1F,0x80,0x20,0x40,0x20,0x40,0x20,0x40,0x1F,0x80,0x00,0x00},/*"0",16*/
{0x00,0x00,0x10,0x40,0x3F,0xC0,0x00,0x40,0x00,0x00,0x00,0x00},/*"1",17*/
{0x18,0xC0,0x21,0x40,0x22,0x40,0x24,0x40,0x18,0x40,0x00,0x00},/*"2",18*/
{0x10,0x80,0x20,0x40,0x24,0x40,0x24,0x40,0x1B,0x80,0x00,0x00},/*"3",19*/
{0x02,0x00,0x0D,0x00,0x11,0x00,0x3F,0xC0,0x01,0x40,0x00,0x00},/*"4",20*/
{0x3C,0x80,0x24,0x40,0x24,0x40,0x24,0x40,0x23,0x80,0x00,0x00},/*"5",21*/
{0x1F,0x80,0x24,0x40,0x24,0x40,0x34,0x40,0x03,0x80,0x00,0x00},/*"6",22*/
```

Figure 42 LCD text work library support

As shown in the Figure 43 is the LCD font generation software used in this design. The software name is PCtoLCD2002.

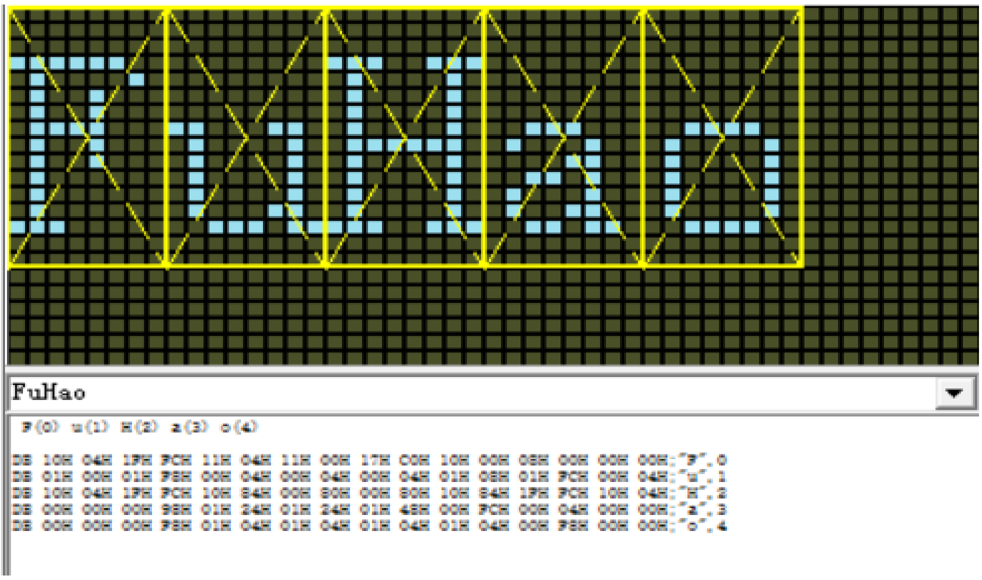

Figure 43 LCD font library generation software

6.2 Keyboard input system design

KEY_Scan function is used to scan whether the 4 IO ports is pressed or not.

KEY_Scan function supports two scanning methods.

Set mode parameter. When mode is 0,

When mode is 0 ,KEY_Scan function will not support continuous pressing, when scanning a key, the button must be released after pressing in order to trigger the second time, otherwise it will not respond to this key, the advantage is that it can prevent multiple triggers once, the disadvantage is that it is not suitable when key need to press and hold.

When mode is 1, KEY_Scan function will support continuous pressing. If a key is pressed all the time, it will always return the key value, which can easily achieve long press detection.

6.3 Camera module design

6.3.1 SCCB configuration·

Due to the description of SCCB timing diagram, the following functions are written to implement the initialization and related settings of SCCB bus.

SCCB Strat signal

The function of SCCB_Start(void) is to start SCCB bus. As seen from the SCCB timing diagram, SCCB start signal is when the clock signal is high-level, and the data line is trending from high level to low level.

SCCB Stop signal

The function of SCCB_Stop(void) is used to implement the abort data transmission. When the clock is at high level, the data line transitions from low level to the off level, which is SCCB stop signal. In idle state, SDA and SCL are both high level.

SCCB Write data function

SCCB_WR_Byte(u8   dat) function is data write function, which is microcontroller writes one byte of data to OV2640 through the SCCB bus.

SCCB Read data function

The SCCB_RD_Byte(void) function is a data read function that is used by the microcontroller to OV2640 camera module to reads one byte of data.

SCCB Write register function

SCCB_WR_Reg(u8   dat) function is register write function, which is microcontroller writes one byte of data to OV2640 through the SCCB bus.

SCCB Read register function

The SCCB_RD_Reg(void) function is a d register read function that is used by the microcontroller to OV2640 camera module to reads one byte of data.

Through the above eight functions, the SCCB bus can access the image sensor and conFigure its corresponding register and control the output image.

6.3.2 OV2640 camera module initialization

When the programming of the SCCB bus is completed, the OV2640 initialization setting can be performed by function. The entire initialization flow chart is shown 44.

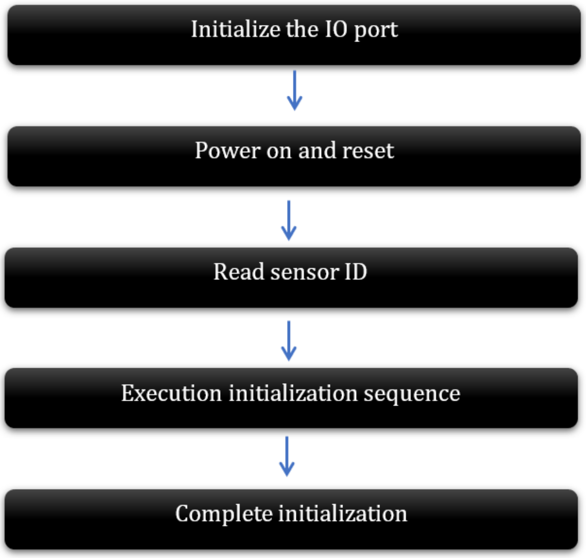

Figure 44 OV2640 Camera module initialization flow chart

6.3.3 Reads image data of OV2640 module

When the initial configuration of the OV2640 and the necessary output image size are completed, the output signal acquisition of the OV2640 can be performed in time series. As shown on Figure 45.

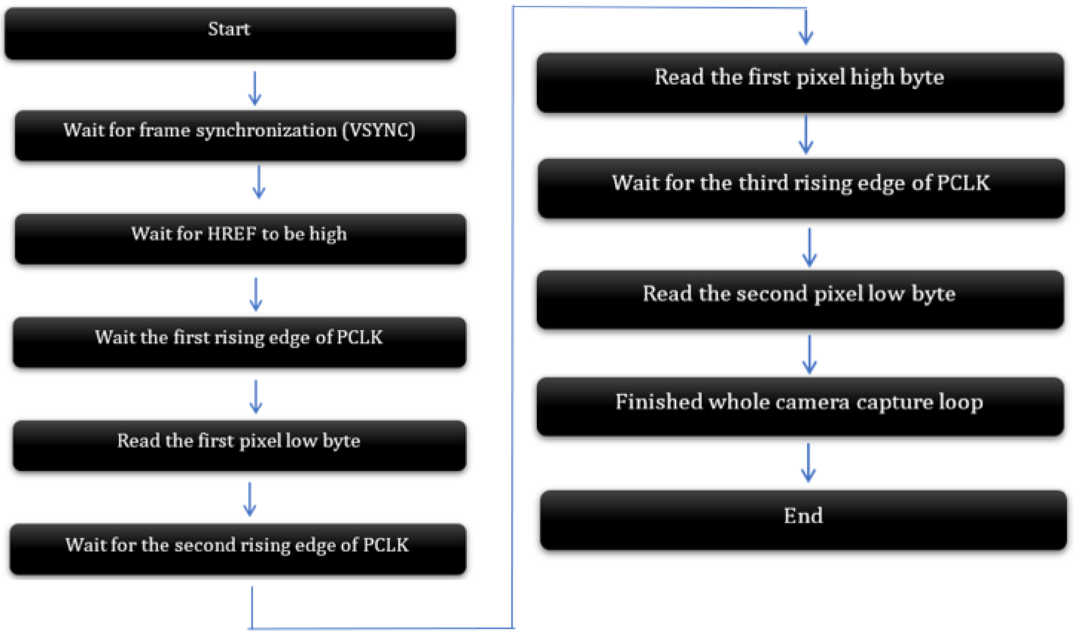

Figure 45 OV2640 Camera module read image data flow chart

6.4 DCMI Interface design

ConFigure the multiplexing function of relevant pins to enable DCMI clock.

To use DCMI, first enable DCMI clock. Secondly, the relevant pin of DCMI should be set output to connect the OV2640 module.

Set DCMI working mode and parameters.

DCMI interface, use 8-bit interface, continuous mode, according to the output timing diagram of OV2640 module, set: PCLK is valid for rising edge, HSYNC and VSYNC are active in low level. At the same time, set parameters such as frame interruption (jpeg data acquisition).

Set DMA to collect data.

DCMI data, generally use DMA to carry, after setting DCMI related parameters, set DMA to collect data.

Start DCMI transmission.

Finally, set the lowest bit of DCM->CR to 1, to start DCMI image data capture.

7. Results and Discussion

7.1 System Operation Diagram

As shown in the Figure 47 is the operation flow chart of PFOA solution identification system. It can be found that the whole operation is divided into three parts which are user selection module, image display module (RGB565/YUV422) and solution identification module.

The entire system steps 1 through 2 require a wait time of 0.5 seconds, and step 2 to step 3 require a wait time of 1.2 seconds. The users complete the image processing time of each solution is about 30 seconds.

At the same time, the image data of the embedded image acquisition system can also be transmitted to the mobile display screen through the SD card.it can achieve image display format fully compatible with mobile display screen.

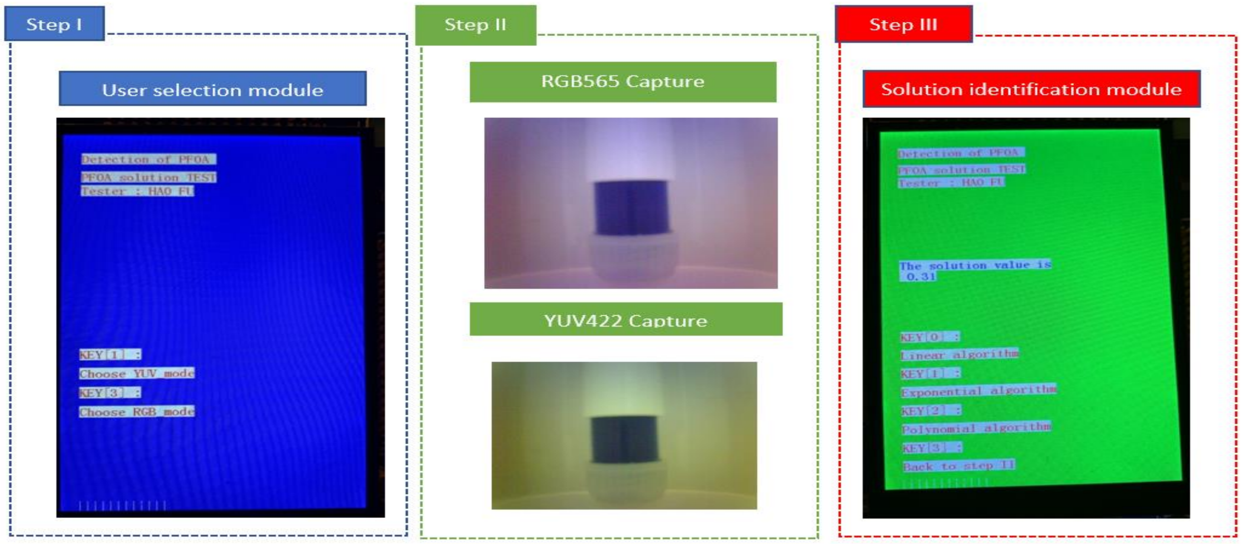

Figure 46 FPOA image system operation diagram

The main function of user selection module (Step I) is to control the image acquisition format of the camera module through different key inputs. The main function of image display module (Step II) is to observe the current state of image acquisition and whether the camera is in a normal operation state. The main function of solution identification module (Step III) is to analyse different algorithms according to the pixels of the image acquisition system.As show in Table 9.

Step I		Step II		Step III	
Key input	**Function**	**Key input**	**Function**	**Key input**	**Function**
KEY[0]		**KEY [0]**	**Change brightness**	**KEY [0]**	**Linear algorithm**
KEY[1]	**Choose YUV_mode**	**KEY [1]**	**Change Contrast**	**KEY [1]**	**Exponential algorithm**
KEY[2]		**KEY [2]**	**To step III**	**KEY [2]**	**Polynomial algorithm**
KEY [3]	**Choose RGB_mode**	**KEY [3]**	**RE-capture**	**KEY [3]**	**Back to step II**
KEY[RESET]	**Back to step**	**KEY[RESET]**	**Back to step I**	**KEY[RESET]**	**Back to step I**

Table 9 the function of key about FPOA image system operation diagram

7.2 RGB565 Brightness mode result

The brightness adjustment of the image acquisition module can be performed by internal register of the camera (refer to 6.3.5 OV2640 brightness setting). Then set camera acquisition format to RGB565 (refer to 6.3.3.2 OV2640 RGB565 Mode function) as shown in Table 10 is RGB image of different solutions when brightness is set to -2.

	0ppb	1ppb	3ppb	5ppb	11ppb
Solution image	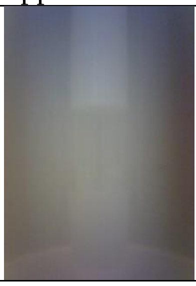				
TEST1					
Red value	144	73	62	46	39
Green Value	146	84	52	55	35
Blue value	136	125	118	118	102
TEST2					
Red value	140	68	61	51	35
Green Value	139	87	58	57	38
Blue value	132	119	111	108	109
TEST3					
Red value	148	74	57	45	31
Green Value	138	81	54	59	40
Blue value	141	121	116	103	110
Average value					
Red value	144	71.6	60	47.3	35
Green Value	141	84	54.6	57	37.6
Blue value	136.3	121.6	115	109.6	107
Shift value					
Red value	8	6	5	6	8
Green Value	8	6	6	4	5
Blue value	9	6	7	15	8

Maximum value					
Red value	148	74	62	51	39
Green Value	146	87	58	59	40
Blue value	141	125	118	118	110
Minimum value					
Red value	140	68	57	45	31
Green Value	138	81	52	55	35
Blue value	132	119	111	103	102

Table 10 RGB565 Brightness mode (-2) result

As shown in Table 11, the RGB565 image of the different solutions when the brightness is set to 0.

	0ppb	1ppb	3ppb	5ppb	11ppb
Solution image					
TEST1					
Red value	181	91	61	66	37
Green Value	180	101	61	55	40
Blue value	173	165	168	157	121
TEST2					
Red value	189	88	58	68	34
Green Value	182	98	59	58	42
Blue value	171	171	160	153	125
TEST3					
Red value	178	86	64	64	33
Green Value	177	103	65	56	48
Blue value	168	174	163	159	119
Average value					
Red value	182.6	88.3	61	66	34.6
Green Value	179.6	100.6	61.6	56.3	43.3
Blue value	170.6	170	163.6	156.3	121.6

Shift value					
Red value	11	5	6	4	4
Green Value	5	5	6	3	8
Blue value	5	9	8	6	6
Maximum value					
Red value	189	91	64	68	37
Green Value	182	103	65	58	48
Blue value	173	174	168	159	125
Minimum value					
Red value	178	86	58	64	33
Green Value	177	98	59	55	40
Blue value	168	165	160	153	119

Table 11 RGB565 Brightness mode (0) result

As shown in Table 12, it is an RGB565 image of a different solution when the brightness is set to +2.

	0ppb	1ppb	3ppb	5ppb	11ppb
Solution image					
TEST1					
Red value	234	131	75	77	60
Green Value	233	139	89	80	50
Blue value	226	217	174	129	113
TEST2					
Red value	233	136	68	72	54
Green Value	232	142	85	85	55
Blue value	220	220	171	131	98
TEST3					
Red value	234	137	79	71	63
Green Value	231	148	81	89	59
Blue value	218	215	179	134	110
Average value					
Red value	233.6	134.6	74	73.3	59
Green Value	232	143	85	84.6	54.6

Blue value	221.3	217.3	174.6	131.3	107
Shift value					
Red value	1	6	11	6	9
Green Value	2	9	8	9	9
Blue value	8	5	8	5	15
Maximum value					
Red value	234	137	79	77	63
Green Value	233	148	89	89	59
Blue value	226	220	179	134	113
Minimum value					
Red value	233	131	68	71	54
Green Value	231	139	81	80	50
Blue value	218	215	171	129	98

Table 12 RGB565 Brightness mode (2) result

7.3 YUV422 Brightness mode result

Set camera acquisition format to YUV422 (refer to 6.3.3.1 OV2640 JPEG Mode function) as shown in Table 13 is YUV image of different solutions when brightness is set to -2. Each solution YUV data was collected 5 times. It can be found that the colour of solutions increases from light blue to dark blue as the concentration of the solution increases.

	0ppb	1ppb	3ppb	5ppb	11ppb
Solution image	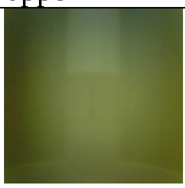				
TEST1					
Y	124	80	54	58	34
U	98	125	150	150	140
V	128	115	120	115	123
TEST2					
Y	118	86	50	55	32
U	95	131	145	148	147
V	131	121	118	127	129
TEST3					
Y	128	81	61	51	39
U	99	122	159	157	139
Y	131	128	127	129	125
Average value					
Y	123.3	82.3	55	54.6	35
U	97.3	126	151.3	151.6	142
V	130	121.3	121.6	123.6	125.6

Shift value					
Y	10	6	11	7	7
U	4	9	14	9	8
V	3	13	9	14	6
Maximum value					
Y	128	86	61	58	39
U	99	131	159	157	147
V	131	128	127	129	129
Minimum value					
Y	118	80	50	51	32
U	95	122	145	148	139
V	128	115	118	115	123

Table 13 YUV422 Brightness mode (-2) result

As shown Table 14, the YUV422 image of the different solutions when the brightness is set to 0. Each solution was subjected to 5 times of YUV data acquisition.

	0ppb	1ppb	3ppb	5ppb	11ppb
Solution image					
TEST1					
Y	156	96	69	71	44
U	92	133	147	150	137
V	128	118	115	115	117
TEST2					
Y	149	94	64	68	48
U	95	139	150	153	141
V	130	110	121	120	121
TEST3					
Y	145	110	60	73	41
U	90	137	154	159	150
Y	124	118	127	119	127
Average value					
Y	150	100	64.3	70.6	44.3
U	92.3	136.3	150.3	154	142.6
V	127.3	115.3	121	118	121.6
Shift value					
Y	11	16	9	5	7
U	5	6	7	9	13
V	6	8	12	5	10
Maximum value					
Y	156	110	69	73	48
U	95	139	154	159	150
V	130	118	127	120	127

Minimum value					
Y	145	94	60	68	41
U	90	133	147	150	137
V	124	110	115	115	117

Table 14 YUV422 Brightness mode (0) result

As shown on Table 15, the YUV422 image is a different solution with a brightness setting of 2. Each solution was subjected to 5 times of YUV data acquisition.

	0ppb	1ppb	3ppb	5ppb	11ppb
Solution image					
TEST1					
Y	205	137	98	84	58
U	79	130	159	181	144
V	125	113	105	105	115
TEST2					
Y	203	133	95	92	55
U	83	128	163	178	142
V	131	119	110	112	120
TEST3					
Y	200	130	90	84	59
U	86	122	151	175	149
Y	121	115	117	110	125
Average value					
Y	202.6	133.3	94.3	86.6	57.3
U	82.6	126.6	157.6	178	145
V	125.6	115.6	110.6	109	120
Shift value					
Y	5	7	8	8	4
U	7	8	12	6	7
Y	10	6	12	7	10
Maximum value					
Y	205	137	98	92	59
U	86	130	163	181	149
V	131	119	117	112	125
Minimum value					
Y	200	130	90	84	55
U	79	122	151	175	142
V	121	113	105	105	115

Table 15 YUV422 Brightness mode (2) result

7.4 RGB565 and YUV 422 Brightness mode discussion

As shown in the Figure, under RGB565 acquisition format with different brightness, RED pixel values can be collected by PFOA solution acquisition system. Red value_-2 represents RED pixel value when the brightness is -2, Red value_0 represents pixel value when the brightness is 0, and Red value_2 represents RED pixel value when the brightness is 2. It can be found that when the brightness is 2 and the concentration of the PFOA solution changes, the change trend of the RED pixel is most obvious.

	0ppb	1ppb	3ppb	5ppb	11ppb
Red value_-2	144	71.6	60	47.3	35
Red value_0	182.6	88.3	61	66	34.6
Red value_2	233.6	134.6	74	73.3	59

Table 16 Compare different brightness mode on RGB565 format about RED

In Table 17, Green value_-2 represents GREEN pixel value when the brightness is -2, Green value_0 represents GREEN pixel value when the brightness is 0, and Green value_2 represents GREEN pixel value when the brightness is 2. It can be found that when the brightness is 2 and the concentration of the PFOA solution changes, the change trend of the GREEN pixel is most obvious.

	0ppb	1ppb	3ppb	5ppb	11ppb
Green Value_-2	141	84	54.6	57	37.6
Green Value_0	179.6	100.6	61.6	56.3	43.3
Green Value_2	232	143	85	84.6	54.6

Table 17 Compare different brightness mode on RGB565 format about GREEN

In Table 18, Blue value_-2 represents BLUE pixel value when the brightness is -2, Blue value_0 represents BLUE pixel value when the brightness is 0, and Blue value_2 represents BLUE pixel value when the brightness is 2. It can be found that when the brightness is 2 and the concentration of the PFOA solution changes, the change trend of the BLUE pixel is most obvious.

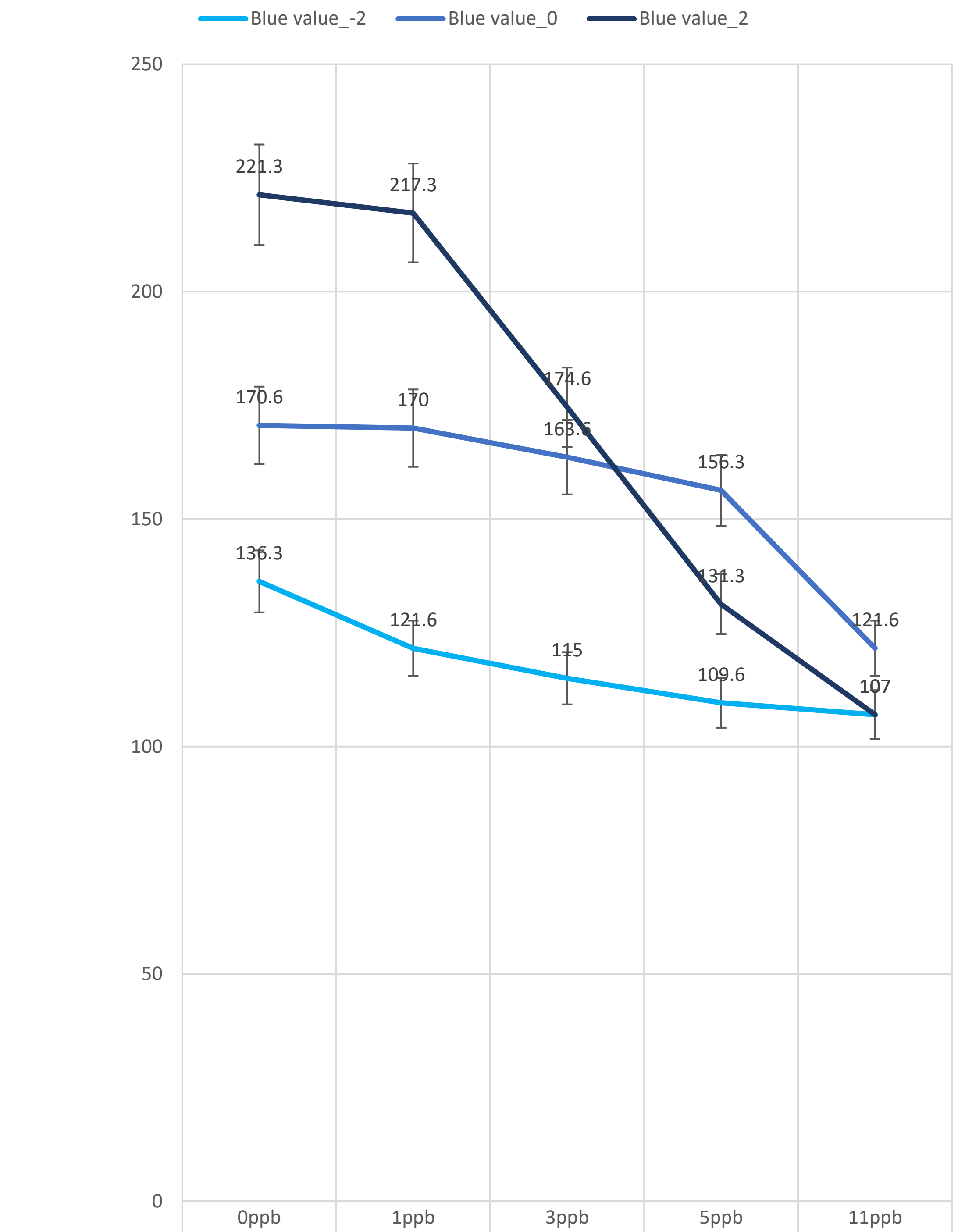

	0ppb	1ppb	3ppb	5ppb	11ppb
Blue value_-2	136.3	121.6	115	109.6	107
Blue value_0	170.6	170	163.6	156.3	121.6
Blue value_2	221.3	217.3	174.6	131.3	107

Table 18 Compare different brightness mode on RGB565 format about BLUE

As shown in Table 19, the Y pixel value acquired by the PFOA solution acquisition system under the YUV422 acquisition format with different brightness. In the Figure, Y_-2 represents the Y pixel value when the brightness is -2, Y_0 represents the Y pixel value when the brightness is 0, and Y_2 represents the V pixel value when the brightness is 2. It can be found that when the brightness is 2, The concentration of the PFOA solution changes, the change trend of the Y pixel is most obvious.

Table 19 Compare different brightness mode on YUV422 format about Y (the brightness)

In Table 20, U_-2 represents the U pixel value when the brightness is -2, U_0 represents the U pixel value when the brightness is 0, and U_2 represents the U pixel value when the brightness is 2. It can be found that when the brightness changes, the U pixel value in the YUV422 format has little effect.

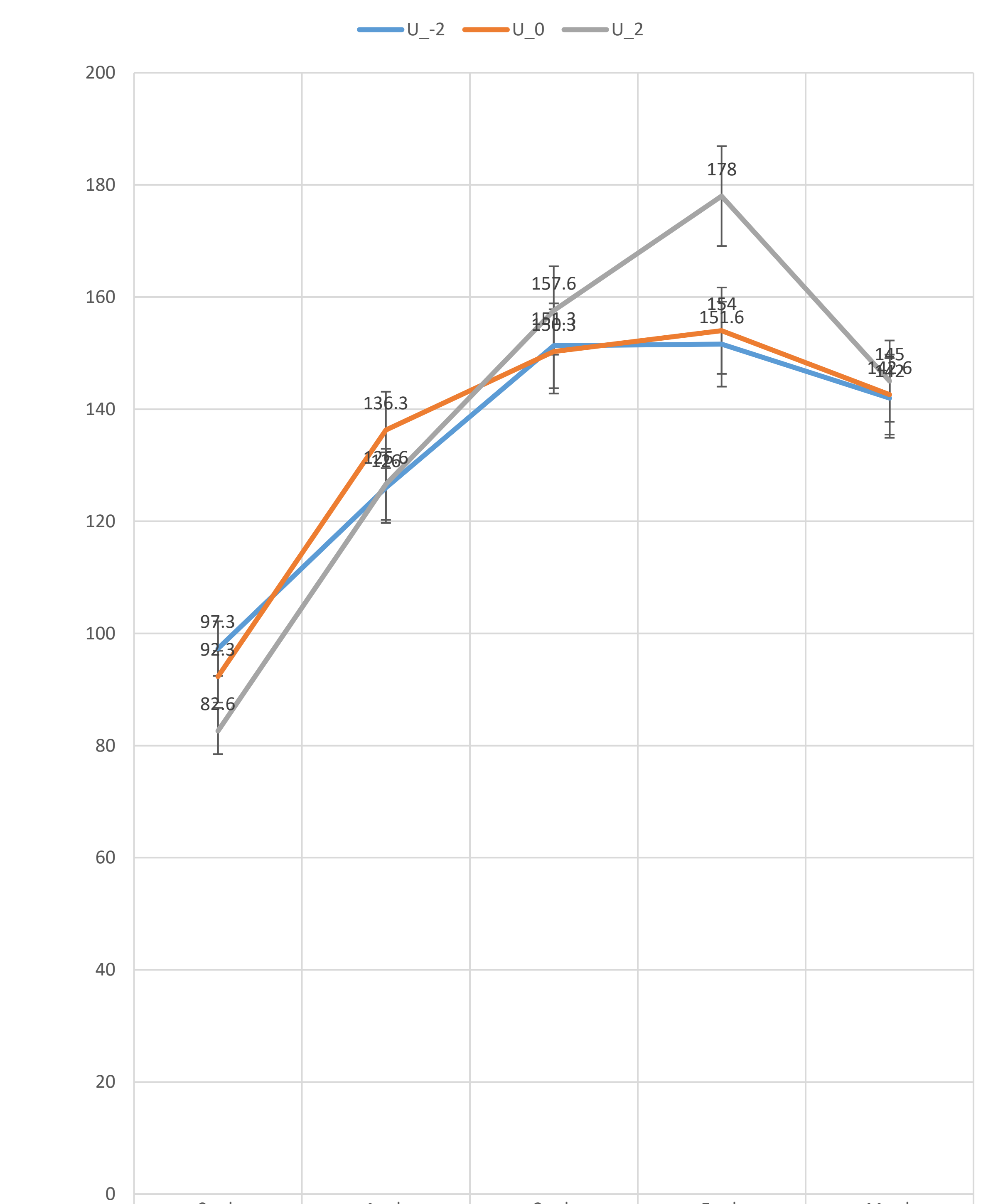

	0ppb	1ppb	3ppb	5ppb	11ppb
U_-2	97.3	126	151.3	151.6	142
U_0	92.3	136.3	150.3	154	142.6
U_2	82.6	126.6	157.6	178	145

Table 20 Compare different brightness mode on YUV422 format about U (blue projection)

In Table 21, V_-2 represents the U pixel value when the brightness is -2, V_0 represents the V pixel value when the brightness is 0, and V_2 represents the V pixel value when the brightness is 2. It can be found that when the brightness changes, the V pixel for the YUV422 format has little effect.

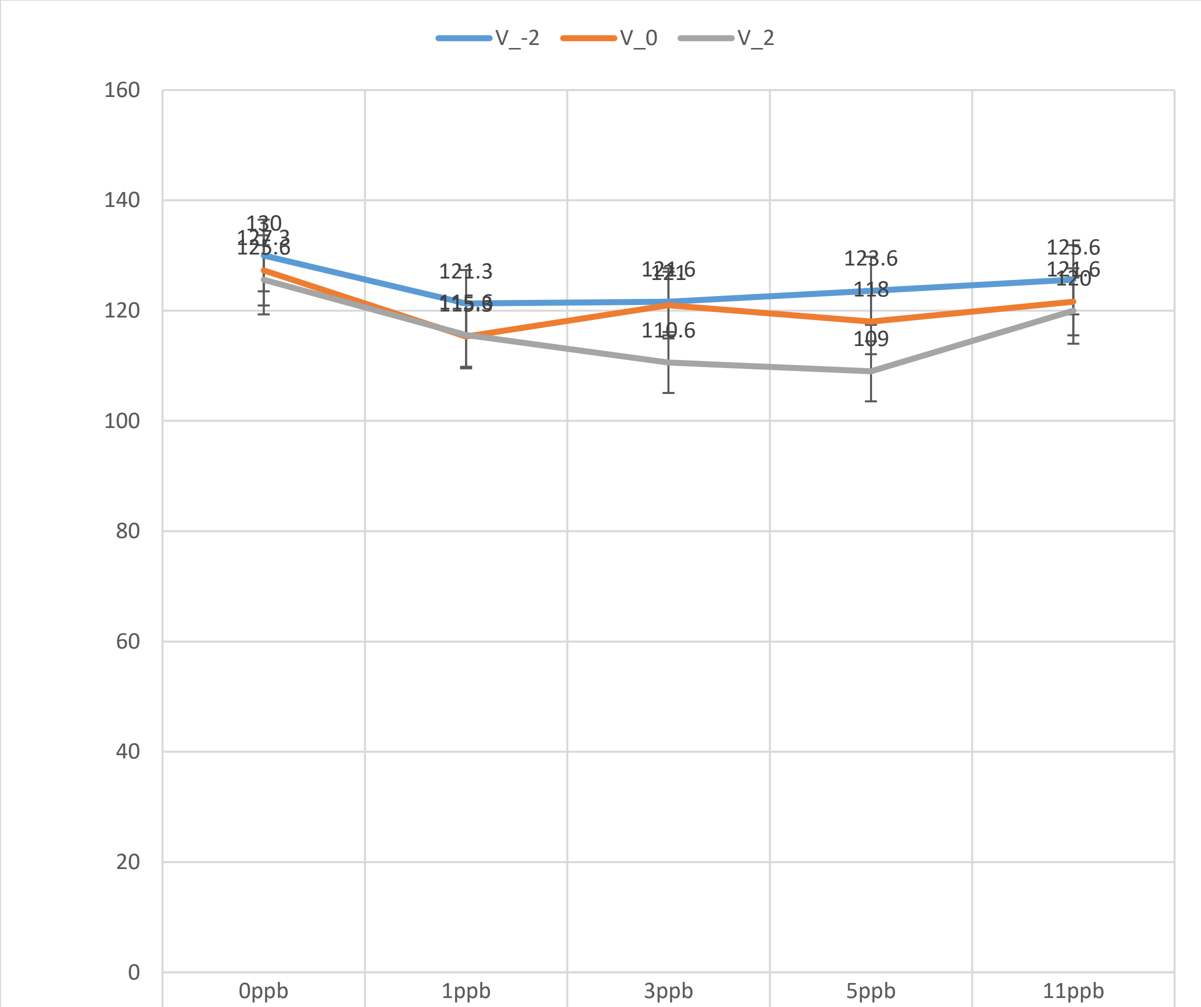

	0ppb	1ppb	3ppb	5ppb	11ppb
V_-2	130	121.3	121.6	123.6	125.6
V_0	127.3	115.3	121	118	121.6
V_2	125.6	115.6	110.6	109	120

Table 21 Compare different brightness mode on YUV422 format about V (red projection)

Through experiments, it can be found that the brightness value set by the camera should be +2 whether the image information is collected using RGB format or YUV422, which is suitable with the standard of the entire identification system. Although the method of adjusting the brightness of camera can significantly improve the quality of the image and the entire curve change is more obvious. However, there are certain drawbacks in the way of adjusting the image quality only by brightness. When the brightness adjustment of the camera is greater than 2, (the maximum value is 3) it will cause distortion. Due to the time and the fact that there is obvious trend curve when the brightness of the camera is set to be 2, the brightness value of the entire image acquisition system is set to 2 in this experiment.

7.5 RGB565 Contrast mode result

When the brightness setting of the camera module is completed (the brightness of this experiment is set to +2), the contrast adjustment of the image acquisition module can be performed through the camera's internal register (refer to 6.3.6 OV2640 Contrast setting). Then set the camera's acquisition format to RGB565 (refer to 6.3.3.2 OV2640 RGB565 Mode function) as shown in the table is the RGB image of the different solutions when the contrast is set to -2. It can be found that the colour of the solution increases from light blue to dark blue as the concentration of the solution increases.

	0ppb	1ppb	3ppb	5ppb	11ppb
Solution image					
TEST1					
Red value	164	109	65	71	64
Green Value	171	112	92	80	60
Blue value	164	169	155	139	109
TEST2					
Red value	172	110	58	65	68
Green Value	174	121	98	88	66
Blue value	170	173	147	133	113
TEST3					
Red value	161	101	55	61	74
Green Value	178	128	102	93	69
Blue value	173	179	143	138	102
Average value					
Red value	165.6	106.6	59.3	65.6	68.6
Green Value	174.3	120.3	97.3	87	65
Blue value	169	173.6	148.3	136.6	108
Shift value					
Red value	11	9	10	10	10
Green Value	7	16	10	13	9
Blue value	9	10	12	6	11
Maximum value					
Red value	172	110	65	71	74
Green Value	178	128	102	93	69
Blue value	173	179	155	139	113

Minimum value					
Red value	161	101	55	61	64
Green Value	171	112	92	80	60
Blue value	164	169	143	133	102

Table 22 RGB565 contrast mode (-2) result

As shown in Table 23, the RGB565 image of the different solution when the contrast is set to 0.

	0ppb	1ppb	3ppb	5ppb	11ppb
Solution image					
TEST1					
Red value	181	91	61	66	37
Green Value	180	101	61	55	40
Blue value	173	165	160	154	121
TEST2					
Red value	185	84	58	60	32
Green Value	182	95	56	50	35
Blue value	178	161	154	137	118
TEST3					
Red value	189	98	53	59	28
Green Value	186	108	53	52	31
Blue value	171	158	152	142	110
Average value					
Red value	185	91	57.3	61.6	32.3
Green Value	182.6	101.3	56.6	52.3	35.3
Blue value	174	161.3	155.3	144.3	116.3
Shift value					
Red value	8	14	8	7	9
Green Value	6	13	8	5	9
Blue value	7	7	8	17	11
Maximum value					
Red value	189	98	61	66	37
Green Value	186	108	61	55	40
Blue value	178	165	160	154	121

Minimum value					
Red value	181	84	53	59	28
Green Value	180	95	53	50	31
Blue value	171	158	152	137	110

Table 23 RGB565 contrast mode (0) result

As shown in Table 24, the RGB565 image of the different solution when the contrast is set to 2.

	0ppb	1ppb	3ppb	5ppb	11ppb
Solution image					
TEST1					
Red value	196	81	30	28	15
Green Value	195	85	49	40	22
Blue value	180	166	170	164	87
TEST2					
Red value	201	85	35	20	23
Green Value	200	90	56	35	28
Blue value	190	156	180	159	93
TEST3					
Red value	205	93	33	18	9
Green Value	191	93	59	43	33
Blue value	187	145	173	170	99
Average value					
Red value	200.6	86.3	32.6	22	15.6
Green Value	195.3	89.3	54.6	39.3	27.6
Blue value	185.6	155.6	174.3	164.3	93
Shift value					
Red value	9	12	5	10	14
Green Value	9	8	10	8	11
Blue value	10	21	10	11	12
Maximum value					
Red value	205	93	35	28	23
Green Value	200	93	59	43	33
Blue value	190	166	180	170	99

Minimum value					
Red value	196	81	30	18	9
Green Value	191	85	49	35	22
Blue value	180	145	170	159	87

Table 24 RGB565 contrast mode (2) result

7.6 YUV422 Contrast mode result

When the brightness setting of the camera module is completed (the brightness of this experiment is set to +2), the contrast adjustment of the image acquisition module can be performed through the camera's internal register (refer to 6.3.6 OV2640 Contrast setting). Then set the camera's acquisition format to RGB565 (refer to 6.3.3.2 OV2640 JPEG Mode function) as shown in Table 25, which is the RGB image of the different solutions with the contrast set to -2. Each solution was subjected to 5 acquisitions of RGB data. It can be found that the colour of the solution increases from light blue to dark blue as the concentration of the solution increases.

	0ppb	1ppb	3ppb	5ppb	11ppb
Solution image	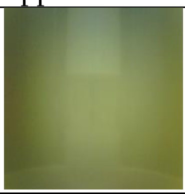	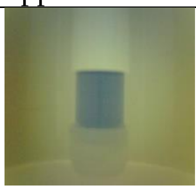			
TEST1					
Y	152	106	88	82	66
U	100	131	148	150	131
V	127	119	117	113	126
TEST2					
Y	143	110	83	89	69
U	103	126	156	160	139
V	118	124	121	123	129
TEST3					
Y	160	115	89	81	59
U	106	121	159	164	126
Y	129	121	129	123	125
Average value					
Y	151.6667	110.3333	86.66667	84	64.66667
U	103	126	154.3333	158	132
V	124.6667	121.3333	122.3333	119.6667	126.6667
Shift value					
Y	17	9	6	8	10
U	6	10	11	14	13
V	11	5	12	10	4
Maximum value					
Y	160	115	89	89	69
U	106	131	159	164	139
V	129	124	129	123	129

Minimum value					
Y	143	106	83	81	59
U	100	121	148	150	126
V	118	119	117	113	125

Table 25 YUV422 contrast mode (-2) result

As shown on Table 26, the YUV422 image of the different solutions with contrast set to 0 is shown.

	0ppb	1ppb	3ppb	5ppb	11ppb
Solution image					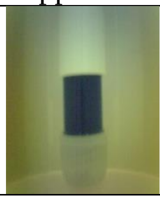
TEST1					
Y	156	96	69	71	44
U	92	133	147	150	137
V	128	118	115	115	117
TEST2					
Y	152	100	62	78	48
U	98	126	154	159	147
V	131	128	121	121	121
TEST3					
Y	148	104	58	126	37
U	82	122	159	168	131
Y	128	134	127	132	110
Average value					
Y	152	100	63	91.66667	43
U	90.66667	127	153.3333	159	138.3333
V	129	126.6667	121	122.6667	116
Shift value					
Y	8	8	11	55	11
U	16	11	12	18	16
V	3	16	12	17	11
Maximum value					
Y	156	104	69	126	48
U	98	133	159	168	147
V	131	134	127	132	121
Minimum value					
Y	148	96	58	71	37
U	82	122	147	150	131
V	128	118	115	115	110

Table 26 YUV422 contrast mode (0) result

As shown, the YUV422 image is a different solution with a contrast setting of 2.

	0ppb	1ppb	3ppb	5ppb	11ppb
Solution image					
TEST1					
Y	166	98	61	52	28
U	81	130	147	168	145
V	128	111	113	98	118
TEST2					
Y	169	92	54	43	30
U	75	139	138	170	156
V	134	120	110	100	122
TEST3					
Y	173	87	59	38	23
U	71	128	140	174	155
Y	139	110	110	108	127
Average value					
Y	169.3333	92.33333	58	44.33333	27
U	75.66667	132.3333	141.6667	170.6667	152
V	133.6667	113.6667	111	102	122.3333
Shift value					
Y	7	11	7	14	7
U	10	11	9	6	11
V	11	10	3	10	9
Maximum value					
Y	173	98	61	52	30
U	81	139	147	174	156
V	139	120	113	108	127
Minimum value					
Y	166	87	54	38	23
U	71	128	138	168	145
V	128	110	110	98	118

Table 27 YUV422 contrast mode (2) result

7.7 RGB565 and YUV 422 Contrast mode discussion

As shown in Table 28, the RED pixel values collected by the PFOA solution acquisition system under the RGB565 acquisition format with different brightness. In the Figure, Red value_-2 represents the RED pixel value when the contrast is -2, Red value_0 represents the pixel value when the contrast is 0, and Red value_2 represents the RED pixel value when the contrast is 2. It can be found that when the contrast is 2, when the concentration of the PFOA solution changes, the change trend of the entire RED pixel is most obvious.

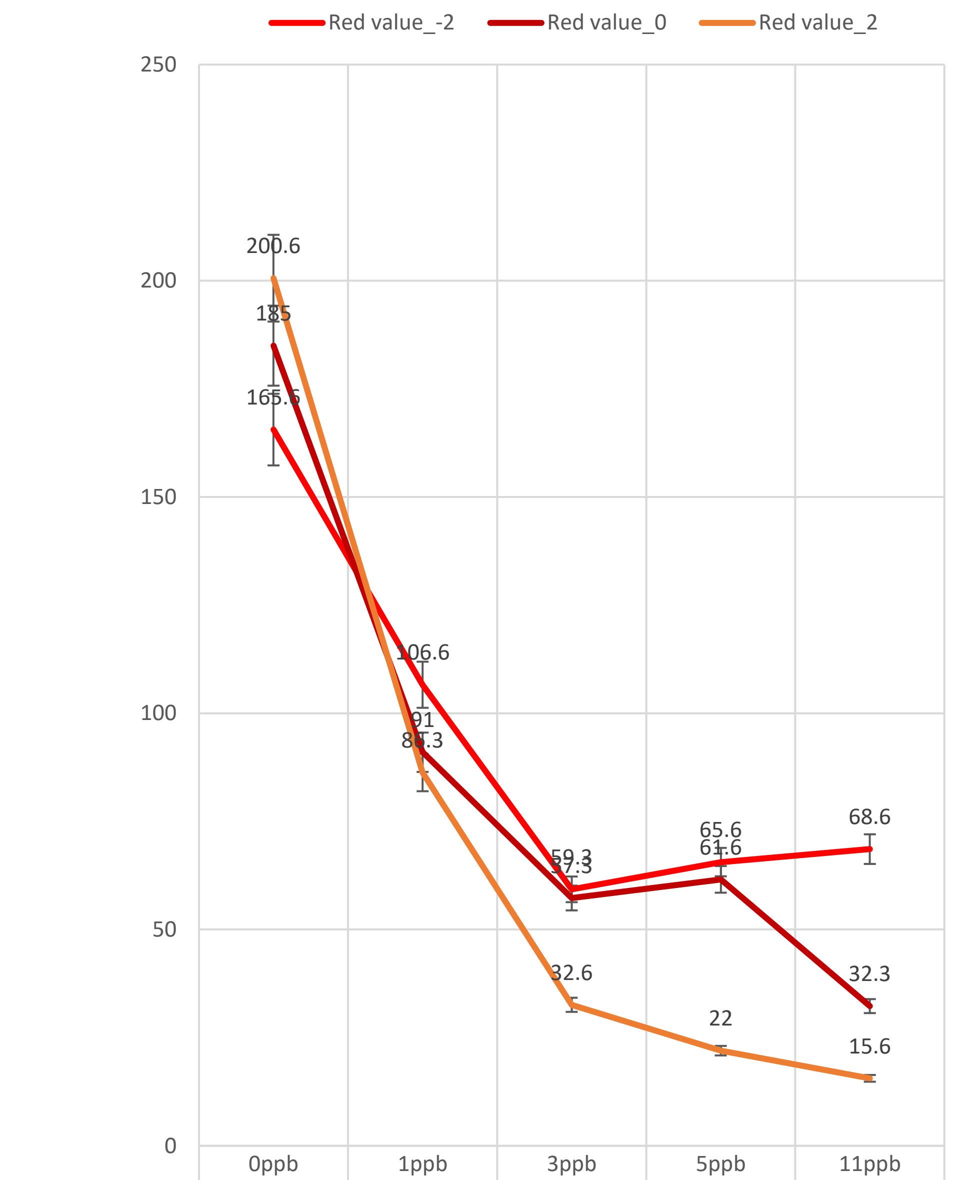

	0ppb	1ppb	3ppb	5ppb	11ppb
Red value_-2	165.6	106.6	59.3	65.6	68.6
Red value_0	185	91	57.3	61.6	32.3
Red value_2	200.6	86.3	32.6	22	15.6

Table 28 Compare different contrast mode on RGB565 format about RED

In Table 29, Green value_-2 represents the GREEN pixel value when the contrast is -2, Green value_0 represents the GREEN pixel value when the contrast is 0, and Green value_2 represents the GREEN pixel value when the contrast is 2. It can be found that when the contrast is 2, when the concentration of the PFOA solution changes, the trend of the entire GREEN pixel is most obvious.

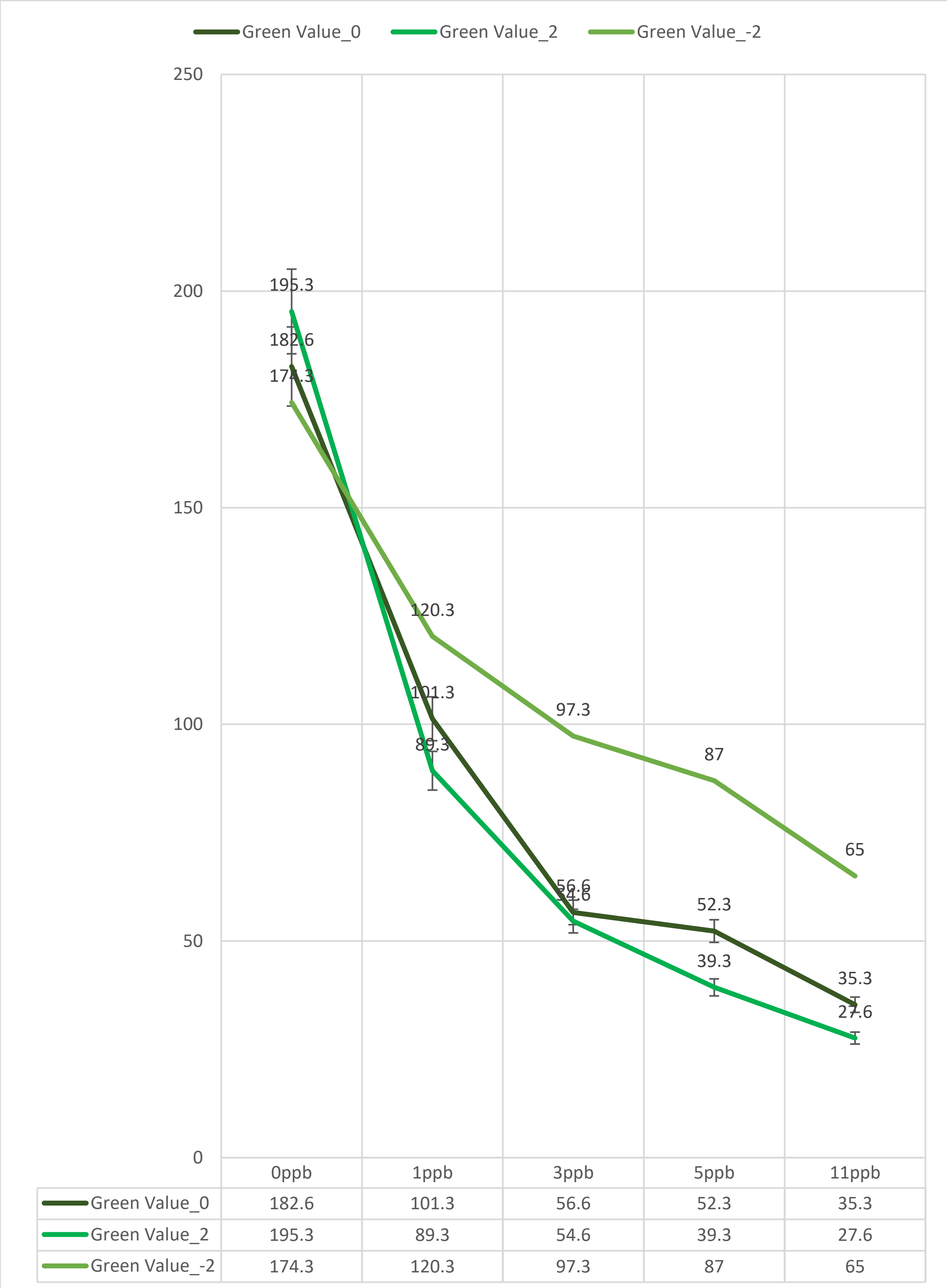

Table 29 Compare different contrast mode on RGB565 format about GREEN

In Table 30, Blue value_-2 represents the BLUE pixel value when the contrast is -2, Blue value_0 represents the BLUE pixel value when the contrast is 0, and Blue value_2 represents the BLUE pixel value when the contrast is 2. It can be found that when the contrast is 2, when the concentration of the PFOA solution changes, the trend of the entire BLUE pixel is most obvious.

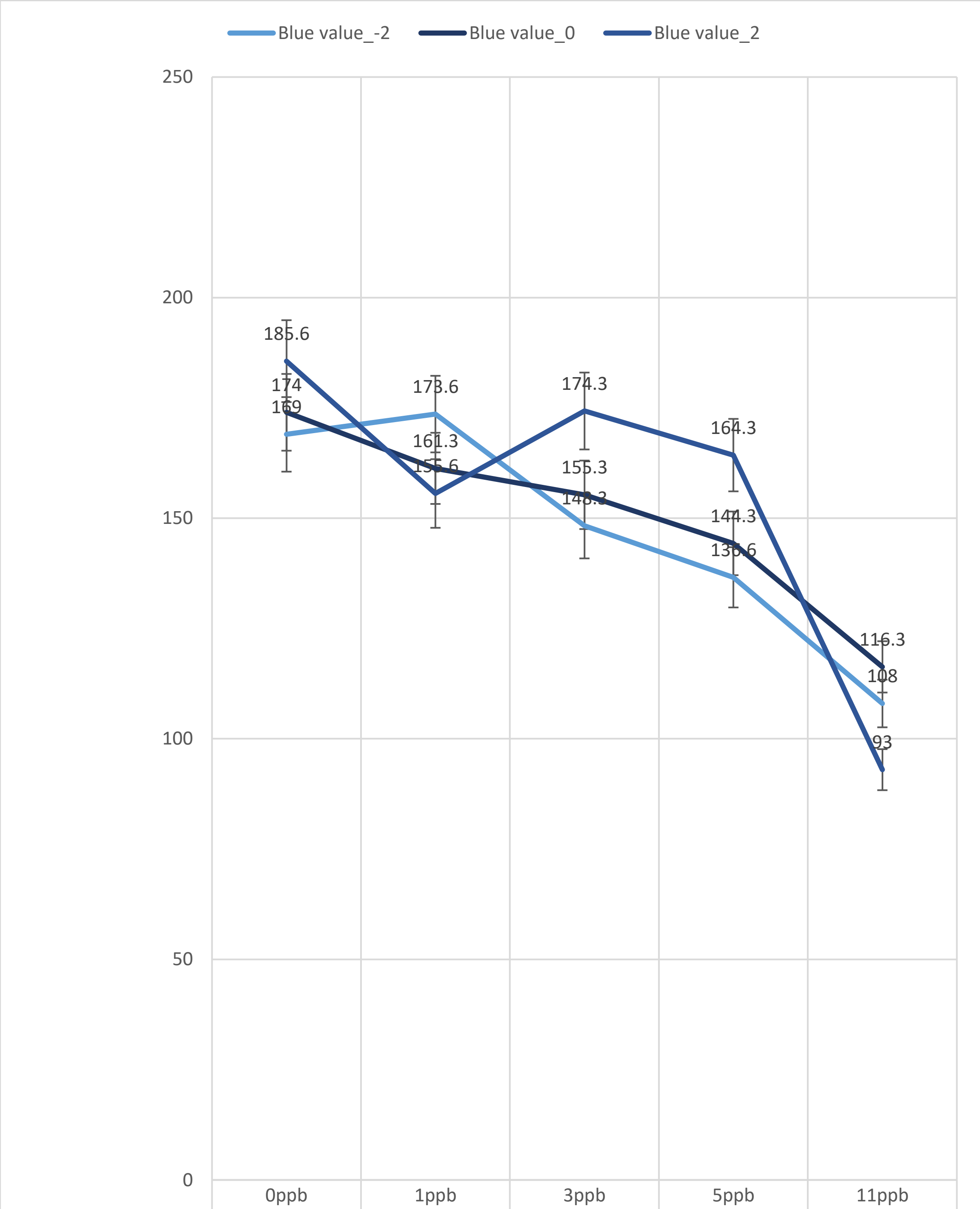

	0ppb	1ppb	3ppb	5ppb	11ppb
Blue value_-2	169	173.6	148.3	136.6	108
Blue value_0	174	161.3	155.3	144.3	116.3
Blue value_2	185.6	155.6	174.3	164.3	93

Table 30 Compare different contrast mode on RGB565 format about BLUE

In Table 31, Y value_-2 represents the Y pixel value when the contrast is -2, Y value_0 represents the Y pixel value when the contrast is 0, and Y value_2 represents the Y pixel value when the contrast is 2. It can be found that when the contrast is 2, when the concentration of the PFOA solution changes, the trend of the entire Y pixel is most obvious.

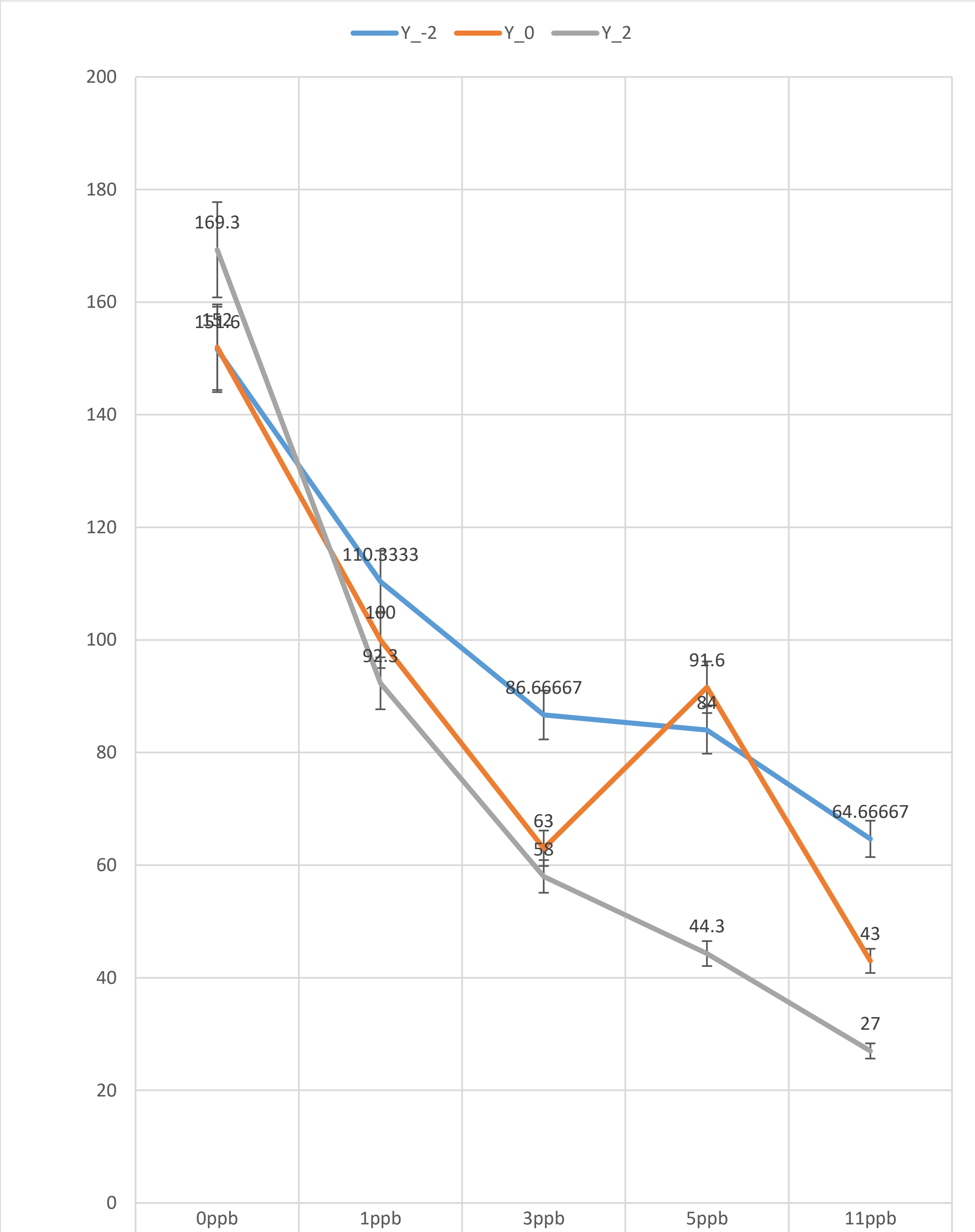

	0ppb	1ppb	3ppb	5ppb	11ppb
Y_-2	151.6	110.3333	86.66667	84	64.66667
Y_0	152	100	63	91.6	43
Y_2	169.3	92.3	58	44.3	27

Table 31 Compare different contrast mode on YUV422 format about Y (the brightness)

In Table 32, U_-2 represents the U pixel value when the contrast is -2, U_0 represents the U pixel value when the contrast is 0, and U_2 represents the U pixel value when the contrast is 2. It can be found that when the contrast changes, the U pixel value in the YUV422 format has little effect.

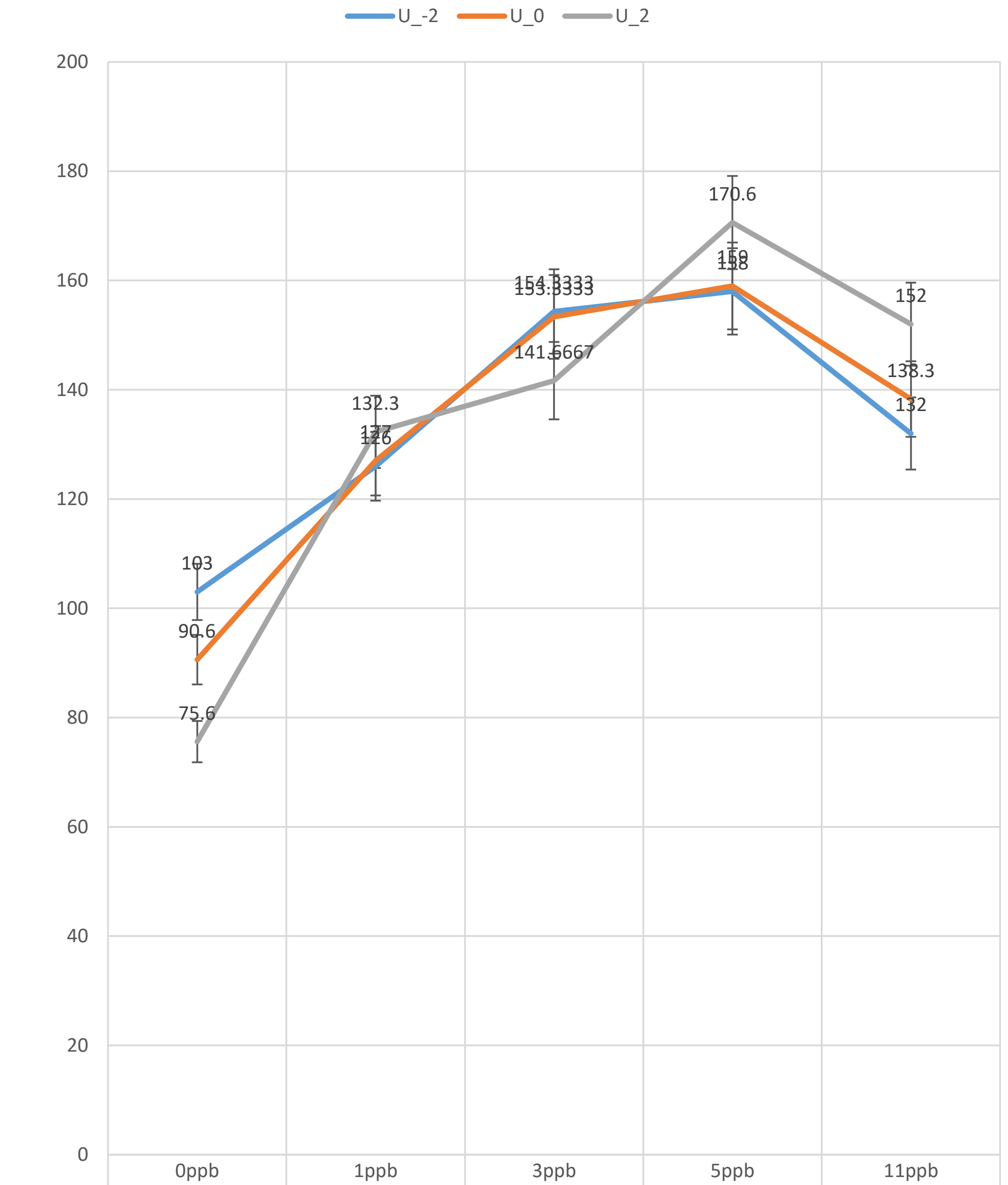

	0ppb	1ppb	3ppb	5ppb	11ppb
U_-2	103	126	154.3333	158	132
U_0	90.6	127	153.3333	159	138.3
U_2	75.6	132.3	141.6667	170.6	152

Table 32 Compare different contrast mode on YUV422 format about U (blue projection)

In Table 33, V_-2 represents the V pixel value when the contrast is -2, V_0 represents the V pixel value when the contrast is 0, and V_2 represents the V pixel value when the contrast is 2. It can be found that when the contrast changes, the V pixel value in the YUV422 format has little effect.

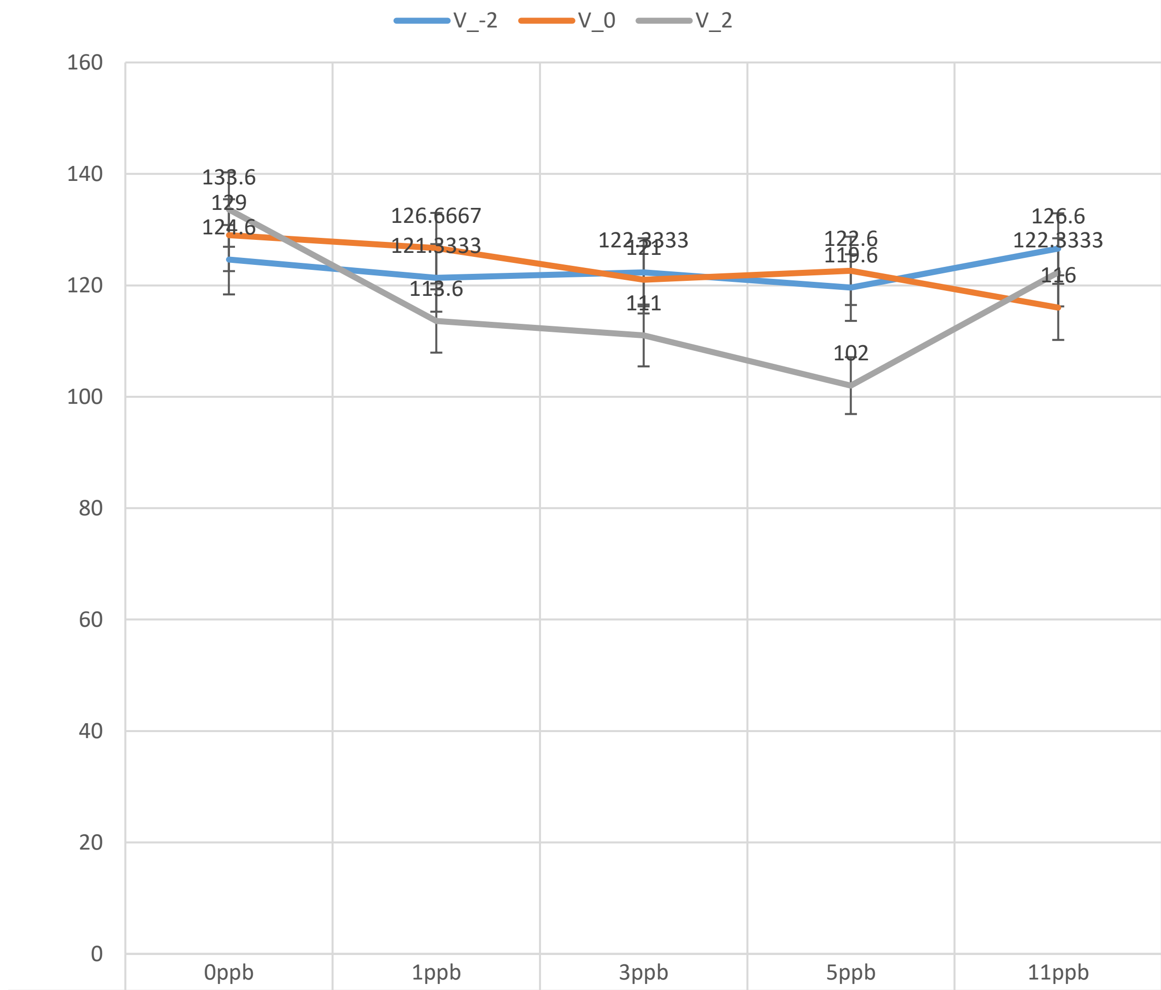

	0ppb	1ppb	3ppb	5ppb	11ppb
V_-2	124.6	121.3333	122.3333	119.6	126.6
V_0	129	126.6667	121	122.6	116
V_2	133.6	113.6	111	102	122.3333

Table 33 Compare different contrast mode on YUV422 format about V (red projection)

Through experiments, it can be found that the contrast value set by the camera should be +2 whether the image information is collected using RGB format or YUV422, which is suitable with the standard of the entire identification system. Due to the time and the fact that there is obvious trend curve when the contrast value of the entire image acquisition system is set to 2 in this experiment.

6. Algorithm design

A total of three different algorithms are used in this design, namely linear algorithm, exponential algorithm and polynomial algorithm. Each algorithm compares the RGB565 image output format to the YUV422 image output format.

8.1 linear algorithm

8.1.1 RGB565 linear algorithm

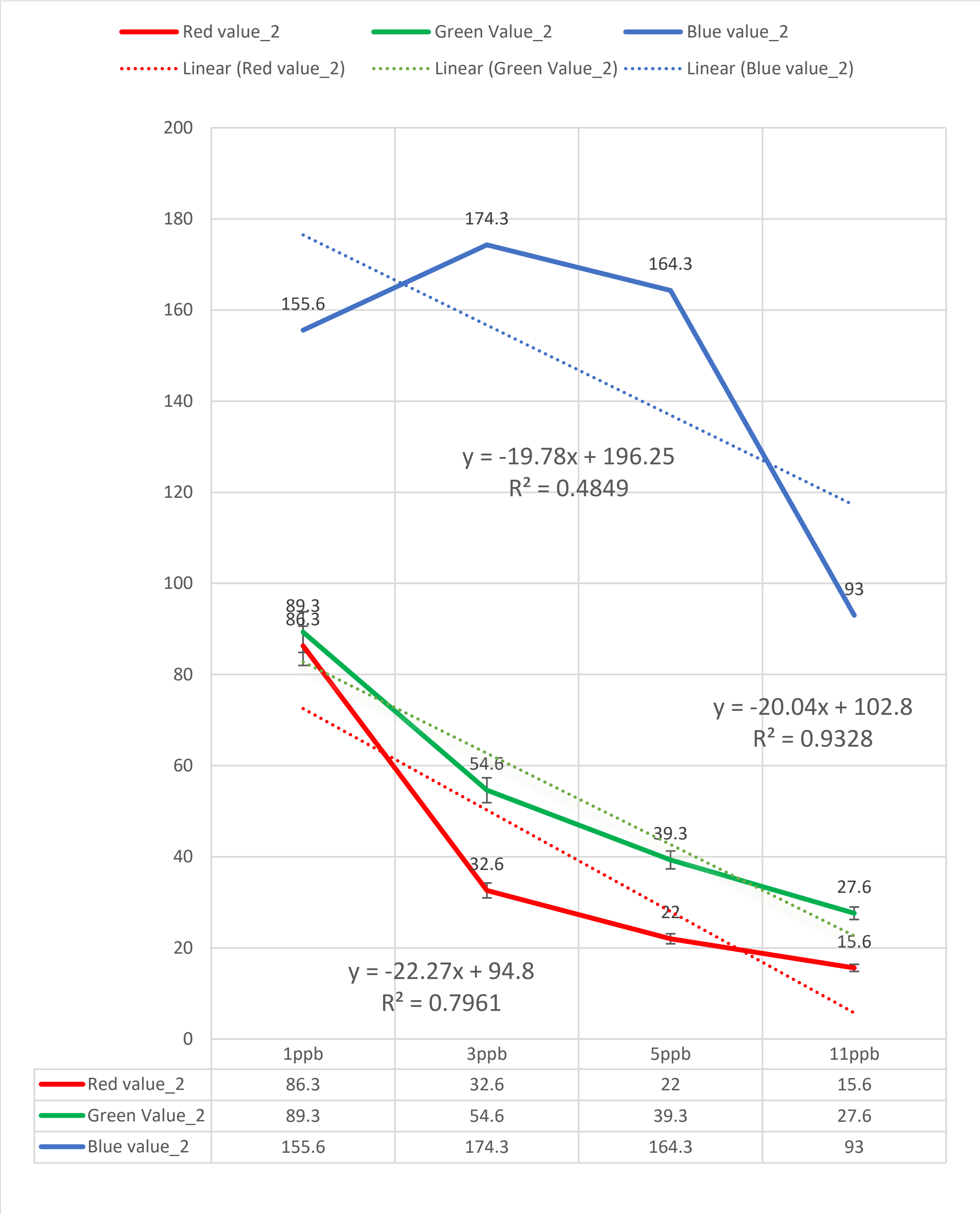

Table 34 RGB565 linear algorithm

	Red	Green	Blue
Linear function	y = -22.27x + 94.8	y = -20.04x + 102.8	y = -19.78x + 196.25
R^2	0.7961	0.9328	0.4849

Table 35 RGB565 linear algorithm coefficient of determination

Equation 5 Calculation factor about Red, Green and Blue on RGB565 linear algorithm

$$F_{red} = \frac{R_{red}^2}{R_{total}^2} = \frac{0.7961}{2.2138} = 0.359, F_{green} = \frac{R_{green}^2}{R_{total}^2} = \frac{0.9328}{2.2138} = 0.421, F_{blue} \frac{R_{blue}^2}{R_{total}^2} = \frac{0.4849}{2.2138} = 0.219$$

Equation 6 The calculation formula on RGB565 linear algorithm

$$Y = Y_R \times F_{red} + Y_g \times F_{green} + Y_B \times F_{blue}$$

$$\begin{aligned} Y &= (-22.27x_{red} + 94.8) \times 0.359 + (-20.04x_{green} + 102.8) \times 0.421 + (-19.78x_{blue} + 196.25) \times 0.219 \\ &= -7.99x_{red} + 34.03 - 8.43x_{green} + 43.27 - 4.33x_{blue} + 42.97 \\ &= -7.99x_{red} - 8.43x_{green} - 4.33x_{blue} + 120.27 \end{aligned}$$

8.1.1 YUV422 linear algorithm

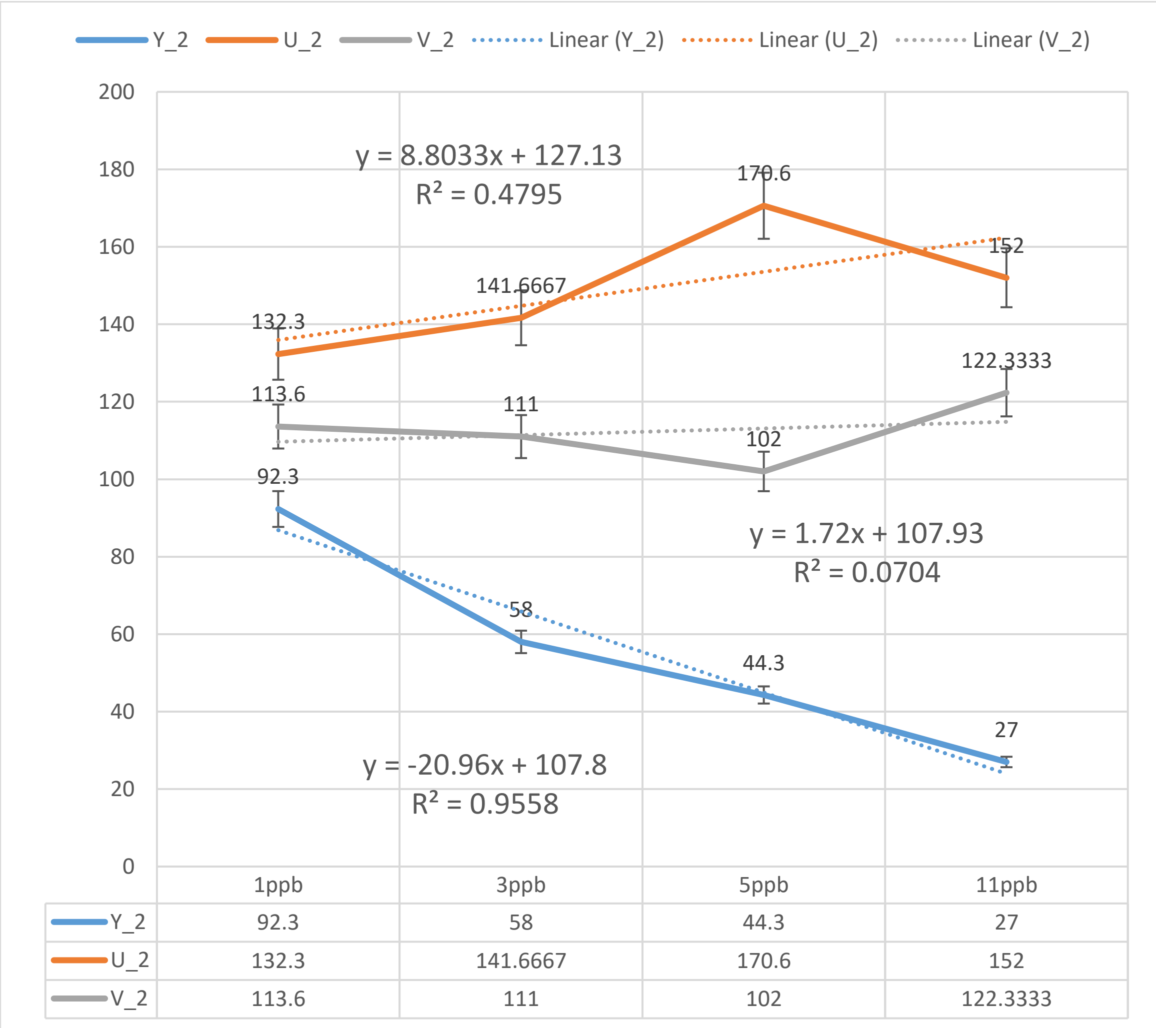

Table 36 YUV422 linear algorithm

	Y	U	V
Linear function	y = -20.96x + 107.8	y = 1.72x + 107.93	y = 8.8033x + 127.13
R^2	0.9558	0.0704	0.4795

Table 37 YUV422 linear algorithm coefficient of determination

Equation 7 Calculation factor about Y U V on YUV422 linear algorithm

$$F_Y = \frac{R_Y^2}{R_{total}^2} = \frac{0.9558}{1.5057} = 0.63, F_U = \frac{R_U^2}{R_{total}^2} = \frac{0.0704}{1.5057} = 0.04, F_V = \frac{R_V^2}{R_{total}^2} = \frac{0.4795}{1.5057} = 0.31$$

Equation 8 The calculation formula on YUV422 linear algorithm

$$Y = Y_Y \times F_Y + Y_U \times F_U + Y_V \times F_V$$
$$Y = (-20.96x_Y + 107.8) \times 0.63 + (1.72x_U + 107.93) \times 0.04 + (8.8033x_V + 127.13) \times 0.31$$
$$= -13.28x_Y + 68.34 + 0.06x_U + 4.31 + 2.73x_V + 39.41$$
$$= -13.28x_Y + 0.06x_U + 2.73x_V + 112.06$$

8.2 Exponential algorithm

8.2.1 RGB565 Exponential algorithm

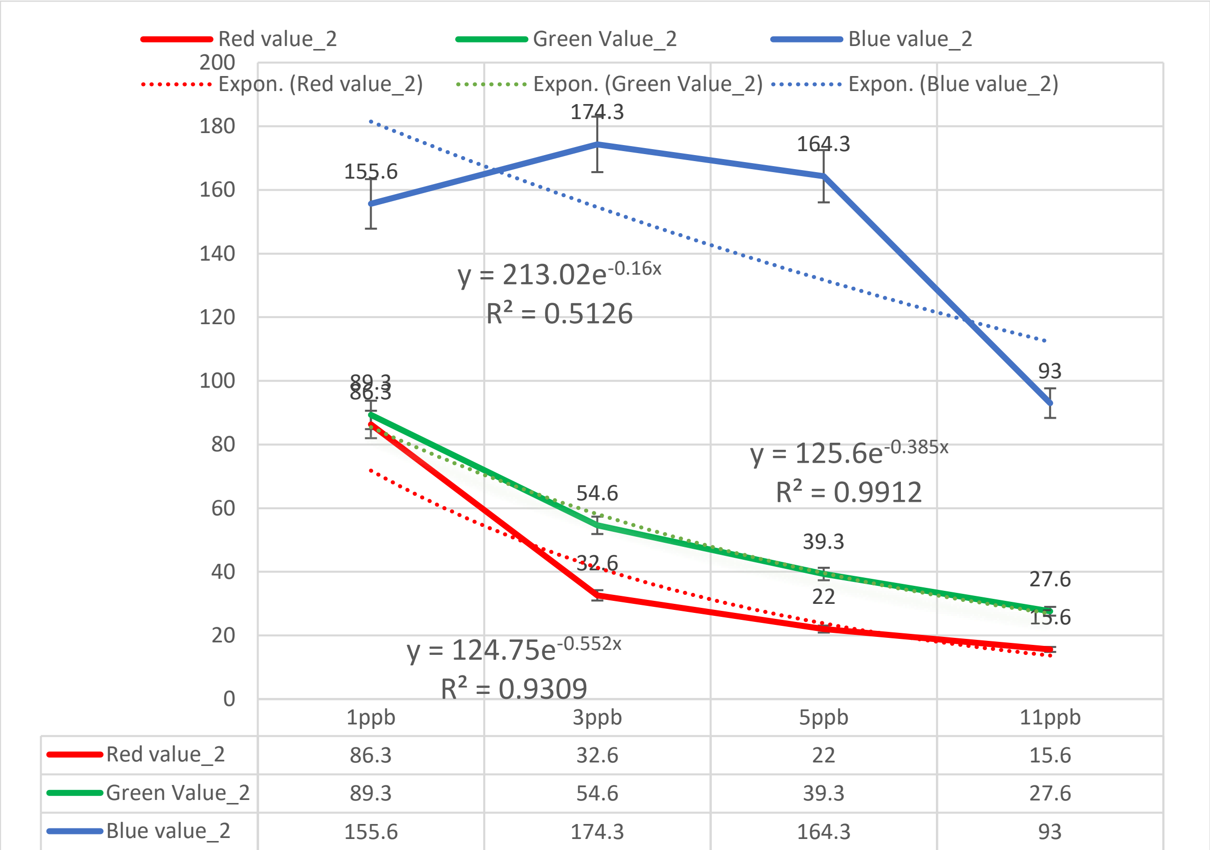

Table 38 RGB565 Exponential algorithm

	Red	Green	Blue
Linear function	$y = 124.75e^{-0.552x}$	$y = 125.6e^{-0.385x}$	$y = 213.02e^{-0.16x}$
R^2	0.9309	0.9912	0.5126

Table 39 RGB565 Exponential algorithm coefficient of determination

Equation 9 Calculation factor about Red, Green and Blue on Exponential algorithm

$$F_{red} = \frac{R^2_{red}}{R^2_{total}} = \frac{0.9309}{2.4347} = 0.38, F_{green} = \frac{R^2_{green}}{R^2_{total}} = \frac{0.9912}{2.4347} = 0.41, F_{blue} = \frac{R^2_{blue}}{R^2_{total}} = \frac{0.5126}{2.4347} = 0.21$$

Equation 10 The calculation formula on RGB565 Exponential algorithm

$$Y = Y_R \times F_{red} + Y_g \times F_{green} + Y_B \times F_{blue}$$

$$Y = (124.75e^{-0.552x\_red}) \times 0.38 + (125.6e^{-0.385x\_green}) \times 0.41 + (213.02e^{-0.16x\_blue}) \times 0.21$$
$$= 47.65e^{-0.552x\_red} + 51.11e^{-0.385x\_green} + 44.73e^{-0.16x\_blue}$$

8.2.2 YUV422 Exponential algorithm

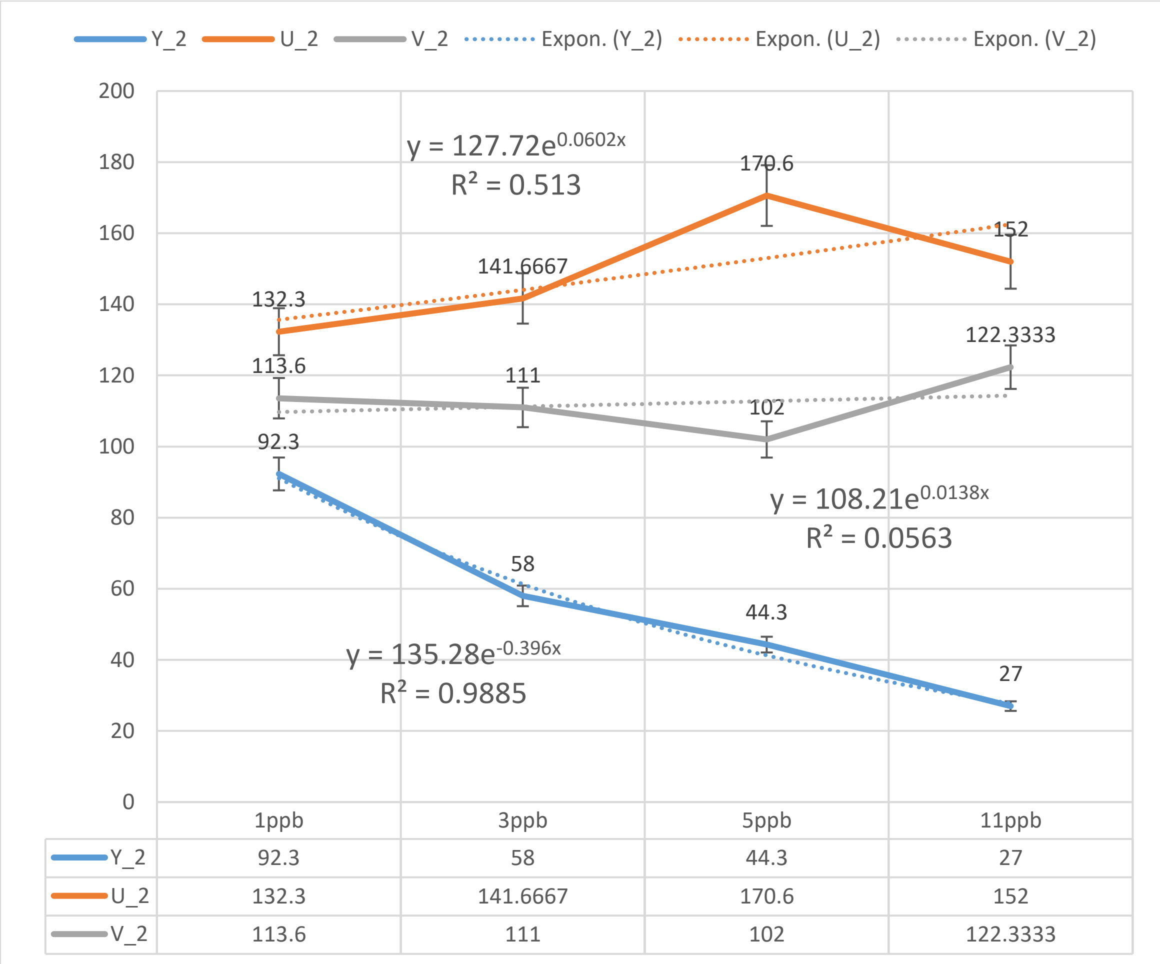

Table 40 YUV422 exponential algorithm

	Y	U	V
Linear function	$y = 135.28e^{-0.396x}$	$y = 108.21e^{0.0138x}$	$y = 127.72e^{0.0602x}$
R^2	0.9885	0.0563	0.513

Table 41YUV422 exponential algorithm coefficient of determination

Equation 11 Calculation factor about Y U V on Exponential algorithm

$$F_Y = \frac{R_Y^2}{R_{total}^2} = \frac{0.9885}{1.5578} = 0.63, F_U = \frac{R_U^2}{R_{total}^2} = \frac{0.0563}{1.5578} = 0.03, F_V = \frac{R_V^2}{R_{total}^2} = \frac{0.513}{1.5578} = 0.32$$

Equation 12 The calculation formula on YUV422 Exponential algorithm

$$Y = Y_Y \times F_Y + Y_U \times F_U + Y_V \times F_V$$
$$Y = (135.28e^{-0.396x\_Y}) \times 0.63 + (108.21e^{0.0138x\_U}) \times 0.03 + (127.72e^{0.0602x\_V}) \times 0.32$$
$$= 85.22e^{-0.396x\_Y} + 3.24e^{0.0138x\_U} + 40.87e^{0.0602x\_V}$$

8.3 Polynomial algorithm

8.3.1 RGB565 Polynomial algorithm

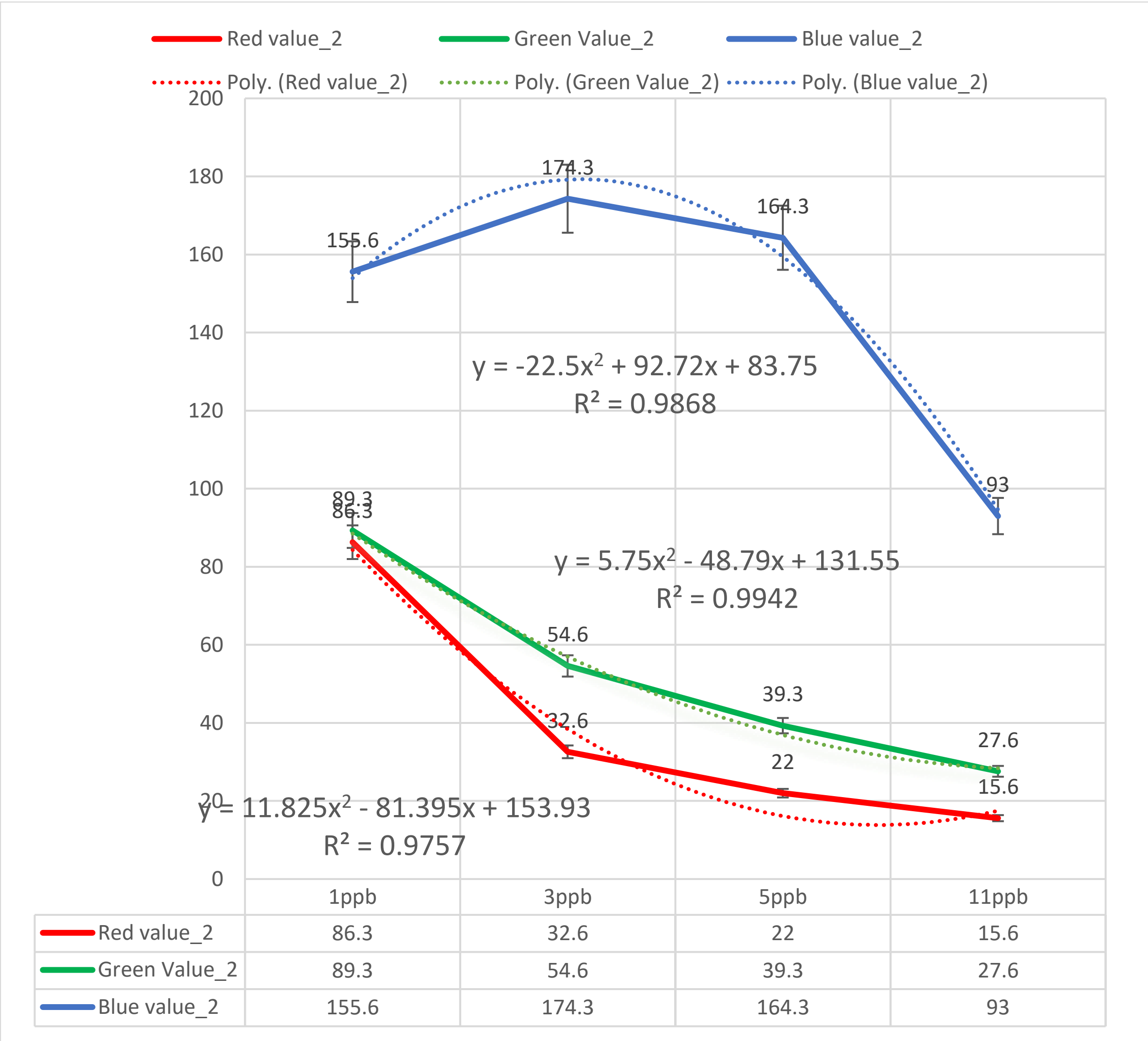

Table 42 RGB565 Polynomial algorithm

	Red	Green	Blue
Linear function	$y = 11.825x^2 - 81.395x + 153.93$	y = 5.75x2 – 48.79x + 131.55	$y = -22.5x^2 + 92.72x + 83.75$
R^2	0.9757	0.9942	0.9868

Table 43 RGB565 Polynomial algorithm coefficient of determination

Equation 13 Calculation factor about Red, Green and Blue on Polynomial algorithm

$$F_{red} = \frac{R^2_{red}}{R^2_{total}} = \frac{0.9757}{2.9567} = 0.329, F_{green} = \frac{R^2_{green}}{R^2_{total}} = \frac{0.9942}{2.9567} = 0.336, F_{blue}\ \frac{R^2_{blue}}{R^2_{total}} = \frac{0.9868}{2.9567} = 0.333$$

Equation 14The calculation formula on RGB565 Polynomial algorithm

$$Y = Y_R \times F_{red} + Y_g \times F_{green} + Y_B \times F_{blue}$$

$$Y = (11.825x_{\mathrm{red}}{}^2 - 81.395x_{red} + 153.93) \times 0.329 + (5.75x_{\mathrm{green}}{}^2 - 48.79x_{green} + 131.55) \times 0.336 +$$

$$(-22.5x_{blue}{}^2 + 92.72x_{blue} + 83.75) \times 0.333$$

$$= 3.890x_{\mathrm{red}}{}^2 - 26.778\ x_{red} + 50.642 + 1.932x_{\mathrm{green}}{}^2 - 16.393x_{green} + 44.200 +$$

$$-7.492x_{blue}{}^2 + 30.875x_{blue} + 27.888$$

$$= 3.890x_{\mathrm{red}}{}^2 - 26.778\ x_{red} + 1.932x_{\mathrm{green}}{}^2 - 16.393x_{green} - 7.492x_{blue}{}^2 + 30.875x_{blue} + 122.73$$

8.3.2 YUV422 Polynomial algorithm

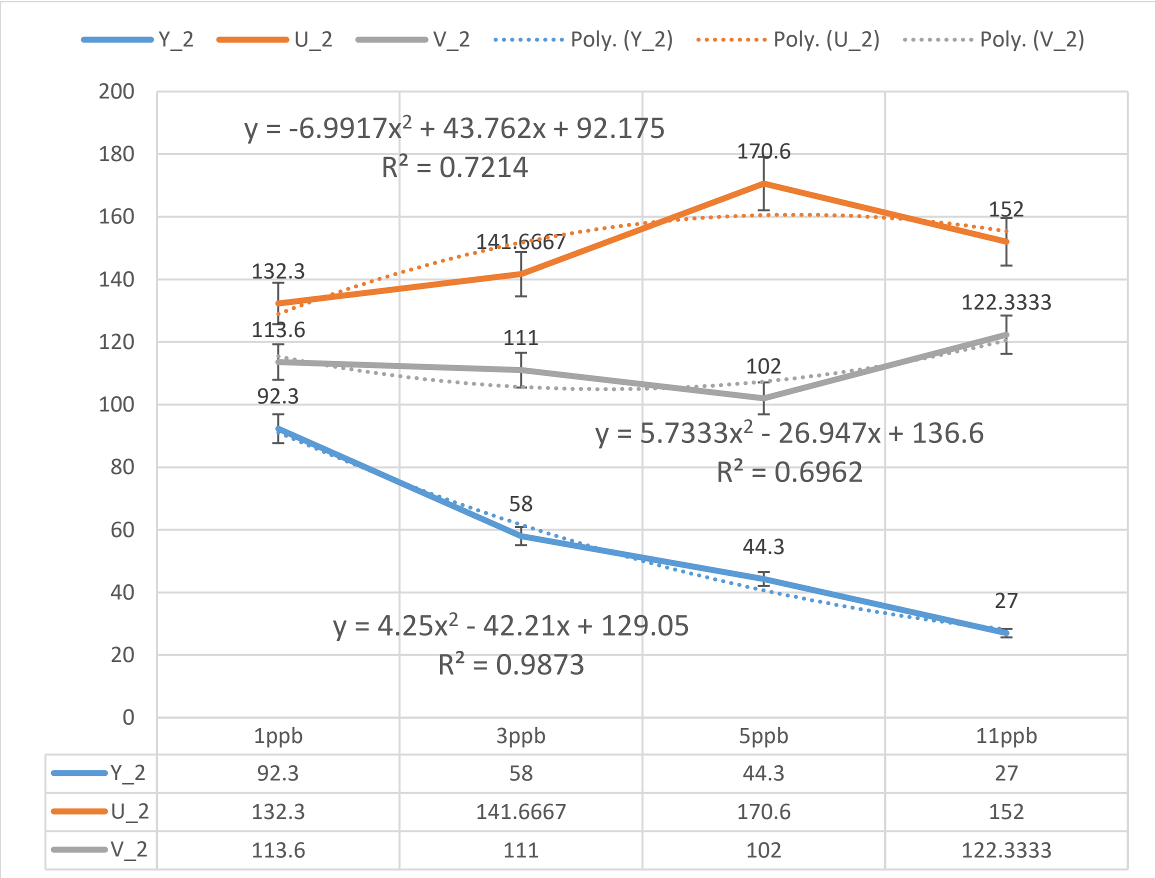

Table 44 YUV422 Polynomial algorithm

	Y	U	V
Linear function	$y = -6.9917x^2 + 43.762x + 92.175$	$y = 5.7333x^2 - 26.947x + 136.6$	$y = 4.25x^2 - 42.21x + 129.05$
R^2	0.7214	0.6962	0.9873

Table 45 YUV422 exponential algorithm coefficient of determination

Equation 15 Calculation factor about Y U V on Polynomial algorithm

$$F_Y = \frac{R_Y^2}{R_{total}^2} = \frac{0.7214}{2.4049} = 0.29, F_U = \frac{R_U^2}{R_{total}^2} = \frac{0.6962}{2.4049} = 0.28, F_V = \frac{R_V^2}{R_{total}^2} = \frac{0.9873}{2.4049} = 0.41$$

Equation 16 The calculation formula on YUV422 Polynomial algorithm

$$Y = Y_Y \times F_Y + Y_U \times F_U + Y_V \times F_V$$
$$Y = (-6.9917x_y^2 + 43.762x_y + 92.175)\times 0.29 + (5.7333x_u^2 - 26.947x_u + 136.6)\times 0.28$$
$$+(4.25x_v^2 - 42.21x_v + 129.05)\times 0.41$$
$$= -2.027x_y^2 + 12.690x_y + 26.730 + 1.605x_u^2 - 7.545x_u + 38.248$$
$$+1.742x_v^2 - 17.306x_v + 52.910$$
$$= -2.027x_y^2 + 12.690x_y + 1.605x_u^2 - 7.545x_u + 1.742x_v^2 - 17.306x_v + 117.88$$

9. Result Verification

As shown in Table 46 the concentration of the actual PFOA solution obtained by three different tests (Linear, Exponential and Polynomial) after five tests when the concentration of the solution to be tested is 1 ppb.

		Theoretical value	Linear	Exponential	Polynomial
RGB565 Format	TEST 1	1ppb	0.31	0.56	0.89
YUV422 Format		1ppb	1.56	1.34	0.99
RGB565 Format	TEST 2	1ppb	2.01	1.23	1.02
YUV422 Format		1ppb	0.12	1.78	1.32
RGB565 Format	TEST 3	1ppb	3.11	0.65	1.23
YUV422 Format		1ppb	1.56	0.89	0.89
RGB565 Format	TEST 4	1ppb	1.13	0.90	0.92
YUV422 Format		1ppb	1.78	1.02	1.15
RGB565 Format	TEST 5	1ppb	1.12	1.45	1.09
YUV422 Format		1ppb	2.94	1.55	1.14

Table 46 1ppb results about PFOA image system

As shown in Table 47, the concentration of the actual PFOA solution when the concentration of the solution to be tested is 3 ppb.

		Theoretical value	Linear	Exponential	Polynomial
RGB565 Format	TEST 1	3ppb	3.35	3.91	3.39
YUV422 Format		3ppb	3.69	3.89	3.11
RGB565 Format	TEST 2	3ppb	1.78	2.76	3.63
YUV422 Format		3ppb	3.53	2.63	2.87
RGB565 Format	TEST 3	3ppb	1.68	3.09	3.16
YUV422 Format		3ppb	1.98	3.36	2.68
RGB565 Format	TEST 4	3ppb	2.66	3.01	3.07
YUV422 Format		3ppb	3.91	3.13	3.47
RGB565 Format	TEST 5	3ppb	2.68	3.09	2.67
YUV422 Format		3ppb	3.35	3.07	2.79

Table 47 3ppb results about PFOA image system

As shown in Table 48, the concentration of the actual PFOA solution obtained when the concentration of the solution to be tested is 5 ppb.

		Theoretical value	Linear	Exponential	Polynomial
RGB565 Format	TEST 1	5ppb	4.69	5.50	5.46
YUV422 Format		5ppb	4.07	4.57	5.43
RGB565 Format	TEST 2	5ppb	3.29	4.48	5.04
YUV422 Format		5ppb	3.37	5.93	5.19
RGB565 Format	TEST 3	5ppb	4.78	5.31	5.36
YUV422 Format		5ppb	6.49	5.12	5.23
RGB565 Format	TEST 4	5ppb	6.46	4.37	4.89
YUV422 Format		5ppb	5.08	4.27	4.91
RGB565 Format	TEST 5	5ppb	3.80	6.26	4.76

YUV422 Format		5ppb	4.69	6.50	4.93

Table 48 5ppb results about PFOA image system

As shown in Table 49, the concentration of the actual PFOA solution obtained by three different tests (Linear, Exponential and Polynomial) after five tests when the concentration of the solution to be tested is 11 ppb.

		Theoretical value	Linear	Exponential	Polynomial
RGB565 Format	TEST 1	11ppb	9.74	11.05	11.43
YUV422 Format		11ppb	11.82	10.66	11.03
RGB565 Format	TEST 2	11ppb	11.54	10.61	11.19
YUV422 Format		11ppb	9.90	11.61	11.30
RGB565 Format	TEST 3	11ppb	10.80	11.87	11.14
YUV422 Format		11ppb	10.10	11.09	10.78
RGB565 Format	TEST 4	11ppb	12.35	11.58	10.80
YUV422 Format		11ppb	11.31	11.34	11.05
RGB565 Format	TEST 5	11ppb	11.81	10.63	11.41
YUV422 Format		11ppb	12.74	11.05	11.43

Table 49 11ppb results about PFOA image system

As shown in Table 50 is the accurate values comparation of RGB565 and YUV422 under three different algorithms. The accurate range of the polynomial algorithm is the smallest, which means the recognition degree of this algorithm is the highest. The accurate range of the Exponential algorithm is the second, and the accurate range of linear algorithm is the largest, which means the recognition degree of this algorithm is the lowest. Through experiments, it can be found that whether the image acquisition is performed using YUV422 format or RGB565 format, the obtained image acquisition results are basically the same. However, image acquisition using YUV422 format can reduce the impact of external light sources on the entire experiment by simply calculating the change in Y value.

		Theoretical value	Min	Max	Accurate range	Average
RGB565 Format	Linear	1ppb	0.31	3.11	2.8	1.53
		3ppb	1.68	3.35	1.67	2.43
		5ppb	3.29	6.46	3.17	4.60
		11ppb	9.74	12.35	2.61	11.24
	Exponential	1ppb	0.56	1.45	0.89	0.95
		3ppb	2.76	3.91	1.15	3.12
		5ppb	4.37	6.26	1.89	5.18
		11ppb	10.61	11.87	1.26	11.14
	Polynomial	1ppb	0.89	1.23	0.34	1.03
		3ppb	2.76	3.91	1.15	3.17
		5ppb	4.76	5.46	0.7	5.10
		11ppb	10.8	11.43	0.63	11.19
YUV422 Format	Linear	1ppb	0.02	1.94	1.92	1.37
		3ppb	1.98	3.91	1.93	3.29
		5ppb	3.37	6.49	3.12	4.74
		11ppb	9.9	12.74	2.84	11.17
	Exponential	1ppb	0.89	1.78	0.89	1.31
		3ppb	2.63	3.89	1.26	3.21
		5ppb	4.27	6.5	2.23	5.27
		11ppb	10.66	11.61	0.95	11.15
	Polynomial	1ppb	0.89	1.32	0.43	1.09
		3ppb	2.63	2.89	0.26	3.21
		5ppb	4.91	5.43	0.52	5.13
		11ppb	10.78	11.43	0.65	11.11

Table 50 Compare three different algorithm results

10. Conclusion

This article explains the importance of PFAS detection. Currently, the use of HPLC-MS instrumentation to detect PFAS concentration is not only need to cost long time period but also is high cost. The solution is detected by using the asktCARE^{TM} test paper, but it involves human eye recognition. The problem is that the external environment is very likely to cause errors in the experimental results. Therefore, the method of recognizing the aktCARE^{TM} test paper by the human eye cannot be widely applied. The current research direction is to use a mobile phone camera to replace the human eye for colour recognition. Interestingly, the value of RGB for reading an image through phone camera is more stable than human eye recognition. However, the method of identifying the colour of the PFAS solution by the mobile phone camera still has certain problems. In order to effectively improve the recognition ability of the image system. I select two effective improvements to the image recognition system of the mobile phone camera which is Image acquisition module and image processing module.

- In the image acquisition module

  By setting the internal registers of the OV2640 to collect Images of different brightness. Through analysis, it can be found that the method of improving brightness can effectively improve the quality of the image. However, this method will cause a certain distortion as the acquired pixel value is greater than the threshold.

  The output format of the image can also be controlled by setting the internal registers of OV2640. This design compared images in RGB565 and YUV422 formats. Through the experimental results, it can be found that the two different acquisition formats have little e ffect on linearity of the data, but because RGB565 receives the influence of external light source, it will generate more optical noise, but if YUV422 format is used for image acqui sition, more storage space of STM407 processing unit will be occupied.

- In the image processing module
  This design uses three different algorithms to process the solution identification algori thm for the image information of RGB565 acquisition format and YUV422 acquisitio n format. Experiments show that Polynomial algorithm has the highest recognition de gree and Coefficient of determination is also close to 1 but the operation time is long. Linear algorithm is simple in design but lowest in recognition. Exponential requires a dditional math library function support. Using DCMI (Digital camera interface) in the ARM Cortex-4 (STMF407) can effectively enhance the processing speed of image information, which can reduce the image distortion caused by insufficient image buffer

The embedded systems to develop image processing modules to replace mobile phone image processing modules has significant advantages. the embedded system can effectively increase the image acquisition quality and can effectively increase the image acquisition speed. It is possible that to achieved low concentration image analysis of PFAS solutions.

Reference

[1] Buck, R.C., Franklin, J., Berger, U., Conder, J.M., Cousins, I.T., de Voogt, P., Jensen, A.A., Kannan, K., Mabury, S.A., van Leeuwen, S.P.J., 2011. Perfluoroalkyl and polyfluoroalkyl substances in the environment: terminology, classification, and origins. Integr. Environ. Assess. Manag. 7 (4), 513-541.

[2] Fang, C and R. Naidu . "Fluoro-spe for Selective Detection of Fluorosurfactants at Ppb Level."

[3] George, A.L., White, G.F., 1999. Optimization of the methylene blue assay for anionic surfactants added to estuarine and marine water. Environ. Toxicol. Chem. 18 (10), 2232e2236

[4] Fang, C and Megharaj, M., Naidu, R., 2016b. Potentiometric detection of AFFFs based on molecular imprinting polymer. Environ. Technol. Innov. 5, 52-59.

[5] Lopez-Ruiz, N., Curto, V.F., Erenas, M.M., Benito-Lopez, F., Diamond, D., Palma, A.J., Capitan-Vallvey, L.F., 2014. Smartphone-based simultaneous pH and nitrite colorimetric determination for paper microfluidic devices. Anal. Chem. 86 (19), 9554-9562.

[6] Apelberg B J, Witter F R, Herbstman J B, et al. Cord serum concentrations of perfluorooctane sulfonate (PFOS) and perfluorooctanoate (PFOA) in relation to weight and size at birth. Environ. Health Perspec., 2007, 115(11): 1670-1676.

[7] Nakayama S, Harada K, Inoue K, et al. Distributions of perfluorooctanoic acid (PFOA) and perfluorooctane sulfonate (PFOS) in Japan and their toxicities. Environmental sciences: an international journal of environmental physiology and toxicology, 2005, 12(6): 293-313.

[8] Johansson N, Fredriksson A, Eriksson P. Neonatal exposure to perfluorooctane sulfonate (PFOS) and perfluorooctanoic acid (PFOA) causes neurobehavioural defects in adult mice. Neurotoxicology, 2008, 29(1): 160-169.

[9] Trudel D, Horowitz L, Wormuth M, et al. Estimating consumer exposure to PFOS and PFOA. Risk Anal., Inter J., 2008, 28(2): 251-269.

[10] Zhang B. et al. The Experiment and Analysis of Image Acquisition System Based on the Hardware Platform. Proceedings of the 2015 International Conference on Communications, Signal Processing, and Systems. Springer, Berlin, Heidelberg, 2016.

[11] Zhang Y., Xiao G., Xu, J. The Wireless Image Transmission System of Capsule Endoscope Based on STM32F103. *DEStech Transactions on Engineering and Technology Research* ICMITE2016 (2016).

[12] Lobb, D. A., Kachanoski, R. G. Modelling tillage translocation using step, linear-plateau and exponential functions. Soil and Tillage Research 51.3-4 (1999): 317-330.

[13] Andrews, S. K., and Rajavarman, V. N. Designing an IoT Enabled Vehicular Diagnostics System using Automotive Sensors and Actuators Integrated with Onboard Video Camera. Inter J Appl Eng Res 12.19 (2017): 8273-8277.

[14] Bright Danakis, C., et al. "Using a CMOS camera sensor for visible light communication. 2012 IEEE Globecom Workshops. IEEE, 2012.

[15] Sohn, S. M., et al. A CMOS image sensor (CIS) architecture with low power motion detection for portable security camera applications. *IEEE Transactions on Consumer Electronics* 49.4 (2003): 1227-1233.

[16] Lee, C., Darling, C. L., Fried, D. In vitro near-infrared imaging of occlusal dental caries using a germanium-enhanced CMOS camera. *Lasers in Dentistry XVI*. 7549. International Society for Optics and Photonics, 2010.

[17] Holst, G. C., Terrence, S. L. CMOS/CCD sensors and camera systems. Reconstruction 9.5 (2011): 2PFC.

[18] Follett, P. A., Neven, L. G. Current trends in quarantine entomology. Annu. Rev. Entomol., 2006, 51: 359-385.

Appendix

LCD internal address structure code

```
//////////////////////////////////////////////////////////////////////////////////
//-----------------LCD Port Definition----------------

//LCD address structure
typedef struct
{
  vu16 LCD_REG;//Register command
  vu16 LCD_RAM;//data command
} LCD_TypeDef;

#define LCD_BASE        ((u32)(0x6C000000 | 0x0000007E))
//A6 output signal changes through LCD_BASE setting
#define LCD             ((LCD_TypeDef *) LCD_BASE)
//////////////////////////////////////////////////////////////////////////////////
```

Write register function

: void LCD_WR_REG(u16 regval)

```
//Write register function
//regval:Register value
void LCD_WR_REG(vu16 regval)
{
  regval=regval;     //add a delay
  LCD->LCD_REG=regval;//Write the register number
}
```

Write LCD data

void LCD_WR_DATA(u16 data)

```
//Write LCD data
//data:The value to be written
void LCD_WR_DATA(vu16 data)
{
  data=data;        //add a delay
  LCD->LCD_RAM=data;
}
```

Read LCD data

u16 LCD_RD_DATA(void)

```
//Read LCD data
//Return value: the read value
u16 LCD_RD_DATA(void)
{
  vu16 ram;      //Defining variables
  ram=LCD->LCD_RAM;
  return ram;
}
```

LCD Set the cursor position

//Xpos: abscissa

//Ypos: ordinate

/ / According to different LCD models, execute different code

/ / Omit part of the code

```
//Set the cursor position
//Xpos
//Ypos
void LCD_SetCursor(u16 Xpos, u16 Ypos)
{
  if(lcddev.id==0X9341)
  {
    LCD_WR_REG(lcddev.setxcmd);
    LCD_WR_DATA(Xpos>>8);LCD_WR_DATA(Xpos&0XFF);    // X Position
    LCD_WR_REG(lcddev.setycmd);
    LCD_WR_DATA(Ypos>>8);LCD_WR_DATA(Ypos&0XFF);   //  Y Position
  }
}
```

LCD Draw points

//x,y: coordinates

//colour : color

```
//draw points
//x,y:Position
//color:
void LCD_Fast_DrawPoint(u16 x,u16 y,u16 color)
{
  LCD_SetCursor(x,y);    //Set the cursor position
  LCD->LCD_REG=lcddev.wramcmd;
  LCD->LCD_RAM=color;
}
```

LCD Display a character

```
//Display a character at the specified location
//x,y: starting coordinates
void LCD_ShowChar(u16 x,u16 y,u8 num,u8 size,u8 mode)
{
  u8 temp,t1,t;
  u16 y0=y;
  u8 csize=(size/8+((size%8)?1:0))*(size/2);
  num=num-' ';//Get the value of the ASCII library
  for(t=0;t<csize;t++)
  {
    if(size==12)temp=asc2_1206[num][t];
    else return;                //not find any matching value on ASCII library
    for(t1=0;t1<8;t1++)
    {
      if(temp&0x80)LCD_Fast_DrawPoint(x,y,POINT_COLOR);
      else if(mode==0)LCD_Fast_DrawPoint(x,y,BACK_COLOR);
      temp<<=1;
      y++;
      if(y>=lcddev.height)return;   //Over size
      if((y-y0)==size)
      {
        y=y0;
        x++;
        if(x>=lcddev.width)return;  //Over size
        break;
      }
    }
  }
}
```

KEY input function

```
//Key processing function
//return key value
//Mode: 0  not continuous press; 1 continuous press;
//return 0 not key retrun
//return 1 key 1 pressed
//return 2 key 2 pressed
//return 3 key 3 pressed
//return 4 key WK pressed
//Response priority,KEY0>KEY1>KEY2>WK_UP!!
u8 KEY_Scan(u8 mode)
{
  static u8 key_up=1;
  if(mode)key_up=1;
  if(key_up&&(KEY0==0||KEY1==0||KEY2==0||WK_UP==1))
  {
    delay_ms(10);//reduce shake effect
    key_up=0;
    if(KEY0==0)return 1;
    else if(KEY1==0)return 2;
    else if(KEY2==0)return 3;
    else if(WK_UP==1)return 4;
  }else if(KEY0==1&&KEY1==1&&KEY2==1&&WK_UP==0)key_up=1;
  return 0;// not keynot key
}
```

Camera module SCCB Start signal

```
//SCCB start signal
//When the clock is high, the data line is high voltage to low voltage , which is the SCCB start signal.
// In the active state, SDA and SCL are low voltage
void SCCB_Start(void)
{
    SCCB_SDA=1;     //Data line keep high level volatge
    SCCB_SCL=1;     //The data line is high voltage to low when the clock line is high
    delay_us(50);
    SCCB_SDA=0;
    delay_us(50);
    SCCB_SCL=0;     //Date line to low level voltage
}
```

Camera module SCCB Stop signal

```
//SCCB stop signal
//When the clock is high, the data line is low voltage to high voltage
//which is the SCCB stop signal.
void SCCB_Stop(void)
{
    SCCB_SDA=0;
    delay_us(50);
    SCCB_SCL=1;
    delay_us(50);
    SCCB_SDA=1;
    delay_us(50);
}
```

Camera module SCCB Write data function

```
//SCCB,Write 8 byte
//return :0,success ;1,failure
u8 SCCB_WR_Byte(u8 dat)
{
  u8 j,res;
  for(j=0;j<8;j++) //repeat 8 times to send data
  {
    if(dat&0x80)SCCB_SDA=1;
    else SCCB_SDA=0;
    dat<<=1;
    delay_us(50);
    SCCB_SCL=1;
    delay_us(50);
    SCCB_SCL=0;
  }
  SCCB_SDA_IN();     //Set SDA Port is input Port
  delay_us(50);
  SCCB_SCL=1;      //receive 9th date to judge communication is success
  delay_us(50);
  if(SCCB_READ_SDA)res=1;  //SDA=1 failure
  else res=0;          //SDA=0 successful
  SCCB_SCL=0;
  SCCB_SDA_OUT();    //Set SDA Port is output Port
  return res;
}
```

Camera module SCCB Read data function

```
//SCCB,Read 8 byte
//return :Read data
u8 SCCB_RD_Byte(void)
{
  u8 temp=0,j;
  SCCB_SDA_IN();      //Set SDA Port is input Port
  for(j=8;j>0;j--)    //repeat 8 times to receive data
  {
    delay_us(50);
    SCCB_SCL=1;
    temp=temp<<1;
    if(SCCB_READ_SDA)temp++;
    delay_us(50);
    SCCB_SCL=0;
  }
  SCCB_SDA_OUT();     //Set SDA Port is output Port
  return temp;
}
```

Camera module SCCB Write register function

```
//SSCB Read Regisiter
//retrun : Read value
u8 SCCB_RD_Reg(u8 reg)
{
  u8 val=0;
  SCCB_Start();               //Start SCCB
  SCCB_WR_Byte(SCCB_ID);      //Write OV2640 ID
  delay_us(100);
    SCCB_WR_Byte(reg);        //Write Register data
  delay_us(100);
  SCCB_Stop();
  delay_us(100);
  //Start Read
  SCCB_Start();
  SCCB_WR_Byte(SCCB_ID|0X01); //Send Read Command
  delay_us(100);
    val=SCCB_RD_Byte();       //Read Regsiter Data
    SCCB_No_Ack();
    SCCB_Stop();
    return val;
}
```

Camera module SCCB Read register function

```
//SCCB,Write Regisiter
//return :0,success ;1,failure
u8 SCCB_WR_Reg(u8 reg,u8 data)
{
    u8 res=0;
    SCCB_Start();           //Strat SCCB
    if(SCCB_WR_Byte(SCCB_ID))res=1; //Write OV2640 ID
    delay_us(100);
      if(SCCB_WR_Byte(reg))res=1;   //Write Register address
    delay_us(100);
      if(SCCB_WR_Byte(data))res=1;  //Write Register data
      SCCB_Stop();
      return  res;
}
```

OV2640 JPEG Mode function

```
//OV2640:JPEG_Mode
void OV2640_JPEG_Mode(void)
{
    u16 i=0;
    //Set:YUV422 Format
    for(i=0;i<(sizeof(ov2640_yuv422_reg_tbl)/2);i++)
    {
        SCCB_WR_Reg(ov2640_yuv422_reg_tbl[i][0],ov2640_yuv422_reg_tbl[i][1]);
    }

    //Set:Output JPEG data
    for(i=0;i<(sizeof(ov2640_jpeg_reg_tbl)/2);i++)
    {
        SCCB_WR_Reg(ov2640_jpeg_reg_tbl[i][0],ov2640_jpeg_reg_tbl[i][1]);
    }
}
```

JPEG camera module internal register command

```
const u8 ov2640_jpeg_reg_tbl[][2]=
{
    0xff, 0x01,
    0xe0, 0x14,
    0xe1, 0x77,
    0xe5, 0x1f,
    0xd7, 0x03,
    0xda, 0x10,
    0xe0, 0x00,
};
```

YUV422 output format camera internal register command

```
const u8 ov2640_yuv422_reg_tbl[][2]=
{
    0xFF, 0x00,
    0xDA, 0x10,
    0xD7, 0x03,
    0xDF, 0x00,
    0x33, 0x80,
    0x3C, 0x40,
    0xe1, 0x77,
    0x00, 0x00,
};
```

OV2640 RGB565 Mode function

```c
//OV2640 :RGB565_mode
void OV2640_RGB565_Mode(void)
{
  u16 i=0;
  //Set:Output RGB565
  for(i=0;i<(sizeof(ov2640_rgb565_reg_tbl)/2);i++)
  {
    SCCB_WR_Reg(ov2640_rgb565_reg_tbl[i][0],ov2640_rgb565_reg_tbl[i][1]);
  }
}
```

RGB565 output format camera internal register command

```c
const u8 ov2640_rgb565_reg_tbl[][2]=
{
  0xFF, 0x00,
  0xDA, 0x09,
  0xD7, 0x03,
  0xDF, 0x02,
  0x33, 0xa0,
  0x3C, 0x00,
  0xe1, 0x67,

  0xff, 0x01,
  0xe0, 0x00,
  0xe1, 0x00,
  0xe5, 0x00,
  0xd7, 0x00,
  0xda, 0x00,
  0xe0, 0x00,
};
```

OV2640 Image window Set function

OV2640 Output window set

```
//Set Image output window
//sx,sy : Start Address
//(width:horizontal)(height:vertical)
void OV2640_Window_Set(u16 sx,u16 sy,u16 width,u16 height)
{
  u16 endx;
  u16 endy;
  u8 temp;
  endx=sx+width/2;  //V*2
  endy=sy+height/2;

  SCCB_WR_Reg(0XFF,0X01);
  temp=SCCB_RD_Reg(0X03);          //Read Vref value
  temp&=0XF0;
  temp|=((endy&0X03)<<2)|(sy&0X03);
  SCCB_WR_Reg(0X03,temp);          //Set Vref Strat and end First two bits
  SCCB_WR_Reg(0X19,sy>>2);         //Set Vref start high 8 bits
  SCCB_WR_Reg(0X1A,endy>>2);         //Set Vref end high 8 bits

  temp=SCCB_RD_Reg(0X32);          //Read Href Value
  temp&=0XC0;
  temp|=((endx&0X07)<<3)|(sx&0X07);
  SCCB_WR_Reg(0X32,temp);          //Set Href start and end First two bits
  SCCB_WR_Reg(0X17,sx>>3);         //Set Href start high 8 bits
  SCCB_WR_Reg(0X18,endx>>3);       //Set Href end   high 8 bits
}
```

OV2640 image window set

```
//Set Image output size
//(width:horizontal)(height:vertical)
//Return :0 :          Successful
//          Other value: Failure
u8 OV2640_OutSize_Set(u16 width,u16 height)
{
  u16 outh;
  u16 outw;
  u8 temp;
  if(width%4)return 1;
  if(height%4)return 2;
  outw=width/4;
  outh=height/4;
  SCCB_WR_Reg(0XFF,0X00);
  SCCB_WR_Reg(0XE0,0X04);
  SCCB_WR_Reg(0X5A,outw&0XFF);     //Set OUTW Low 8 bits
  SCCB_WR_Reg(0X5B,outh&0XFF);     //Set OUTH Low 8 bits
  temp=(outw>>8)&0X03;
  temp|=(outh>>6)&0X04;
  SCCB_WR_Reg(0X5C,temp);        //Set OUTH/OUTW High bits
  SCCB_WR_Reg(0XE0,0X00);
  return 0;
}
```

OV2640 brightness setting

```
//Brightness Set
//0:(0X00)-2
//1:(0X10)-1
//2,(0X20) 0
//3,(0X30)+1
//4,(0X40)+2
void OV2640_Brightness(u8 bright)
{
  SCCB_WR_Reg(0xff, 0x00);
  SCCB_WR_Reg(0x7c, 0x00);
  SCCB_WR_Reg(0x7d, 0x04);
  SCCB_WR_Reg(0x7c, 0x09);
  SCCB_WR_Reg(0x7d, bright<<4);
  SCCB_WR_Reg(0x7d, 0x00);
}
```

OV2640 contrast setting

```
void OV2640_Contrast(u8 contrast)
{
  u8 reg7d0val=0X20;// 0
  u8 reg7d1val=0X20;// 0
    switch(contrast)
  {
    case 0://-2
      reg7d0val=0X18;
      reg7d1val=0X34;
      break;
    case 1://-1
      reg7d0val=0X1C;
      reg7d1val=0X2A;
      break;
    case 3://1
      reg7d0val=0X24;
      reg7d1val=0X16;
      break;
    case 4://2
      reg7d0val=0X28;
      reg7d1val=0X0C;
      break;
  }
  SCCB_WR_Reg(0xff,0x00);
  SCCB_WR_Reg(0x7c,0x00);
  SCCB_WR_Reg(0x7d,0x04);
  SCCB_WR_Reg(0x7c,0x07);
  SCCB_WR_Reg(0x7d,0x20);
  SCCB_WR_Reg(0x7d,reg7d0val);
  SCCB_WR_Reg(0x7d,reg7d1val);
  SCCB_WR_Reg(0x7d,0x06);
}
```

DCMI Interface design

Enable DCMI clock.

```
RCC_AHB1PeriphClockCmd(RCC_AHB1Periph_GPIOA|RCC_AHB1Periph_GPIOB|RCC_AHB1Periph_GPIOC|RCC_AHB1Periph_GPIOE, ENABLE);
//Strat GPIO_Clock
RCC_AHB2PeriphClockCmd(RCC_AHB2Periph_DCMI,ENABLE);//Enable DCMI Clock
```

Set DCMI working mode and parameters.

```
GPIO_PinAFConfig(GPIOA,GPIO_PinSource4,GPIO_AF_DCMI); //PA4,AF13  DCMI_HSYNC
GPIO_PinAFConfig(GPIOA,GPIO_PinSource6,GPIO_AF_DCMI); //PA6,AF13  DCMI_PCLK
GPIO_PinAFConfig(GPIOB,GPIO_PinSource7,GPIO_AF_DCMI); //PB7,AF13  DCMI_VSYNC
GPIO_PinAFConfig(GPIOC,GPIO_PinSource6,GPIO_AF_DCMI); //PC6,AF13  DCMI_D0
GPIO_PinAFConfig(GPIOC,GPIO_PinSource7,GPIO_AF_DCMI); //PC7,AF13  DCMI_D1
GPIO_PinAFConfig(GPIOC,GPIO_PinSource8,GPIO_AF_DCMI); //PC8,AF13  DCMI_D2
GPIO_PinAFConfig(GPIOC,GPIO_PinSource9,GPIO_AF_DCMI); //PC9,AF13  DCMI_D3
GPIO_PinAFConfig(GPIOC,GPIO_PinSource11,GPIO_AF_DCMI);//PC11,AF13 DCMI_D4
GPIO_PinAFConfig(GPIOB,GPIO_PinSource6,GPIO_AF_DCMI); //PB6,AF13  DCMI_D5
GPIO_PinAFConfig(GPIOE,GPIO_PinSource5,GPIO_AF_DCMI); //PE5,AF13  DCMI_D6
GPIO_PinAFConfig(GPIOE,GPIO_PinSource6,GPIO_AF_DCMI); //PE6,AF13  DCMI_D7
```

Set DMA to collect data.

```
DCMI_InitStructure.DCMI_CaptureMode=DCMI_CaptureMode_Continuous;//Continuous mode
DCMI_InitStructure.DCMI_CaptureRate=DCMI_CaptureRate_All_Frame;//Full frame capture
DCMI_InitStructure.DCMI_ExtendedDataMode= DCMI_ExtendedDataMode_8b;//8-bit data
DCMI_InitStructure.DCMI_HSPolarity= DCMI_HSPolarity_Low;//HSYNC
DCMI_InitStructure.DCMI_PCKPolarity= DCMI_PCKPolarity_Rising;//PCLK Valid on rising edge
DCMI_InitStructure.DCMI_SynchroMode= DCMI_SynchroMode_Hardware;//HSYNC,VSYNC
DCMI_InitStructure.DCMI_VSPolarity=DCMI_VSPolarity_Low;//VSYNC
DCMI_Init(&DCMI_InitStructure);
```

Start DCMI transmission.

```
//DCMI Start Communication
void DCMI_Start(void)
{
  DMA_Cmd(DMA2_Stream1, ENABLE);//Enable DMA2,Stream1
  DCMI_CaptureCmd(ENABLE);//DCMI Capture enable
}
```